

Doctoral Dissertation

**Study on Thermal Performance of Sunagoke Moss
Green Roof in Mitigating Urban Heat Island**

(ヒートアイランド現象の緩和の為の
スナゴケ屋根緑化法の熱的性能に関する研究)



March 2018

MUHAMMAD AMIR AISAR BIN KHALID

Department of Systems Design and Engineering

Graduate School of Science and Engineering

Yamaguchi University

Abstract

In order to mitigate the Urban Heat Island (UHI) effects, green roof is proposed to be a technique to increase the green region in urban area, as it is a method where the unused part of the roof of buildings is utilised for vegetation. A type of moss identified as Sunagoke (*Racomitrium Canescens*) was found to be the only truly draught tolerant species, and started to gain its popularity as a green roof candidate.

However, the discovery on thermal performance of Sunagoke moss green roof are insufficient. Therefore, the objective of this dissertation is to deliver the evaluations on thermal performance of Sunagoke moss green roof in addressing UHI. Previous researches have been surveyed and organized in Chapter 1 to increase the comprehension relating to the role of plants in green roof application. This dissertation aimed to explore the thermal performance of Sunagoke moss green roof with two different experimental approaches: laboratory based indoor experiment, and the actual outdoor experiment.

In Chapter 2, the green roof implementation method utilised in this research has been explained. Several conditions of model houses made from box-shaped Polystyrene foams were utilized throughout the experiments. A model house which was installed with a naturally dry Sunagoke moss green panel on the top, was used as the main experiment subject. The Sunagoke moss green panel was made by attaching 3 mm thickness of Sunagoke moss-mat on a galvalume steel plate. There was no substrate layer since Sunagoke does not require them. Besides, model houses with 30mm thickness of Sunagoke moss, 30mm thickness grass and soil, and a control model house were also used as the comparison subjects.

Chapter 3 reviewed the green roof thermal performance evaluation method. Temperature analysis was conducted by examining the changes of surface, and interior temperature of each model house. Moreover, the heat energy balance were determined to analyse the heat contribution on model houses. The heat balance equation consists of irradiance, reflected radiation, latent heat, convection heat, and conduction heat.

Chapter 4 presented the main results for indoor experiment: effects of convection heat transfer on Sunagoke moss green roof. The indoor experiments were piloted in an enclosed Artificial Climate Chamber, facilitated at Yamaguchi Prefectural Industrial Technology Institute where the measurement environment can be adjusted so that naturally changing external factors will not affect the experimental result. Important parameters that influence the thermal exchange between roof surface and environment: wind velocity, irradiance, and evaporation were altered to simulate an average summer condition in Japan. Here, the dry and moist model house with 3mm Sunagoke moss, and control model house were utilised.

As the results, the convection heat was found to dominate the whole heat transfer in dry Sunagoke moss and control roof surfaces which lack evaporation. Contrarily, the latent heat of moist Sunagoke green roof governed and diverted 70% in natural, and 91% in forced convection from the whole heat transfer process, individually. Besides moist Sunagoke moss in combined and forced convection, there were no correlation between irradiance and

convection heat transfer coefficient. Nevertheless, the effects of wind velocity on Sunagoke moss green roof above 2 m/s were clarified identical since no significant changes were found in the convection coefficient, surface and interior temperature afterwards.

In Chapter 5, the relationship between the irradiation angle of radiation device which considered as sunlight, and the Sunagoke moss green roof has been examined in a similar indoor experimental setup as in previous chapter. In the experiment, the changes of model houses surface temperature were measured under irradiance strength of 200 to 1000 W/m², and irradiance angle of 30 to 90°. The experiment was conducted in a windless condition, and with the change of the angle of sunlight, it was possible to know the basic characteristics of irradiance angle and surface temperature.

Meanwhile, the results for experiment performed at the main office building rooftop of Yamaguchi University Engineering Campus were discussed in Chapter 6. This time, four dry model houses of 3mm Sunagoke moss, 30mm Sunagoke moss, 25mm grass with 5mm soil layer, and control were utilised as the test subjects. The three green panels displayed better convection heat transfer coefficient than the control roof, however, the thinnest Sunagoke moss was the highest. The 30mm thickness Sunagoke moss did not deliver heat as good as 3mm Sunagoke moss and 25mm grass in term of convection heat, but the suppression of interior temperature was the most superior. Despite the absence of soil, both Sunagoke moss green roofs showed decent insulation effect and provide thermal comfort comparable to grass.

Chapter 7 describes a summary of the effectiveness of the basic characteristics obtained in indoor experiments, and their relationship with outdoor experiments. With a certain degree, the corresponding results in outdoor environments can be interpreted in detail by referring to the results of forced and combined convection in indoor experiments. In addition, it is possible to quantitatively select appropriate heat insulation performance and evaporative cooling performance when adjusting the heat balance equation on the roof surface, regardless of whether the Sunagoke moss green panel is dry or wet. These results are extremely useful for establishing the Sunagoke Moss Green Roof Control System, and are expected to be used especially when conducting a theoretical approach (three dimensional thermal fluid numerical simulation).

要旨

ヒートアイランド現象(UHI : Urban Heat Island)を緩和させるために、建物や家屋の屋根の未使用の部分に植生し活用する屋根緑化法があり、それは都市部の緑地を増やすのに理想的な手法である。とりわけスナゴケ(*Racomitrium Canescens*)と称されるコケの一種、唯一真の乾燥耐性種であるこれは、特に屋根緑化の素材として注目を集め始めている。しかしながら、スナゴケ屋根緑化法の熱的性能などまだ深く研究評価されていない。さらにその評価法も確立されていない。本研究の目的は、UHIにおけるスナゴケ屋根緑化法の熱的性能に関する実験的検討とその評価法を提供することである。

第 1 章では、屋根緑化法に関するその役割と期待される性能との理解を深めるために多くの屋根緑化関連の先行研究の文献を調査整理し、その内容などから本研究の意義などを述べている。特に本論文では二つの異なる実験手法（実験室ベースの屋内実験と実環境における屋外実験）の得失から、スナゴケ屋根緑化の熱的性能評価へと研究展開することを目指した。

第 2 章では、屋根緑化法の実験装置、方法に関して説明した。屋内外の実験では、主たるパラメーター（照射量、風速、温度、湿度）に基づき 4 種の条件下で箱型モデル管体を用いた。屋根上に自然乾燥したスナゴケ緑化パネルの有無（2つの条件、後者を特にコントロールパネルと称す）のモデル管体が特に主実験対象である。スナゴケ緑化パネルは、スナゴケと有機接着剤にてガルバニウム鋼板の上に任意の厚み（この場合 3 mm, 30 mm）で貼り付けることで製作している。その他、芝生 30 mm 厚（土壌の厚みを含む）の条件も比較対象のため実験を実施した。

第 3 章では、屋根緑化の熱性能評価方法の詳細を検討したことを述べている。特に各モデル管体の表面・管体内温度の変化を調べることによる温度解析や、さらに、モデル管体における各種熱の寄与度を分析するため熱収支式の作成とその構成などを検討した。式中の熱は、ここでは全受熱、反射熱、放射熱、蒸発潜熱、対流熱および伝導熱から成り立つと考えている。

第 4 章では、屋根表面温度に対流熱伝達が及ぼす影響に限定して実施した屋内実験の結果に対する考察を記述している。自然に変化する様々な外的要因が実験結果に影響を与えないように、屋内実験を山口県産業技術センター密閉型人工気候室で実施した。ここでは計測環境の調整が可能でかつ風速、受熱および蒸発である屋根の表面と環境の間の熱交換に影響を与える重要なパラメータを、日本の平均的夏の環境を再現するように変更できた。評価の 1 つとして、熱収支を構成する各熱の全熱に対する割合を知ることで、顕熱が蒸発を伴わない乾燥スナゴケ、またはコントロールパネルの全ての熱輸送を支配することが分かった。また、一方、湿ったスナゴケ屋根での蒸発潜熱は、それぞれ全熱の熱輸送から自然対流では 70%、強制対流

では 91%を支配し熱輸送に極めて抑制的であることも知ることができた。さらには複合対流と強制対流における湿ったスナゴケ以外の場合、風速 2 m/s 以上では受熱と対流熱伝達係数には然したる相関はないことも知ることができた。全般に対流熱伝達係数、表面温度、伝導熱流束、室内温度などへの風速の影響が小さく、2 m/s 以上の風速領域における対流熱伝達がスナゴケ屋根緑化の場合、同等程度の影響しか及ぼさない事も明らかにした。

第 5 章では、太陽光に見立てた照明器具の照射角度とスナゴケ屋根緑化の関係について、室内実験にてその影響を調べた結果を考察している。実験は、照射強度 200～1000W/m²の下、照射角度を 30～90° と変えながら、筐体表面温度の変化を測定した。実験は無風状態にて行い、太陽光角度の変化に伴い、照射角度と表面温度の基本特性を知ることができた。

第 6 章では、山口大学工学部本館屋上における屋外実験結果に関する考察を記述した。屋外実験ではスナゴケ厚さ 3mm と 30mm、土壌を含んだ芝生厚さ 30mm、コントロールパネルの 4 種の条件を有するモデル筐体を試験対象とした。環境変化での影響は否めないが 3 種の緑化パネルはコントロールパネルよりもより高い対流熱伝達係数を示し、とりわけ厚さ 3mm の場合が最も高い値を示した。スナゴケパネルの厚さ 30mm は厚さ 3mm や芝生のパネルに比べ、対流熱輸送に関しては劣るが、筐体内温度では最も低く安定した温度を示しており、抑制性能が最も優れていることがわかる。厚みの大小にかかわらずスナゴケ屋根緑化は適度な断熱効果を示し、土壌を有する芝生に匹敵する熱的快適性を提供できることが確認された。

第 7 章では、屋内実験で得られた基本特性の有効性と屋外実験のそれらとの関係に関するまとめを記述した。特定の度合いでは、屋内実験における強制、複合対流領域での結果を参考にして屋外環境での対応する結果を詳細に解釈することができた。また、スナゴケパネル屋根緑化が乾燥状態でも湿潤状態でも、屋根表面上での熱収支式を調整する際に、適切な遮熱性能と蒸発冷却性能の定量的選択を可能とした。これらの成果は、スナゴケ屋根緑化制御システムを確立する上に極めて有用であり、とりわけ理論的アプローチ（3次元熱流体数値シミュレーション）を行う際に利用されることが期待される。

Contents

| | |
|---|-----|
| Nomenclatures | VII |
| Chapter 1 – Introduction | 1 |
| 1-1 Research Background | 1 |
| 1-2 Green Roof Characteristics | 2 |
| 1-3 Previous Researches | 5 |
| 1-4 Research Objectives | 9 |
| Chapter 2 – Green Roof Implementation Method | 10 |
| 2-1 Introduction to Green Roof Technique | 10 |
| 2-2 Green Panel | 10 |
| 2-3 Model House | 13 |
| Chapter 3 – Green Roof Thermal Performance Evaluation Method | 15 |
| 3-1 Introduction to Evaluation Method | 15 |
| 3-1-1 Thermal Insulation Effect | 15 |
| 3-1-2 Evaporation Cooling Effect | 15 |
| 3-2 Temperature Analysis | 16 |
| 3-2-1 Temperature Measuring Method | 16 |
| 3-2-2 Dimensionless Temperature | 17 |
| 3-3 Heat Energy Balance in Model house | 17 |
| 3-3-1 Total Radiation Received by a Subject Surface | 18 |
| 3-3-2 Conduction Heat Flux | 19 |
| 3-3-3 Latent Heat Flux | 21 |
| 3-3-4 Convection Heat Flux | 22 |
| 3-4 Evaporation Efficiency of Moist Green Panel | 22 |
| 3-5 Ratio of Grashof Number and Square of Reynolds Number | 24 |
| Chapter 4 – Indoor Experiment: Effects of Convection Heat Transfer on Sunagoke Moss Green Roof | 25 |
| 4-1 Experiment Introduction | 25 |
| 4-2 Experimental Methodology | 25 |
| 4-3 Experimental Conditions | 31 |
| 4-4 Results and Discussion | 31 |
| 4-4-1 Convection Heat Transfer Characteristics | 31 |
| 4-4-2 Effects of Wind Velocity on Heat Balance | 35 |
| 4-4-3 Relation of Wind Velocity and Temperature Profile | 45 |
| 4-5 Chapter Summary | 50 |
| 4-6 Equipment List in Chapter 4 | 51 |

| | |
|--|------------|
| Chapter 5 – Indoor Experiment: Effects of Irradiance Angle on Sunagoke Moss | 54 |
| Green Roof | |
| 5-1 Experiment Introduction | 54 |
| 5-2 Experimental Conditions | 58 |
| 5-3 Experimental Methodology | 60 |
| 5-4 Results and Discussion | 62 |
| 5-4-1 Effects of Irradiance Angle on Heat Balance | 62 |
| 5-4-2 Model Houses Interior Temperature Differences | 77 |
| 5-5 Chapter Summary | 79 |
| 5-6 Equipment List in Chapter 5 | 80 |
| | |
| Chapter 6– Outdoor Experiment and Relationship with Indoor Experiment | 82 |
| 6-1 Experiment Introduction | 82 |
| 6-2 Experimental Conditions | 83 |
| 6-3 Experimental Methodology | 84 |
| 6-4 Results and Discussion | 84 |
| 6-4-1 Convection Heat Transfer Characteristics in Outdoor Environment | 84 |
| 6-4-2 Heat Balance on Model Houses | 88 |
| 6-4-3 Temperature Profile | 92 |
| 6-5 Chapter Summary | 98 |
| 6-6 Equipment List in Chapter 6 | 99 |
| | |
| Chapter 7– General Conclusion | 101 |
| 7-1 Relation between Indoor and Outdoor Experiments | 101 |
| 7-2 Comparison between Green Roof Plants | 102 |
| 7-3 Comparison between Green Roof, High Reflective Roof, and Solar Panel Roof | 103 |
| 7-4 Future Exploration | 104 |
| | |
| Acknowledgement | 105 |
| | |
| References | 106 |
| | |
| Appendix | 111 |

Nomenclatures

| | | |
|------------------|--|-------------------------------|
| Ar | Archimedes number = Ratio of Grashof number and square of Reynolds number | [-] |
| A_s | Outermost surface area | [m ²] |
| B | Bowen ratio | [-] |
| c | Instrument sensitivity constant | [mV/kWm ²] |
| c_p | Specific heat of air | (=1.00) [kJ/kgK] |
| E_i | Instrument output voltage | [mV] |
| e | Evaporation amount | [g] |
| Gr | Grashof number | [-] |
| g | Acceleration due to gravity | [m/s ²] |
| h | Convection heat transfer coefficient | [W/m ² K] |
| k | Thermal conductivity | [W/mK] |
| k_n | Thermal conductivity of n th material | [W/mK] |
| k_x | Mass transfer rate | [kg/m ² s] |
| L | Representative dimension | [m] |
| Le | Lewis number | (=0.83) [-] |
| L_n | Thickness of n th material | [m] |
| l | Latent heat coefficient of water | (=2257) [kJ/kg] |
| Nu | Nusselt number | [-] |
| n | Evaporation rate | [-] |
| P | Ground air pressure | [hpa] |
| P_l | Representative air pressure | [hpa] |
| P_∞ | Saturated water vapour partial pressure | [hpa] |
| $Q_{conduction}$ | Conduction heat flux | [W/m ²] |
| $Q_{convection}$ | Convection heat flux | [W/m ²] |
| Q_{latent} | Latent heat flux | [W/m ²] |
| q_{cond} | Conduction heat proportion | (= $Q_{conduction}/R_n$) [%] |
| q_{conv} | Convection heat proportion | (= $Q_{convection}/R_n$) [%] |
| q_{latent} | Latent heat proportion | (= Q_{latent}/R_n) [%] |
| $q_{reflect}$ | Reflected radiation proportion | (= R_R/R_n) [%] |
| Re | Reynolds number | [-] |
| RH | Relative humidity | [%RH] |
| RH_h | Absolute humidity | [kg/kg] |
| R_l | Irradiance | [W/m ²] |
| R_R | Reflected radiation flux | [W/m ²] |
| R_T | Total/net radiation flux | [W/m ²] |
| r | Thermal resistance | [m ² K/W] |

| | | |
|------------|--|--|
| r_T | Total thermal resistance | [m ² K/W] |
| r_n | Thermal resistance of n th material | [m ² K/W] |
| T_c | Ceiling (roof plate back) temperature | [°C] |
| T_i | Model house interior cavity temperature | [°C] |
| T_s | Outermost surface temperature | [°C] |
| T_∞ | Ambient temperature | [°C] |
| t | Measuring interval | [s] |
| U | Local wind velocity | [m/s] |
| U_{ave} | Average wind velocity | [m/s] |
| u | Conduction heat transfer coefficient | [W/m ² K] |
| ν | Kinematic viscosity of fluid | (=1.38 x10 ⁻⁵) [m ² /s] |
| ΔT | Temperature difference | [°C] |
| α | Albedo | (= R_R/R_I) [-] |
| β | Coefficient of expansion of fluid | (=3.4 x10 ⁻³) [1/K] |
| θ | Temperature ratio | (= $(T_s - T_i)/(T_i - T_\infty)$) [-] |
| φ | Irradiance angle | [°] |

Subscripts

| | |
|-------------------|--|
| <i>air</i> | Fluid, air |
| <i>C</i> | Control roof without green panel |
| <i>c</i> | Ceiling of model house (back of roof plate) |
| <i>conduction</i> | Refers to conduction heat transferred from the subjected surface |
| <i>convection</i> | Refers to convection heat transferred from the subjected surface |
| <i>G</i> | Grass, 25[mm] thickness, with soil layer, 5[mm] thickness |
| <i>gr</i> | Refers to reading near ground surface |
| <i>I</i> | Incident radiation or irradiance |
| <i>i</i> | Refers to interior cavity of model house |
| <i>latent</i> | Refers to latent heat transferred from the subjected moist surface |
| <i>n</i> | Refers to n th number material |
| <i>R</i> | Refers to reflected heat from the subjected surface |
| <i>S3</i> | Sunagoke moss, 3[mm] thickness |
| <i>S30</i> | Sunagoke moss, 30[mm] thickness |
| <i>s</i> | Heat transfer surface |
| <i>T</i> | Total amount |
| ∞ | Ambient condition |

Chapter 1 - Introduction

1-1 Research Background

Urban heat island (UHI) is one of those environmental issues that need to be solved adequately in every scale of methods. UHI is a phenomenon where the air temperature in the urban area is relatively higher than that of the suburbs [1, 2]. For example, the air temperature isotherm line in Tokyo or Osaka focuses higher at the centre of the city and make up a heat island image. This phenomenon occurs in huge cities around the world regardless of the local climate nature. Studies about UHI have been widely performed and reported that the city air temperature was higher than the rural environment at approximately 2.5 °C [3, 4], while Niewolt [5] stated that compared to airport, city air temperature was warmer and drier by 3.5 °C. Another study conducted by Bowler et al. [6] found that the urban green park air temperature was near 1 °C cooler than the area without any plants. Furthermore, the temperature differences were in the range of 5-11 °C between the city and rural area as testified by Aniello et al. [7].

Urban areas which are hit by this problem will encounter health problems [8], increase demand on electricity for cooling [4], and high possibility of smog [9]. The outcomes of UHI are not preferable to mankind as it damages our body and the surrounding environment. Areas affected by the UHI encounter frequent tropical day and sultry night phenomena. Furthermore, the incident of heatstroke, heat exhaustion, heat syncope and heat cramps also have been reported [10].

As the UHI effects progress parallel with urban development, this phenomenon is hugely contributed by the following causes [1, 8, 11, 12, 13, 14]:

- i. Reduction of green region by urbanisation,
- ii. Modification on thermal properties in urban, i.e., usage of high thermal storage materials,
- iii. Lowered evaporative cooling and more energy converted to convection heat,
- iv. Multifaceted surface of cityscape and increased impervious cover,
- v. High usage of fossil fuels by vehicles and industries,
- vi. Circulation of heat in the city through prolonged practice of air-conditioner, and
- vii. Absorption of solar radiation from low albedo materials.

Knowing the seriousness of this problem, many mitigation measures have been conducted at the area affected by UHI. The methods focus on two main objectives; mitigating the heat absorbed by building and reducing the temperature loads inside the building. In order to mitigate the UHI effects, the method of roof spray cooling [15] and practising high albedo materials in urban construction [3, 16] have been encouraged. However, Akbari et al. [9] proposed that improving well-watered vegetation area in urban region will deliver fast, clean, and ecologically friendly measure towards UHI. The known merits of improving greenery in urban area also involve increasing albedo and interception of solar radiation, providing shading effect, promoting evapotranspiration and reducing convection heat by consuming latent heat, absorbing carbon dioxide and releasing oxygen, elevating aesthetical value, preventing urban flooding by increasing water retention, and also providing habitats for animals [1, 9, 14, 17, 18, 19, 20, 21, 22, 23] [24, 25, 26, 27, 28, 29, 30].

Nevertheless, city area is packed with buildings, concrete, and asphalt, thus, making the effort of planting new plants to be a real challenge. Consequently, the variation of greening methods can be classified to green wall, green rooftop and green roof, to match the application location. Although greening method has attracted a huge attention as a good mitigation measure, the degree of the effectiveness of greening method due to the different type of plants, application methods and thermal effect evaluation are still uncertain. Therefore, this research will focus on evaluating the effectiveness of green roof, especially with the use of Sunagoke moss in the method that can be applied on existing roofs in order to mitigate the UHI effects.

1-2 Green Roof Characteristics

Green roof is likely to be an ideal technique to increase the green region in urban area, as it is a method which the unused part of the roof of buildings or houses is utilized to plant trees or plants. It is an effective method to increase green region in the concrete forest to create a new model of buildings to make use of the effectiveness of plants in heat insulation. Green roof is also performed in various regions to improve the scenery aspect together with technology purposes. The application of green roof was investigated and proven to provide benefits in Malaysia [2], Greece [18], Spain [27], the United States [19, 31], Lebanon [32], Sweden [33], and Japan [34] regardless of the climatic condition.

By implementing the green roof, we can suppress the amount of heat received by sun by improving the heat insulation performance and at the same time reducing the interior

temperature of the building. This may result in the reduction of air-conditioner usage and load, thus reducing the anthropogenic heat. Furthermore, as the plants performing photosynthesis and evapotranspiring the rain water, the plants are responsible for promoting the relaxation of the surrounding air temperature by releasing oxygen and absorb carbon dioxide. The selection of plant types depends on the range and the layout of the green roof, maintenance cost, and initial construction plans.

The typical green roof's construction involves four layers; drainage materials, filter to prevent loss of soil particles, soil substrates, and vegetation layer [30]. However, generally, green roof can be classified to intensive and extensive types. The intensive green roof covers wide range of plants selection of lawn and trees, and required special construction method to support the weight of the green roof as shown in Fig. 1-1. Intensive green roof normally weight around 180-500 kg/m² depends on the layout. On the other hand, the extensive green roof shown in Fig. 1-2 represents a modern modification of the concepts with simpler, lighter, and shallower soil and low-growing ground cover usually uses moss-sedum or grasses types of plants. In contrast to the intensive green roof, the extensive green roof do not require any reinforcement to support the green roof model as they weight about 60-150kg/m² and this helps to reduce the initial cost. As it is easier to be maintained, the extensive green roof has been preferred in most of the application nowadays. The Table 1-1 summarized the typical aspects of intensive and extensive green roof [24, 29, 30, 32].



Fig. 1-1. Example of intensive green roof implementation.



Fig. 1-2. Example of extensive green roof implementation.

Table 1-1. Comparison between intensive and extensive green roof.

| Aspects | Intensive Green Roof | Extensive Green Roof |
|-----------------------------|--|---|
| Maintenance frequency | High | Low |
| Irrigation | Regularly | Irregularly |
| Plant communities | Lawn or Perennials, Flower, Shrubs and Trees | Moss, Sedum, Herbs and Grasses |
| System build-up height [mm] | 150-1000 | 10-200 |
| Weight [kg/m ²] | 180-500 | 60-150 |
| Installation costs | High | Low |
| Usage | Park like garden | Vegetation panel or ecological protection layer |

Figuring that the extensive green roof system is more preferable and can be implemented on the existing roof type, this dissertation will discuss more on the study about extensive green roof system. Since the extensive green roof is easier and simpler to be applied, the author expect the extensive green roof technology will illustrate an excellent prospect in future.

1-3 Previous Researches

Since the roofs are exposed to extreme temperature changes, high solar radiation intensities, irregular rain events and atmosphere, these environments are very severe to plants [35]. Therefore, the selection of the green roof plant candidates is a crucial criterion to determine the initial and maintenance costs, longevity, energy saving, and thermal performance of the system. Among the most well-known plants normally used in extensive green roofs are sedum and grass types [22, 23, 27, 30, 33, 36, 37, 38, 39, 40]. Other researches also utilised flowers, herbaceous perennials, and other types of plants [26, 32, 33, 36, 41]. Starting over a decade ago, mosses have been selected as a research green roof option as they are believed to have high water holding capacities of 8-10 times of their weight compared to only 1.3 times for other typical green roof mediums [34, 40, 42, 43]. Moss is a non-vascular plant that can survive drought by drying out and going dormant [44].

Moreover, a type of moss identified as Sunagoke moss (*Racomitrium Canescens*) (Fig. 1-3) was found to be the only truly draught tolerant species when tested [31]. This judgment was supported by Anderson et al. [43], as they mentioned that Sunagoke is an acrocarp that

grows in tight colonies with upright shoots and is likely to be able to hold more interstitial water than other life forms in their report. The authors also highlighted the ability of green roofs planted solely with Sunagoke that had 12-24% higher stormwater retention than vascular or medium only candidates. Moreover, cooling under Sunagoke surface was nearly 6 times faster than the only medium candidate. This study showed the capability of Sunagoke in improving temperature fluctuations on the application of the system.

Sunagoke moss is viable in locations where the presence of small amount of water such as rain and dew, and light. Sunagoke moss as well resistant to drying and can withstand high ambient temperature without wilt. Besides, Sunagoke moss prefer the inorganic substrate which do not require soil to grow and this make the weight reduction in green roof became easier. Practically, light weight green roof system is acknowledged since it can contribute to reducing the initial cost as it is not necessary to carry out reinforcement in the existing building to support the plants' foundation weight. From the maintenance point of view, Sunagoke moss can be said as a maintenance-free plant because it grows only with natural water (rain or dew), thus frequent watering is unnecessary and the running cost can be saved, therefore, making Sunagoke a worthy prospect for green roof candidate [42].

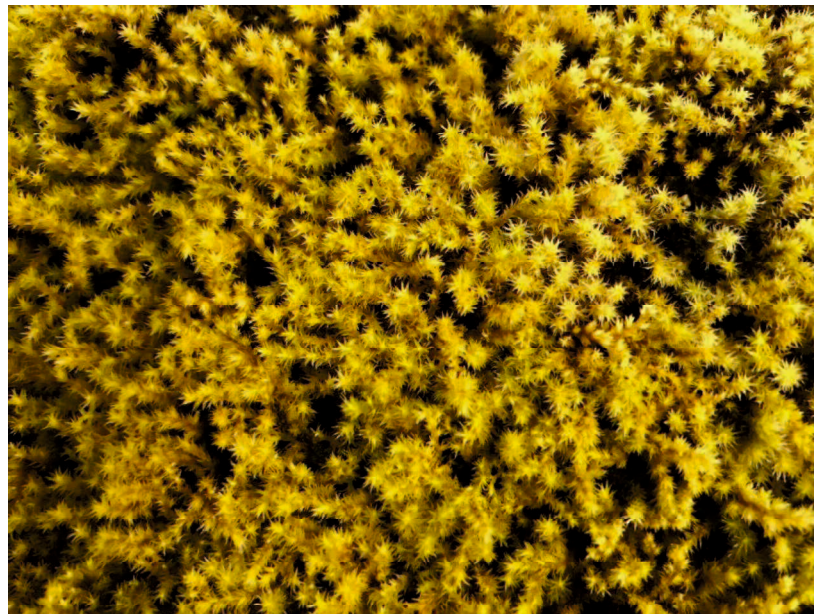


Fig. 1-3. Sunagoke moss (*Racomitrium Canescens*).

From thermal property aspects, compared with sedum and grass which regularly used in green roof application, Sunagoke moss shows better features as represented in Table 1-2. Although Sedum and Grass candidates presents higher thermal resistance, both candidates make use of soil and need appropriate maintenance. Contrarily, Sunagoke moss does not require any substrate, therefore deep investigations have to be made to clarify the effectiveness of Sunagoke moss in suppressing thermal load.

Table 1-2. Characteristics comparison between Sunagoke, Sedum and Grass.

| Aspects | Sunagoke* | Sedum* | Grass* |
|--|-----------------------------------|--|--|
| Weight [kg/m ²] | ~10 | 30~60 | ~300 |
| Thermal Conductivity, k [W/mK] | 0.014 | 0.011 | 0.007 |
| Thermal Resistance, r [m ² K/W] | 2.21 | 3.13 | 4.35 |
| Maintenance | Maintenance-free | Fertilization once a year | Lawn 3-5 times a year, fertilization 6 times a year |
| Construction | Can be installed on existing roof | Can be installed on most existing roof | Require waterproof sheet, soil and reinforcement on roof |

*Data presented based on thickness of Sunagoke 30mm, Sedum 25mm (+soil 10mm), Grass 25mm (+soil 5mm), retrieved from Taufik [45].

Sunagoke moss (*Racomitrium Canescens*) has attracted a lot of attention as a decent option for a green roof especially in Japan [13, 14, 34, 46]. An interesting research made by Suzuki et al. [34] presented the cooling performance of Sunagoke green roof compared to artificial turf and conventional roof. The study described that, on a rainy day, the Sunagoke surface temperatures were 2 °C and 4 °C cooler than that of the artificial turf and conventional roof, respectively. During a clear day (after a rainy day), the Sunagoke surface temperatures were recorded as 17 °C and 4 °C cooler than the artificial turf and conventional roof, correspondingly. The study clearly showed that the slabs that were covered with Sunagoke had elongated periods of effective cooling.

As shown above, most studies examined the effects of applying green roof by conducting the experiments outdoor [18, 32, 39, 41, 43] and by means of simulations [39, 47, 48]. However, the actual outdoor environmental parameters affecting the thermal performance

of a green roof are very complicated as they change through time. The parameters that co-exist involving the ambient temperature and humidity, solar radiation, surrounding radiation, wind velocity, and thermal properties of the green roof system, are making the previous and current evaluations difficult to be analysed. Thus, it is crucial to quantitatively examine the effect of each parameter to study how they affect the heat transfer process of the system. Due to the difficulties discussed above, the objective of this research is to deliver the evaluations on thermal performance of Sunagoke green roof by doing a pilot experiment in an enclosed laboratory environment. The evaluation will be focusing on heat balance, albedo, Bowen ratio, and the interior temperature of the examined model house when Sunagoke green panel was installed. Plus, since there are very few studies that report the performance of Sunagoke moss, this dissertation will also provide a novel data for the future research.

Along the research conducted by Applied Thermal Engineering Laboratory Yamaguchi University, Okamoto [49] had prepared two model houses evaluated the thermal insulation effect of Sunagoke green roof by installing Sunagoke on the roof part of a model house. The thermal insulation effect evaluation has been achieved by examining the conduction heat passes through the roof part of the model houses. In the evaluation of the penetrating conduction heat, Komizo [50] had investigated the calculation for thermal conductivity of model house. He conducted the experiments by the non-stationary method to enable the calculation of the values in a water-containing state. Next, Ishida [51] utilized two model houses and installed the Sunagoke-pre-attached green panel on both of them. One model house was left dried while the other one was applied with water and experiments were conducted to obtain the interior temperature and conduction heat data in order to evaluate the thermal insulation effect the evaporation effect in his graduation thesis.

Thus far most of the experiments were conducted at the actual outdoor environment. However the outdoor influencing parameters were too complicated and affect the evaluation results, Ishida [51] had proposed to evaluate the effect of green roof with a laboratory-adjustable measuring environment. In his completion thesis, he investigated the effect of irradiance magnitude, ambient temperature and humidity on green panel against the suppression of conduction heat and convection heat. As a continuity, this dissertation focuses on other parameters such as irradiance strength, irradiance angle, presence of evaporation, and wind velocity.

1-4 Research Objectives

The usage of Sunagoke moss in green roof application especially in Japan is increasing, however, there are many unknown features that need to be clarified. Therefore, the main objective of this research is to quantitatively evaluate the thermal engineering effects of the Sunagoke moss green roof system. The experiments were conducted by utilizing the green panel pre-attached model houses to simulate buildings. As the thermal engineering effects of green roof are divided into the thermal insulation effect and evaporation effect, each effect was evaluated by both outdoor and laboratory experiments, but explored more in detail in laboratory experiments.

The laboratory based indoor experiments were conducted in an Artificial Climate Chamber that capable of controlling most of the parameters in order to learn their influence individually. Parameters such as irradiance intensity, irradiance angle, water presence and wind velocity were tested chronologically.

The outdoor experiments focused on the evaluation of four different model houses in the outdoor environment parameter which consists of the total radiation, ambient temperature, humidity, wind velocity and cloud coverage. These parameters cannot be controlled and play a major role in deciding the evaluation. The results for outdoor experiments together with the relationship with indoor experimental results will be discussed in the chapter 7 of this dissertation.

This dissertation also proposed the evaluation method in order to thoroughly evaluate the thermal performance of a green roof system. Not only the temperature analysis, but also the entire heat balance, including evaporation latent heat occurred on the green roof. The outline of this dissertation is described as following contents:

Chapter 2 - Green Roof Implementation Method

Chapter 3 - Green Roof Thermal Performance Evaluation Method

Chapter 4 - Indoor Experiment: Effects of Convection Heat Transfer on Sunagoke Moss

Green Roof

Chapter 5 - Indoor Experiment: Effects of Irradiance Angle on Sunagoke Moss Green Roof

Chapter 6 - Outdoor Experiment and Relationship with Indoor Experiment

Chapter 7 - General Conclusion

Chapter 2 - Green Roof Implementation Method

2-1 Introduction to Green Roof Technique

In recent years, among the outdoor greening methods that have been introduced, green roof has attracted the most attraction. Green roof is a method to vegetate the roof of buildings such as residential, houses, factories and buildings with plants or trees. Nevertheless, the green roof application on the existing houses and buildings is difficult to be attempted due to the lack of durability of the roof to support the weight of green roof. Therefore, lightweight model of green roof is necessary to ease the construction process. In this study, the green roof was implemented by utilizing the green panels that can be installed easily on the existing typical roof. Furthermore, to make the evaluation easier, simple but homogenous model houses were used to simulate buildings or houses.

2-2 Green Panel

This experimental research carries out the green roof method by installing a green panel as illustrated in Fig. 2-1 on top of model house. The green panel is a thin removable metal plate which has been covered with vegetation on the surface, and provided with air layer on the back side. Since the green panel will always be exposed to outdoor environment, Galvalume steel was chosen as the material for the metal plate to withstand the rust or corrosion by rain water. On the back side of the Galvalume steel plate, a layer of Styrofoam; a fire plastic-base thermal insulator was attached to increase the heat suppression.

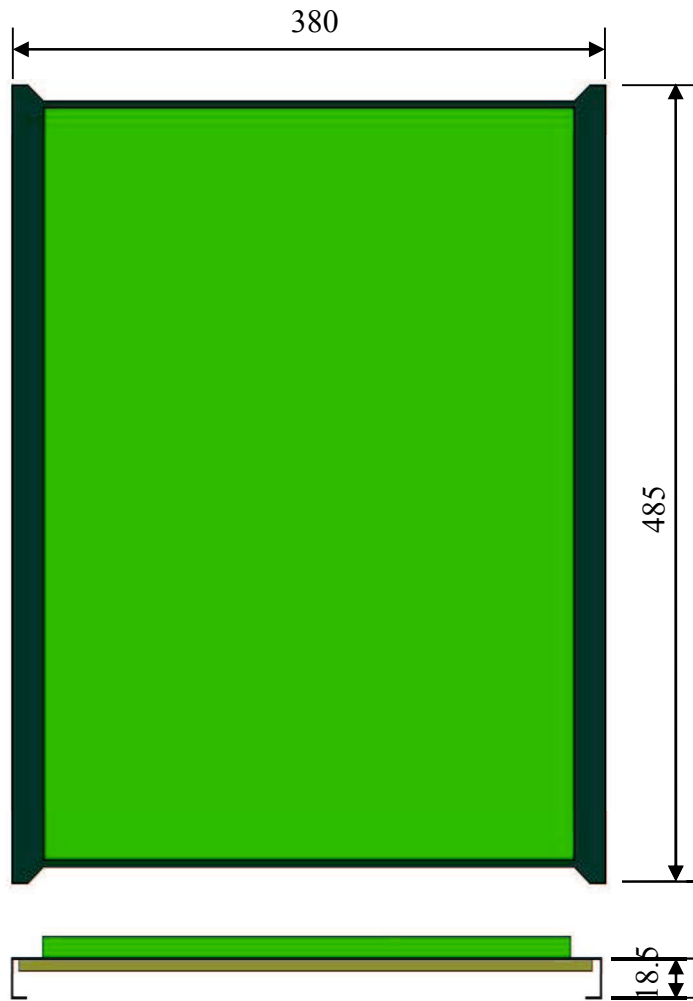
To evaluate the thermal performance of multiple green roofs, three types of green panels were prepared and the specifications are shown in Table 2-1. There were no substrate layers on both Sunagoke moss green panels (S3 and S30) since Sunagoke does not require them to cultivate. Only green panel S3 was attached by the urethane-base adhesive on the galvalume steel plate.

Table 2-1. Green panels specification.

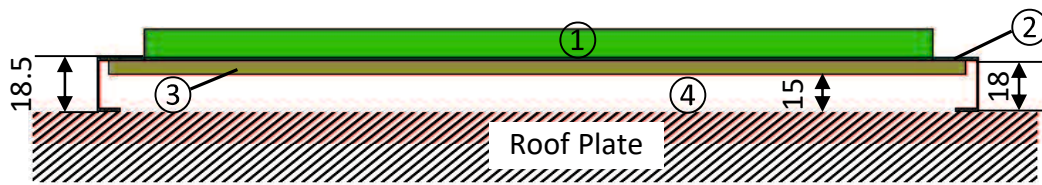
| Plant mat | Scientific name | Thickness [mm] | Growing medium | Surface Area [m ²] | *Area coverage [%] |
|---------------|------------------------------|--------------------|--------------------|--------------------------------|--------------------|
| Sunagoke, S3 | <i>Racomitrium canescens</i> | 3 (with adhesives) | - | 0.156 | 89 |
| Sunagoke, S30 | <i>Racomitrium canescens</i> | 30 | - | 0.161 | 84 |
| Grass, G | <i>Zoysia matrella</i> | 25 | 5 mm of soil layer | 0.152 | 98 |

*Area coverage was determined from image analysis.

An enlarged sectional view of the green panel is shown in Fig. 2-2. For the structure, when the green panel is in installed state, the materials thickness marked from above: Galvalume steel plate 3.5 [mm], Styrofoam 3.0 [mm], and air layer (cavity area) 15.0 [mm]. Even though the plant mats are fixed on the Galvalume steel plate, the thickness varies on each measuring point. Thus the average value for the plant thickness was taken.



Above: Top view, Below: Side view
Fig. 2-1. Green panel schematic drawing.



- ① Plant mat, and substrate layer if any
- ③ Styrofoam
- ② Galvalume steel plate
- ④ Air layer

Fig. 2-2. Enlarged cross-sectional side view of green panel.

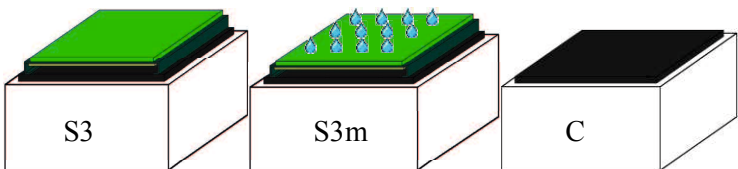
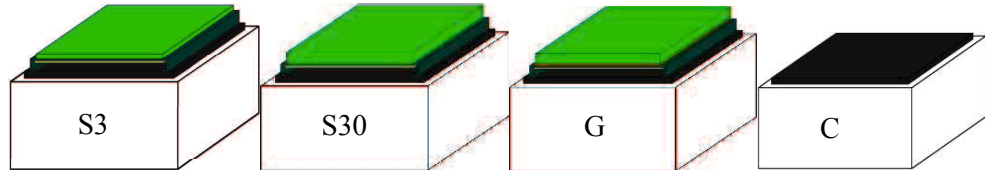
2-3 Model House

In consideration to carry out comparison experiments to evaluate the thermal insulation and evaporation effect of green panel, four homogeneous model houses were prepared according to objectives in laboratory and outdoor experiments. To create an enclosed space, the material for model houses was chosen to be a house-shaped polystyrene foam with thermal conductivity of 0.035 [W/mK]. Fig. 2-3 shows the appearance of model house in green panel-installed-state.

As illustrated in Fig. 2-4, the outer dimensions of model house are length 575 [mm] × width 455 [mm] × height 260 [mm]. Meanwhile, the interior cavity dimensions measured are length 475 [mm] × width 355 [mm] × height 210 [mm] which makes the interior air cavity volume of 0.035 [m³]. Besides, the roof plate of the model house was made from 20 [mm] thickness of polystyrene foam. To make sure the absorption and reducing the reflection of the irradiance flux, the roof plate was painted with black water-base coating. Additionally, to ensure only the influence from the roof part is evaluated during experiments, the outer parts of the model house have been covered with a white Styrofoam of 30 [mm] thickness and 0.031 [W/mK] of thermal conductivity.

Besides, a model house named C was used as the control house; i.e., a representative of a conventional dry untreated roof. Table 2-2 summarizes the classification of model houses used in laboratory and outdoor experiments. Only in laboratory experiment, the evaporation characteristics of green panel S3 were investigated. Thus, the condition where the S3 was thoroughly sprayed with 100 [ml] of water was labelled as “S3m”, where the letter “m” indicates the “moist” condition.

Table 2-2. Model houses classification.

| Experiment | Model House |
|------------|--|
| Indoor |  |
| Outdoor |  |

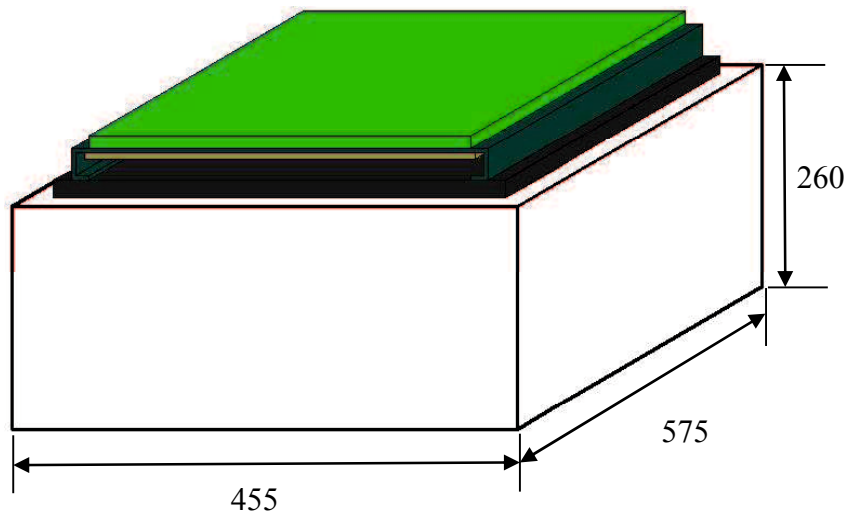
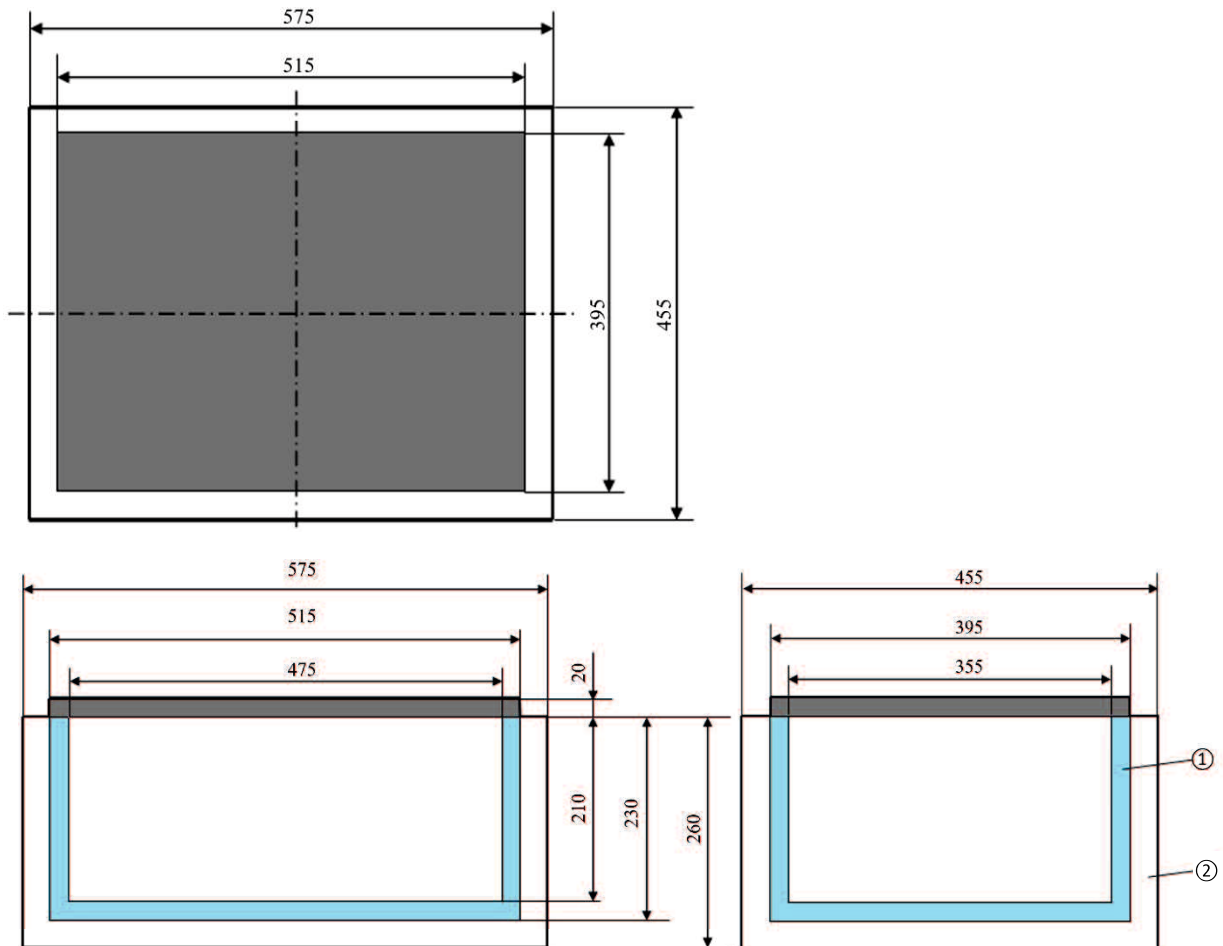


Fig. 2-3. Appearance of model house in green panel-installed-state.



① Polystyrene foam ② Styrofoam

Fig. 2-4. Model house dimensions. All measurements are in millimetre unit.

Chapter 3 - Green Roof Thermal Performance

Evaluation Method

3-1 Introduction to Evaluation Method

This study focuses on two approaches of experiment methods; the indoor laboratory-based experiments and outdoor experiments. The two experiments differ on the environment aspects. The environment of outdoor experiments is the actual environment where the green roof is applied. Meanwhile, the indoor experiments were carried out in an Artificial Climate Chamber (ACC) which the environment was made by some extent similar to the outdoor environment. These two approaches of experiment methods are taken as the evaluation subjects. Furthermore, the evaluation process will view the two effects of green roof; the thermal insulation effect and the evaporation effect.

3-1-1 Thermal Insulation Effect

The thermal insulation effect evaluation focuses on the comparison of conduction heat of each model houses in the experiments. The conduction heat represents numerically by the amount of heat passing through a certain system. In this research, the subjected conduction heat refers to the heat passing through the green panel and roof part of model houses. The roof parts in both experiments have similar sizes but the installation of green panel is different. As the result of changes of roof part attributes, the conduction heat will affect the interior side of model houses thus the changes of model houses' interior temperature evaluation is also appropriate to be carried out. Moreover, the insulation effect is the passive ability of green roof to reduce heat absorption from exterior radiations. The better the thermal insulation effect of a green roof, the better cooling energy savings!

3-1-2 Evaporation Cooling Effect

Indoor experiments will utilise the moist Sunagoke moss green panel (S3m) which made by optionally applying water on the green panel. As the S3m contains water, the cooling effect by the latent heat transport will occur. This effect is namely as the evaporation cooling

effect of Sunagoke. Since the evaporation word came from the evaporation and transpiration, the evaporation effect evaluation will contain both processes in parallel. The heat balance equation which applied will also considered the latent heat transportation expression. As a result of latent heat transport, the changes of conduction and convection heat will also be taken into the evaluation. In addition, the evaporation efficiency will be calculated to observe the evaporation characteristics.

3-2 Temperature Analysis

3-2-1 Temperature Measuring Method

In order to make assessment on the thermal performance of the model houses, the temperature measurement on each point of model houses has to be validated. As illustrated in Fig. 3-1, the temperature measuring points are set at the positions of the red dots which are at the green panel surface, green panel soffit, roof plate surface, ceiling, and three points in model house interior cavity which made up total of seven points of temperature measuring points. The three temperature measuring points in the interior cavity of model house were fixed at each position of 1:4 of vertical interior height of model house. These three temperature measuring points are later processed as average value and hereafter stated as the model house interior temperature, T_i .

On each temperature measuring point, T-type thermocouples are installed as the temperature sensor. In the thermocouples installation process, since the green panel surface is covered with vegetation, the usage of cellophane tape is avoided because there is possibility that the evaporation and water absorption properties of Sunagoke will be affected. Alternatively, the thermocouples (wire diameter 300 μm) on the green panel's surface are fixed by adhesive. Therefore, for positions of green panel soffit, roof plate surface, and ceiling, the thermocouples (wire diameter 100 μm) were attached by cellophane tape. For the three thermocouples inside the model house, both sides wall of model house were penetrated to fix them. The drilled holes are then covered with silicone to maintain the enclosed space. All the installed thermocouples are connected to Datum-Y XL100 Data Logger to record the readings.

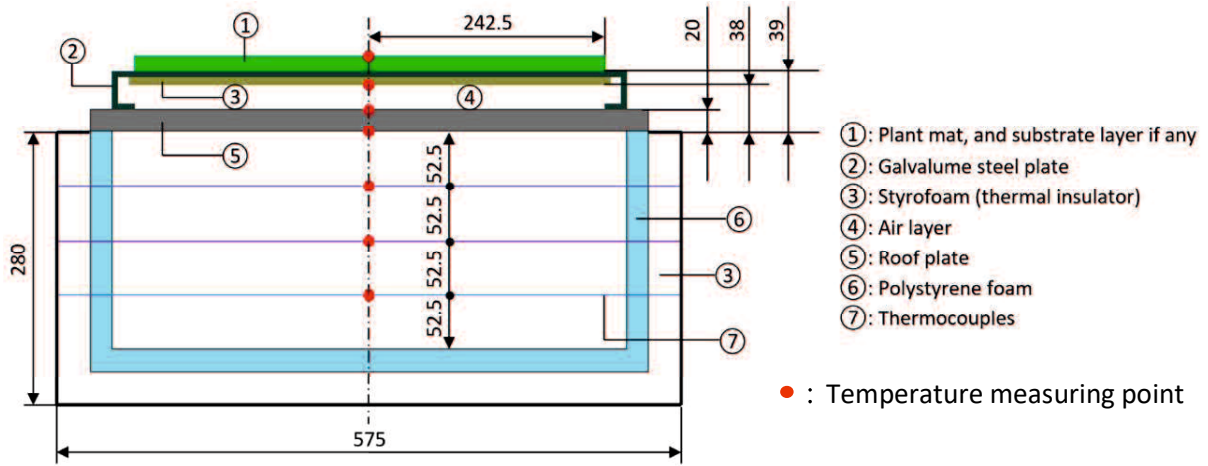


Fig. 3-1. Temperature measuring points in a model house.

3-2-2 Dimensionless Temperature

To further analyse the cooling characteristic that occurred in the model houses, a dimensionless temperature ratio was proposed to determine the normalised temperature difference. The temperature ratio was constructed by taking the differences in temperature between surface and interior temperatures, relative to differences in temperature between interior and ambient temperatures. High ratio in Eq. (3-1) specifies more influence from the roof surface condition, affecting the rise of interior temperature. On the other hand, low ratio meant there was more heat transferred to the atmosphere and less heat penetration into the interior cavity.

$$\theta = \frac{T_s - T_i}{T_i - T_\infty} \quad (3 - 1)$$

3-3 Heat Energy Balance in Model House

In mitigating urban heat island (UHI), the extent of heat transported by implementing each mitigation method has to be clearly clarified. Correspond to this necessity, in order to evaluate the green roof effects, the heat transport occurred by implementing green roof were calculated via the heat balance equation. Theoretically, in order to derive the heat balance around green panel and roof plate of a model house, the total radiation R_T [W/m^2] received by a subject surface will be taken equal to the sum of convection heat $Q_{convection}$ [W/m^2], latent heat of evaporation Q_{latent} [W/m^2], and conduction heat $Q_{conduction}$ [W/m^2] as represented in Eq. (3-2) and Fig. 3-2 [18, 26, 52]. In Tabares-Valesco et al. [52] model, there are other fractions of

heat such as thermal and metabolic storage. However, both fractions only made up about 1-2% of the whole heat balance, thus neglected in Eq. (3-2).

$$R_T = Q_{conduction} + Q_{latent} + Q_{convection} \quad (3-2)$$

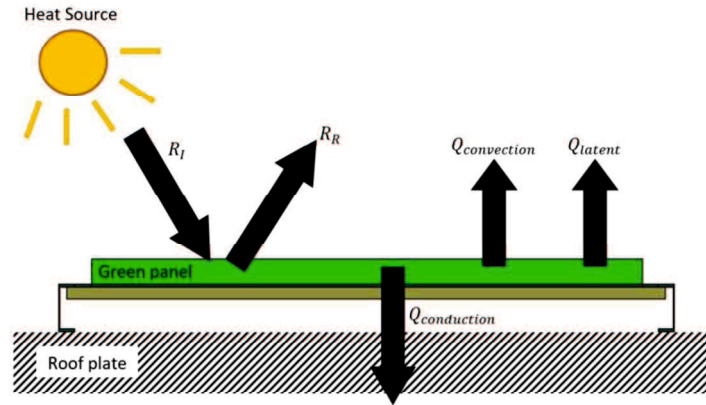


Fig. 3-2. Heat balance model at roof section.

3-3-1 Total Radiation Received by a Subject Surface

The total radiation R_T [W/m^2] received by a subject surface is a summary of the solar radiation, reflected radiation, atmosphere radiation from moisture and etc., and radiation emitted to atmosphere by subject surface. The strength of total radiation is affected by the position of subject surface position on longitude and latitude, weather and time. Therefore, the total radiation R_T can also be derived by subtracting the irradiance R_I irradiated by the heat source, with the reflected radiation R_R as shown in Eq. (3-3). During the experiments, the irradiance and reflected radiation were measured by MS-402 pyranometer and LP-PYRA-06 albedometer, respectively, and fitted with Eq. (3-4) which calculates the output voltage E_i [mV] of both devices. For reference, the sensitivity constant c of pyranometer and downward albedometer used in this study was 6.99 and 15.55 [mV/kWm^2], respectively. Meanwhile, both devices are able to measure energy spectral in wavelength range of 285-2800 [nm] and 305-2800 [nm], individually. Consecutively, the albedo of each model house surface was determined from Eq. (3-5).

$$R_T = R_I - R_R \quad (3-3)$$

$$R_I \text{ or } R_R = \frac{E_i}{c} \quad (3-4)$$

$$\alpha = \frac{R_R}{R_I} \quad (3-5)$$

3-3-2 Conduction Heat Flux

Conduction heat formed as a result of the total radiation received passes through the subject surface. The conduction heat is hugely related to the building's thermal load. The increment of conduction heat will result in the increase of building's interior temperature. As the consequence, people tend to use the air-conditioner to reduce the interior temperature but at the same time releasing the anthropogenic heat outside. The conduction heat may changes depend on the building's surface temperature, interior temperature, and thermal resistance.

In this study, the author evaluate the thermal insulation effect of green panel by comparing the conduction heat passes through each model house. This calculation method considered the inflow and outflow of heat from the roof part as one-dimensional from the roof cross-sectional direction. Firstly, the total thermal resistance from each material constituting the roof part have to be determined. The thermal resistance is representing the hardness of heat passing through a material, and the reciprocal of thermal resistance represents the overall conduction heat transfer coefficient u [W/m²K]. The thermal resistance r_n [m²K/W] of each material can be calculated by using Eq. (3-6) marking the material thickness L_n [mm] and thermal conductivity k_n [W/mK].

$$r_n = \frac{L_n}{k_n} \quad (3 - 6)$$

The value of thermal resistance and thermal conductivity of each material is tabled in Table 3-1. The thermal conductivity of each material in green panel was calculated by Komizo [50] and Taufik [45] in advance. The thermal conductivity values calculated by Komizo and Taufik were based on the changes in the moisture content from the green panel. However, in this dissertation, the conduction heat flux calculation was conducted by assuming that the thermal conductivity is constant even though the green panel is in sufficient moist state.

Table 3-1. Physical and thermal properties of materials on roof section.

| Material | Thickness, L_n [m] | Thermal conductivity, k_n [W/mK] | Thermal resistance, r_n [m ² K/W] | | | |
|---|-------------------------|--|--|-----------------------|-----------------------|-----------------------|
| | | | S3 | S30 | G | C |
| Plant mat (Sunagoke + adhesive) | 3.5×10^{-3} | 1.13 | 3.1×10^{-2} | - | - | - |
| Plant mat (Sunagoke) | 3×10^{-2} | 1.4×10^{-2} | - | 2.21 | - | - |
| Plant mat (Grass + soil) | 3×10^{-2} | 6.9×10^{-3} | - | - | 4.35 | - |
| Galvalume steel plate | 5×10^{-3} | 44 | 1.14×10^{-5} | 1.14×10^{-5} | 1.14×10^{-5} | - |
| Styrofoam | 3×10^{-3} | 3.1×10^{-2} | 9.7×10^{-2} | 9.7×10^{-2} | 9.7×10^{-2} | - |
| Air layer | 15×10^{-3} | 2.4×10^{-2} | 6.22×10^{-1} | 6.22×10^{-1} | 6.22×10^{-1} | - |
| Polystyrene foam | 20×10^{-3} | 3.5×10^{-2} | 5.71×10^{-1} | 5.71×10^{-1} | 5.71×10^{-1} | 5.71×10^{-1} |
| Total thermal resistance, r_T (m ² K/W) | - | - | 1.321 | 3.504 | 5.638 | 0.571 |

Therefore, the calculated thermal resistance r_n can be substituted in Eq. (3-7) to determine the total thermal resistance r_T for every type of model houses.

$$r_T = r_1 + r_2 + \dots + r_n = \sum_n r_n \quad (3-7)$$

Next, the established total thermal resistance r_T [m²K/W] and the measured temperature difference ΔT [°C] on the surface and back of roof parts are substituted in Eq. (3-8) to obtain the conduction heat $Q_{conduction}$ [W/m²] passing through the roof part [53]. Eq. (3-8) was derived from Fourier equation which generally used when the temperature changes do not depend on time. The evaluation in laboratory experiment was conducted in equilibrium state where the temperature changes did not affected by time. However in outdoor experiment, the amount of heat transferred to model houses dependent on the environment conditions and changes with time thus the evaluation were conducted in a non-steady state. Nevertheless, during the both experiments, the results are recorded within 1 minute interval and applied Eq. (3-8) by regarding the quasi-steady state where no temperature changes within the 1 minute. Note that the flow of heat was defined as the inflow of heat which is the amount of heat entering the room through the roof, while the outflow of heat is the amount of heat emanating from the room to the roof.

$$Q_{conduction} = \frac{\Delta T}{r_T} \quad (3-8)$$

The temperature difference ΔT [$^{\circ}\text{C}$] can be calculated by Eq. (3-9). Note that for model house C, the value for T_s [$^{\circ}\text{C}$] refers to the temperature of roof surface, while for S3, S3m, S30, and G, the T_s [$^{\circ}\text{C}$] refers to the temperature of green panel surface. On the other hand, T_c [$^{\circ}\text{C}$] refers to the ceiling temperature; the back side of roof plate for every model houses.

$$\Delta T = T_s - T_c \quad (3 - 9)$$

In addition, in order to find out the contribution of conduction heat in the heat balance, the conduction heat flux proportion q_{cond} of a model house is determined from Eq. (3-10).

$$q_{cond} = \frac{Q_{conduction}}{R_n} \quad (3 - 10)$$

3-3-3 Latent Heat Flux

Latent heat flux Q_{latent} [W/m^2] denotes the amount of heat collected by water moisture when the watered surface received total radiation flux R_T [W/m^2]. As the evaporation hypothetically provides an extra cooling aid to the model house, this paper will also investigate the effects of evaporation on the Sunagoke moss green panel. By measuring the real-time water content by EK-6100i electronic balance, the latent heat flux of evaporation Q_{latent} can be calculated from Eq. (3-11), while the latent heat proportion q_{latent} was derived in Eq. (3-12). The latent heat coefficient of water l was assumed 2257 [kJ/kg] for model house S3m in all laboratory experimental conditions. Note that in this report, the latent heat was not considered in the heat balance equation (Eq. (3-2)) at the beginning of the experiment since the Sunagoke moss green panel was assumed to be in a naturally dried condition. The latent heat was only considered during the active evaporation period. Evaporation is literally the combination of evaporation and transpiration process by plant, nevertheless in this paper the amount of water used in both processes cannot be analysed separately, thus, the latent heat calculated was assumed to consist of both processes simultaneously. As a remark, latent heat flux only exist on a moist surface which undergone evaporation process, therefore, the calculation of latent heat was only performed on model house S3m in laboratory experiments.

$$Q_{latent} = \frac{l \cdot e}{t \cdot A_s} \quad (3 - 11)$$

$$q_{latent} = \frac{Q_{latent}}{R_T} \quad (3 - 12)$$

3-3-4 Convection Heat Flux

The convection heat $Q_{convection}$ [W/m²] refers to the amount of heat exchanged between the subject surface that received total radiation, and ambient air. The convection heat is also considered as the heat energy transferred by both natural and forced convection reactions. The rise of convection heat lead to higher amount of heat transferred from subject surface to the ambient air. Thus, bigger convection heat flux will lead to a better thermal comfort on the building. The convection heat is hugely affected by subject surface temperature, ambient temperature, total radiation flux and wind velocity. From the heat balance equation Eq. (3-2), convection heat flux is calculated by taking the revenue minus of each heat transport quantity from total radiation as shown by Eq. (3-13). Also, the conduction heat flux proportion q_{cond} of a model house is represented in Eq. (3-14).

$$Q_{convection} = R_T - Q_{conduction} - Q_{latent} \quad (3 - 13)$$

$$q_{conv} = \frac{Q_{convection}}{R_T} \quad (3 - 14)$$

Meanwhile, the Bowen ratio, B [-] as in Eq. (3-15) was determined to compare the different processes of surface cooling that occurred especially on the moist S3m green panel. Since the ratio was constructed as the proportion of convection heat to latent heat, the association between these two heat fluxes can be characterised. If the ratio is lower than 1, a larger proportion of the energy on the green panel surface will be delivered to the atmosphere as latent heat instead of convection heat, and vice versa.

$$B = \frac{Q_{convection}}{Q_{latent}} \quad (3 - 15)$$

3-4 Evaporation Efficiency of Moist Green Panel

Through evaporation effect evaluation, the evaporation efficiency of Sunagoke on green panel is verified to indicate the evaporation characteristics. The evaporation efficiency is calculated by each heat transport values. By using the cooling law of Eq. (3-16), the convection heat transfer coefficient, h [W/m²K] of ambient air can be found by substituting convection heat flux $Q_{convection}$ [W/m²], outermost surface temperature T_s [°C], and ambient temperature T_∞ [°C].

$$h = \frac{Q_{convection}}{(T_s - T_\infty)} \quad (3 - 16)$$

Next, as shown in Eq. (3-17), the mass heat transfer rate k_x can be calculated by substituting the calculated heat transfer rate h , Lewis number Le and specific heat of air c_p . Mass heat transfer rate refers to the movement of water amount per unit time. Lewis number represents the ratio of heat transfer by thermal diffusion, and mass transfer by mass diffusion. In this thesis, Lewis number of 0.83 was applied.

$$k_x = \frac{h}{(c_p - Le)} \quad (3 - 17)$$

From the ratio of evaporation amount e and the product of calculated mass heat transfer rate k_x and the difference of saturated humidity of roof surface and ambient humidity, the evaporation efficiency can be calculated as shown in Eq. (3-18). Here, RH_{hs} indicates the absolute humidity of surface temperature, while RH_{hgr} indicates the absolute humidity around ground surface. In the calculation for RH_{hs} , the relative humidity of surface vicinity are taken as the surface are in wet state, the relative humidity are assumed to be 80%.

$$n = \frac{e}{k_x \times (RH_{hs} - RH_{hgr})} \quad (3 - 18)$$

The calculation for water vapour partial pressure is done by substituting the ambient temperature and humidity that are measured during experiments, and Eq. (3-19) to (3-22). Note that RH is relative humidity, P_∞ is saturated water vapour partial pressure with respect to the outside temperature, and T_∞ is the outside ambient temperature. For the ground surface pressure, the author used the weather data from Japan Meteorological Agency. RH_{hgr} is the absolute humidity of ground surface vicinity calculated by using the ambient temperature and humidity measured from 1.2 m above the surface that received total radiation.

$$RH_{hgr} = 0.622 \times \frac{P_l}{(P_\infty - P_l)} \quad (3 - 19)$$

$$P_l = RH \times P_\infty \quad (3 - 20)$$

$$P_\infty = 6.11 \times 10^{T_r} \quad (3 - 21)$$

$$T_r = \frac{7.5T_\infty}{T_\infty + 273.15} \quad (3 - 22)$$

3-5 Ratio of Grashof Number and Square of Reynolds Number

The ratio of the Grashof number and the square of Reynolds, Ar number was determined to observe the wind flow characteristic generated by the blower fan or the natural wind. The Grashof number itself is explained in Eq. (3-23) where it is a nondimensional parameter usually used to define the heat and mass transfer due to convection on a solid surface. Another parameter to express wind characteristics is by referring to its Reynolds number as defined in Eq. (3-24). The wind velocity term reflects to average velocity in indoor experiment, but local velocity in the case of outdoor experiment. By finding the ratio of the Grashof number and the square of Reynolds number as in Eq. (3-25), the natural and forced convection can be clearly classified. Value of Ar less than 0.1 specifies the forced convection dominating the heat transfer, and contrarily, the natural convection will dominate when the value is bigger than 10. When the ratio is between 0.1 and 10, the combination of forced and natural convection need to be considered [54, 55]. In the notations, g denotes acceleration due to Earth's gravity, β coefficient of thermal expansion of fluid, T_s surface temperature, T_∞ ambient temperature, L heat transfer surface length, ν kinematic viscosity, and U_{ave} average velocity.

$$Gr = \frac{g\beta(T_s - T_\infty)L^3}{\nu^2} \quad (3 - 23)$$

$$Re = \frac{U_{ave} L}{\nu} \quad (3 - 24)$$

$$Ar = \frac{Gr}{Re^2} \quad (3 - 25)$$

Another parameter that can express the convection characteristics is the Nusselt number. Nusselt number is the ratio of convective to conductive heat transfer across the surface boundary. Nusselt number is represented by Eq. (3-26), where h is convection heat transfer coefficient calculated in Eq. (3-16), and k_{air} is the thermal conductivity of the fluid.

$$Nu = \frac{hL}{k_{air}} \quad (3 - 26)$$

Chapter 4 - Indoor Experiment: Effects of Convection Heat Transfer on Sunagoke Moss Green Roof

4-1 Experiment Introduction

Along with ambient temperature, humidity, irradiance strength, and irradiance angle, the outdoor environment also consists of wind velocity parameter. Wind velocity is another important influential parameter besides irradiance strength that affect the heat transfer characteristics on a building, in this case, the model house. In this chapter, the evaluation of the effects of wind velocity i.e., convection heat transfer on dry and moist Sunagoke moss green panel (S3 and S3m) together with control model house C will be piloted and discussed in detail. Moreover, the evaluation of the effect of convection heat transfer on green roof were conducted by configuring five levels of average wind velocity, U_{ave} (0, 1, 1.5, 2, and 3 m/s). The selection of wind velocity was referred to the average wind events during summer in Japan.

4-2 Experimental Methodology

Researches regarding green roofs have been conducted widely since a few years ago. However, the experiments were mostly conducted in an actual environment where a lot of uncontrollable parameters were affecting the evaluations of green roof performance. In order to quantitatively evaluate the performance of green roofs according to each parameter, the experiments were suggested to be performed in an enclosed environment by using the MC-402 Artificial Climate Chamber (ACC) at Yamaguchi Prefectural Industrial Technology Institute. Interior dimension of the ACC is 4500W × 3020D × 3020H. Fig. 4-1 demonstrated the interior walls location relation, while Fig. 4-2 illustrated the equipment setup in the ACC.

The effect of walls and floor have been investigated and clarified about 3 to 6% relative to total radiation, respective to irradiance. Since the experiment setup is located in the centre, and far from the walls, the effects of walls and floor have been neglected in the evaluation in this chapter. The details on the experiments to investigate the effect of wall have been discussed in the Appendix (I).

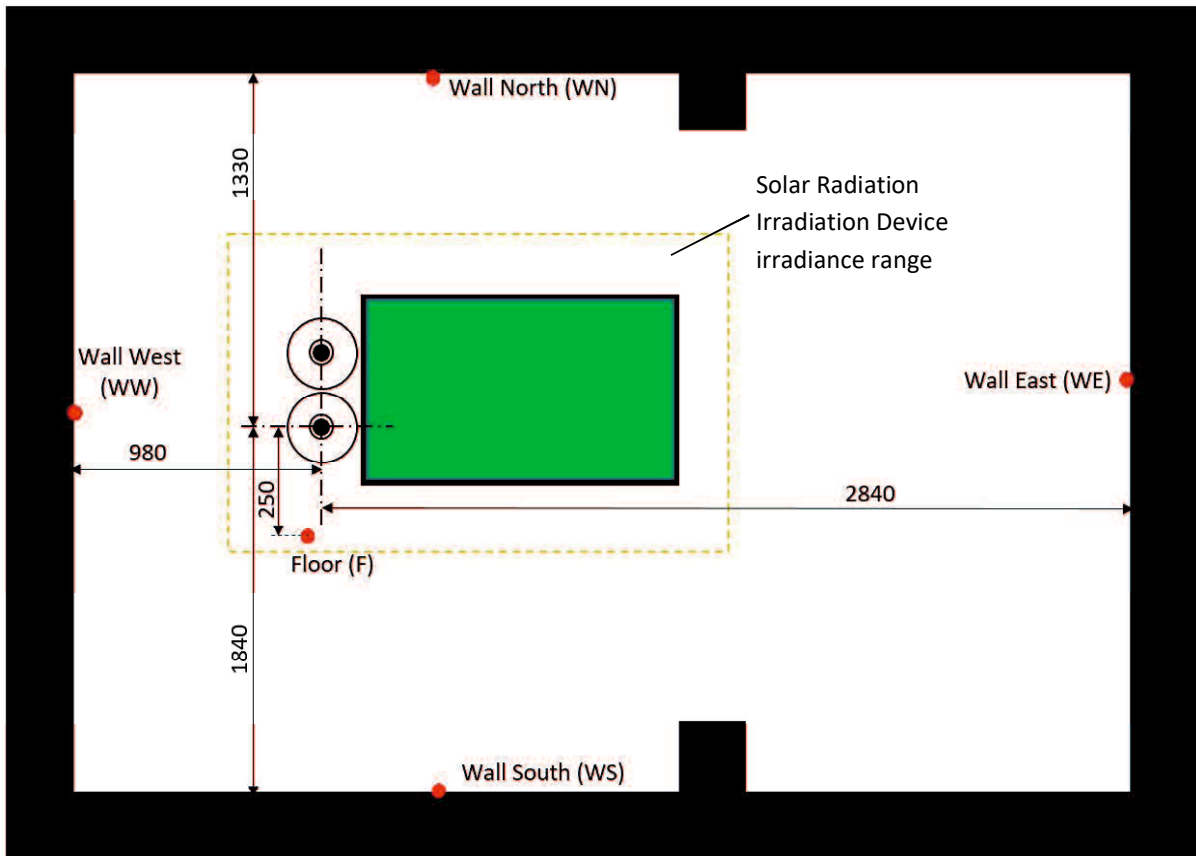


Fig. 4-1. Upper view in Artificial Climate Chamber; interior walls location relation. Red dots represents temperature measuring locations.

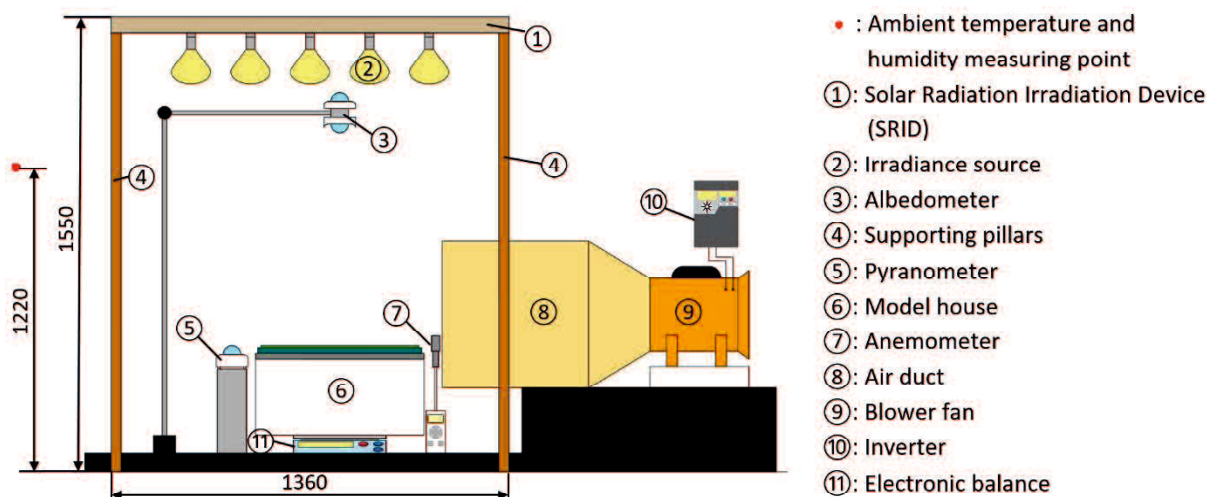


Fig. 4-2. Experimental equipment in Artificial Climate Chamber.

Ambient conditions

The ambient temperature and humidity were set fixed at 30 °C and 70 % RH, respectively, to simulate the average summer environmental condition at Tokyo, Japan in August 2016 based on the data surveyed [56]. Although the initial ambient temperature and humidity of about 1.2 m above ground inside an instrument shelter, in the ACC, were set to be constant, the actual measured values were 30 ± 0.3 °C and 65 ± 3.6 %RH, respectively. The actual value wavered slightly because the machine adjusted the pre-set environment condition along with the condition of the experiment that changed continuously. As shown in Fig. 4-3, the ambient temperature slowly increased as the experiment started. This happened since the heat from Solar Radiation Irradiation Device was warming the space inside ACC. Humidity was also affected by the same reason in the first 90minutes. Humidity escalated as soon as the wind velocity was generated on the 91st minute. Nevertheless, both ambient temperature and humidity were considered acceptable as their error were significantly small, only diverted 0.2% and 5.7% from the desired value, respectively.

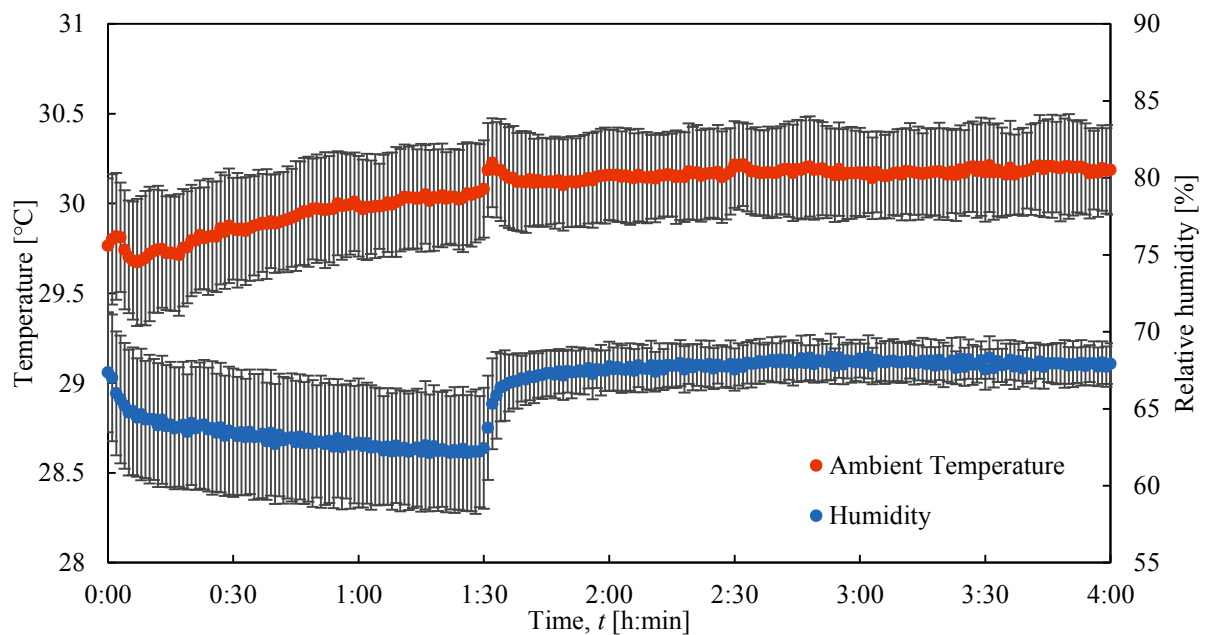


Fig. 4-3. Average ambient temperature and humidity for indoor experiments inside Artificial Climate Chamber.

Irradiance source

By installing the Solar Radiation Irradiation Device (SRID), the strength of irradiance R_I can be set to three different intensities (600, 800, and 1000 W/m²). To get a more accurate readings of irradiance, two MS-402 pyranometers (one for input control, and another one for actual measurement) were positioned at the same level with model house roof plate. Meanwhile, the LP-PYRA-06 albedometer was located in centre about 0.8m above of model house. Only downward albedometer was used in the experiments because the upward albedometer was too close to the irradiance source. While the spectral irradiation energy is shown in Fig. 4-4, the irradiance intensities were chosen to imitate a typical solar radiation range during a clear summer day in Japan. In addition, as understood in previous investigation (Master Thesis) that at irradiance angle of 90°, the thermal effects were affected the most, all experiments in this chapter were conducted at 90°.

The irradiances generated by the SRID were recorded with minimal fluctuation for 600, 800, and 1000 W/m². As depicted in Fig. 4-5, the irradiance error was below than 0.8% in all cases, noting 598 ± 4.2 [W/m²], 794 ± 7.0 [W/m²], and 993 ± 9.7 [W/m²] as the average actual measurement. Here, the measured irradiance was treated to consist of not only the main irradiance, but also some portions of secondary radiation from surrounding floor and walls inside ACC. According to calculation in Appendix I, it was estimated that there were 3 to 5% of radiation coming from floor and walls, measured together with the irradiance by the pyranometer. However, the secondary radiation portions from atmosphere are undistinguishable in the experimental setup.

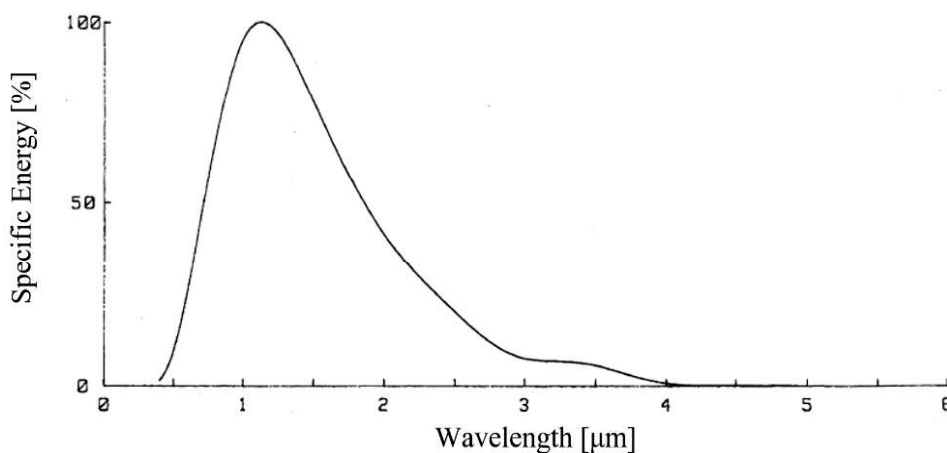


Fig. 4-4. Spectral irradiation energy irradiated by Solar Radiation Irradiation Device.

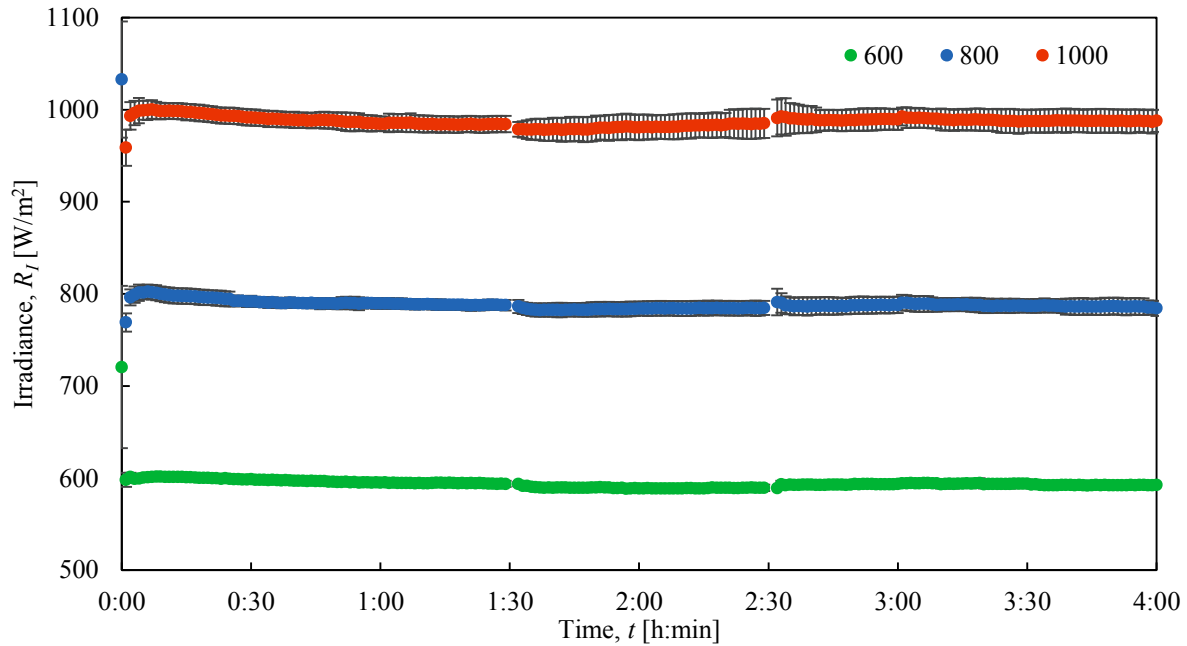


Fig. 4-5. Average Irradiance, R_I for all experiments.

Generation of wind

In order to evaluate the effect of convection heat transfer on green roof, five levels of average wind velocity, U_{ave} (0, 1, 1.5, 2, and 3 m/s) were configured by a FR-FS2-0.4K fan inverter and calibrated in the preliminary experiments. Wind velocity of 0 m/s illustrates the natural convection condition where there is no wind movement involved. Meanwhile, the wind velocity was generated by SHT-250 blower fan attached with 500×500 mm cross-sectional area air duct and V-13-100 honey-comb funnel to treat the wind stream (refer Fig. 4-2). The wind velocity profile was determined from the lower-half of the air duct outlet since the wind profile was found as symmetric through the middle point during the preliminary procedure. An EM-SD vane-type anemometer probe with a pre-attached T-type thermocouple was fixed at the air duct outlet to validate the wind velocity and temperature at the air duct outlet. The anemometer came along with a logger which enabled the data to be recorded.

Experiment procedures

All experiments were carried out in three halves; the first 90 minutes for natural convection ($U_{ave} = 0$ [m/s]), the next 60 minutes with wind velocity, and the last 90 minutes involved both wind and evaporation process. In order to simulate a condition after a rain event, the evaporation was initiated by spraying 100 mL of water on the green panel thoroughly within one minute (average spraying speed of 1.67 mL/s) for each experiment condition. The evaporation was determined by measuring the real-time weight changes by an EK-6100i electronic balance mounted below the model house. Each experiment was conducted twice to increase the accuracy and reliability, and the average results were determined.

Experiment procedures were as below:

- 1- Remove the green panel and roof plate from the model house.
- 2- Set the ambient temperature at 30°C and humidity at 70%.
- 3- Wait about one hour until every temperature measuring points including the measuring points in model house to reach steady 30°C.
- 4- Close the model house tightly with the roof plate, and install the green panel.
- 5- Close the Artificial Climate Chamber door tightly.
- 6- Set the irradiance to 600 W/m², and at the same time, start logging all sensors on Portable Data Logger, Anemometer Logger, and Electronic Balance Logger.
- 7- Wait for 90 minutes until uniform temperature reading is achieved. Turn on the Fan Inverter to generate 1m/s of wind velocity.
- 8- Wait 60 minutes until uniform temperature reading is achieved. Apply 100ml of water thoroughly on green panel by using water sprayer.
- 9- Let the experiment run for another 90 minutes. Turn off all equipment.
- 10- Repeat procedure 1 to 9 for 800 and 1000 W/m² of irradiance, and 1.5, 2, and 3 m/s of wind velocity.
- 11- Execute same procedures for control model house C, but neglect procedure number 8.
- 12- Repeat each experiment three times to increase data accuracy.

4-3 Experimental Conditions

Table 4-1 below summarized the experimental conditions for the experiments in this chapter.

Table 4-1. Summary of experimental conditions in Chapter 4.

| Parameter | Value |
|--|--|
| Ambient Temperature, T_{∞} [°C] | 30 |
| Ambient Humidity, RH [%RH] | 70 |
| Irradiance angle, φ [°] | 90 |
| Irradiance, R_I [W/m ²] | 600, 800, 1000 |
| Wind Velocity, U_{ave} [m/s] | 0, 1, 1.5, 2, 3 |
| Model houses | Dry Sunagoke S3, Moist Sunagoke S3m, Dry Control C |
| Hydration Water Volume on S3m [mL] | 100 |

4-4 Results and Discussion

4-4-1 Convection Heat Transfer Characteristics

Since wind velocity is an important parameter in the experiment, it is essential to study the behaviour of the wind flow as it will give the basic understanding on how the wind reacts and affects the heat transfer system of the whole model house. Fig. 4-6 illustrates the derived ratio of the Grashof number and the square of Reynolds number, Ar from Eq. (3-25). The model houses were indicated in the graph legend as S3 for dry Sunagoke moss, S3m for moist Sunagoke moss, and C for dry control roof, while the numbers such as 600 indicated the irradiance irradiated in the experiment.

The ratio of Grashof number and square of Reynolds number indicated a natural convection if the value exceeds 10, combination of forced and natural convection in between 0.1 and 10, and forced convection if the value was less than 0.1. At wind velocity of 0 m/s, the ratio extended to infinity, thus the natural convection was assumed to dominate the heat transfer on the three model houses in such wind conditions. The region of $0 < U_{ave} < 2$ m/s was considered as the transition region where the combined convection took place. Although the ratio for dry and moist Sunagoke green roof reached below 0.1, at wind velocity value of 1.5 m/s, the surface condition was assumed to be unstable in that wind velocity, since the surface temperature was still decreasing. Hence, wind velocity of 2 m/s ($Re=74,500$) was considered as the critical point

where the forced convection started to dominate the heat transfer on all model houses. Gaffin et al. [19] supported this finding, where wind velocity of 1.75 m/s was verified to be the indicator of forced convection in their study.

To support the findings in Fig. 4-6, the relation of Nusselt number (calculated from Eq. 3-26) and ratio of Grashof number and square of Reynolds number has been demonstrated in Fig. 4-7. According to the graph, high Nusselt number mostly presented between ratio of Grashof number and Reynolds number of below than 0.1. Hence, approved the domination of forced convection above 2 m/s of wind velocity.

Apparently the ratios for dry and moist Sunagoke moss were lower compared to the ratio for untreated model house. This occurred because the surface and ambient temperature differences of model houses S3 and S3m were much lower. The same concept also applies to higher irradiance condition where a higher irradiance will elevate the surface temperature and the temperature differences as well. Thus, the ratio increases in higher irradiance.

Unlike the ratio of Grashof number and square of Reynolds number, the increased wind velocity had reduced the surface temperature along with the temperature differences with ambient temperature, causing the convection heat transfer coefficient calculated from Eq. (3-16) to increase, as depicted in Fig. 4-8. At the time when the wind velocity was getting faster, the surface temperature remained almost constant which caused the heat transfer coefficient to remain similar with the wind velocity of 2 m/s onwards (forced convection region).

The convection heat transfer coefficient for each model house was estimated by the approximation equations that are shown in Table 4-2. Given that the R^2 values, for each roof condition were close to 1, the approximation equations have a good fitment with the average values for each wind parameter. Generally, there were no correlations between the irradiance and the coefficient since only $\pm 1\%$ variations were found for model house S3 and C. However, only for moist Sunagoke moss, with exception in natural convection, there were positive correlations in irradiance and convection heat transfer coefficient. Particularly in forced convection region, the convection heat transfer coefficient varied $\pm 9\%$ from the mean value, depending on the irradiance intensities. It was noted that the estimation equations were constructed based on the ambient temperature of 30 °C, therefore different environment may result in different accuracy.

In a natural convection region, the resulting average convection heat transfer coefficients were $24.5 \pm 0.31 \text{ W/m}^2\text{K}$, $23.7 \pm 0.97 \text{ W/m}^2\text{K}$, and $14.5 \pm 0.16 \text{ W/m}^2\text{K}$ for model

house d-A, m-A and d-B, respectively. Meanwhile, the convection heat transfer coefficients of $116.1 \pm 0.99 \text{ W/m}^2\text{K}$, $108.3 \pm 9.10 \text{ W/m}^2\text{K}$, and $37.8 \pm 0.24 \text{ W/m}^2\text{K}$ in the same model houses order were obtained in a forced convection region. Therefore, the application of Sunagoke moss green roof was clarified to improve the convection heat transfer ability of the model houses by a factor of 1.6 in natural convection and 2.9 in forced convection.

As a comparison with common plants, Kumar et al. [57] reported that the maximum convection heat transfer coefficient in natural convection was $26.8 \text{ W/m}^2\text{K}$ for peperomia, $10.1 \text{ W/m}^2\text{K}$ for egg-plant, and $23.5 \text{ W/m}^2\text{K}$ for wax-bean, as acquired in experiments conducted in a wind tunnel. The convection heat transfer coefficient increased to $59.5 \text{ W/m}^2\text{K}$ for peperomia and egg-plant, and $42.7 \text{ W/m}^2\text{K}$ for wax-bean in forced convection. The convection heat transfer coefficients for Sunagoke moss, especially in the forced convection, were 2 times higher than the reference, and may result from the different heating intensities to the subject plant. Therefore the data presented in this paper were considered valid.

Table 4-2. Estimation equations for convection heat transfer coefficient according to wind velocity range.

| Model house | For $0 < U_{ave} < 2$ | For $U_{ave} > 2$ |
|-------------|-------------------------------|------------------------------|
| S3 | $h = 25.428e^{0.7478U_{ave}}$ | $h = 9.1232U_{ave} + 88.697$ |
| S3m | $h = 24.041e^{0.7506U_{ave}}$ | $h = 5.448U_{ave} + 91.983$ |
| C | $h = 14.949e^{0.4311U_{ave}}$ | $h = 3.1186U_{ave} + 28.396$ |

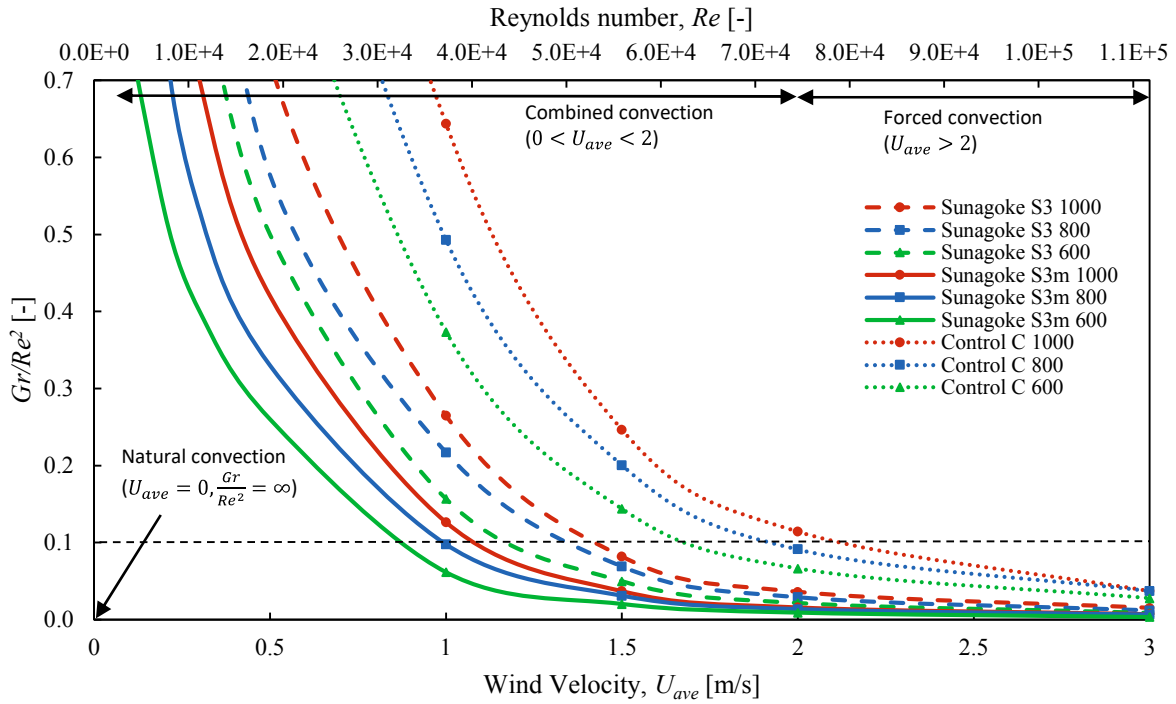


Fig. 4-6. Ratio of Grashof number and square of Reynolds number. Irradiance strength is denoted by color; the moss-free house is marked by dotted lines, the moss covered house is marked by dashed lines if dry, solid lines if moist.

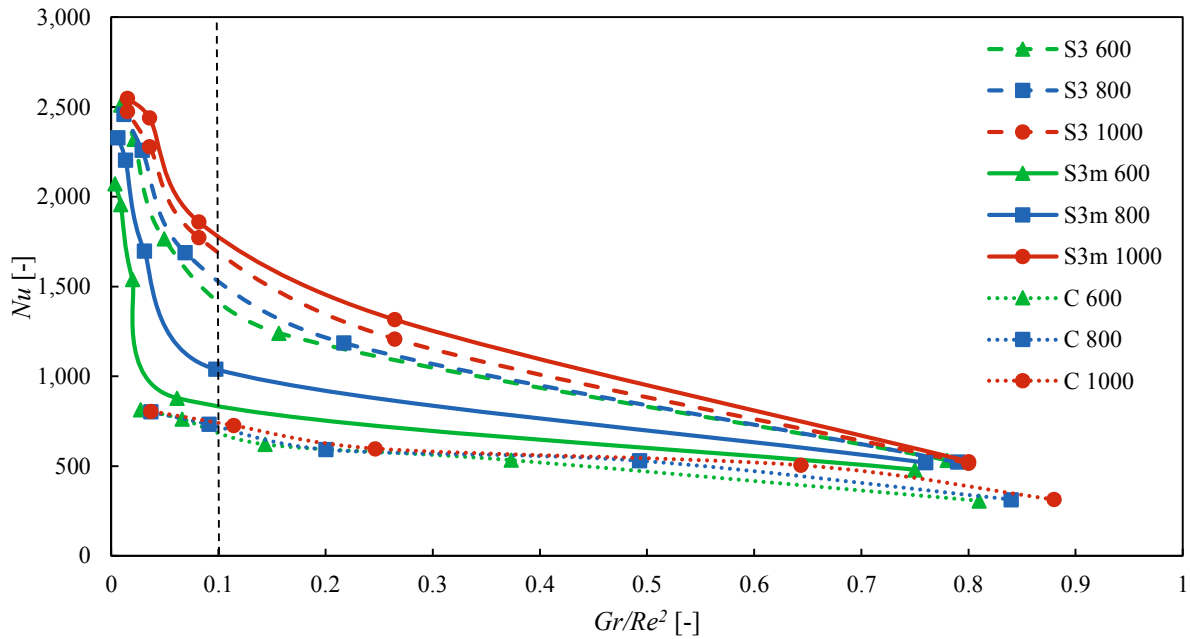


Fig. 4-7. Relation between Nusselt number and ratio of Grashof number and square of Reynolds number.

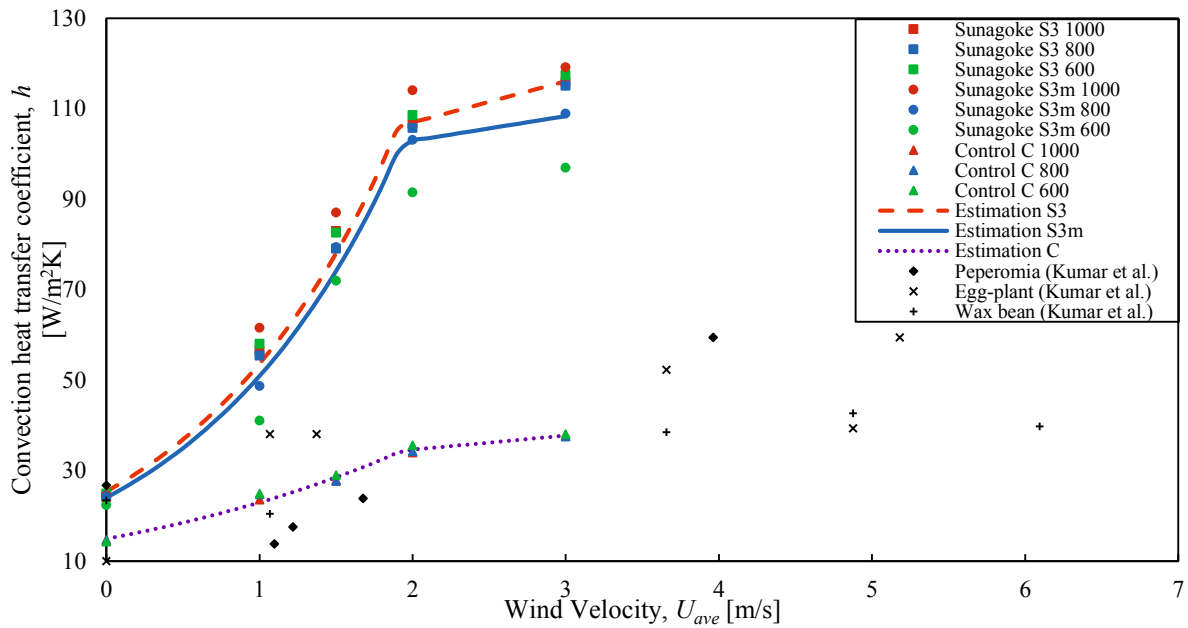


Fig. 4-8. Convection heat transfer coefficient for each model house in different wind velocity and irradiance. Convection heat transfer coefficient for model house S3, S3m and C are presented with estimation equation, while data for Peperomia, Egg-plant, and Wax bean are retrieved from Kumar et al..

4-4-2 Effects of Wind Velocity on Heat Balance

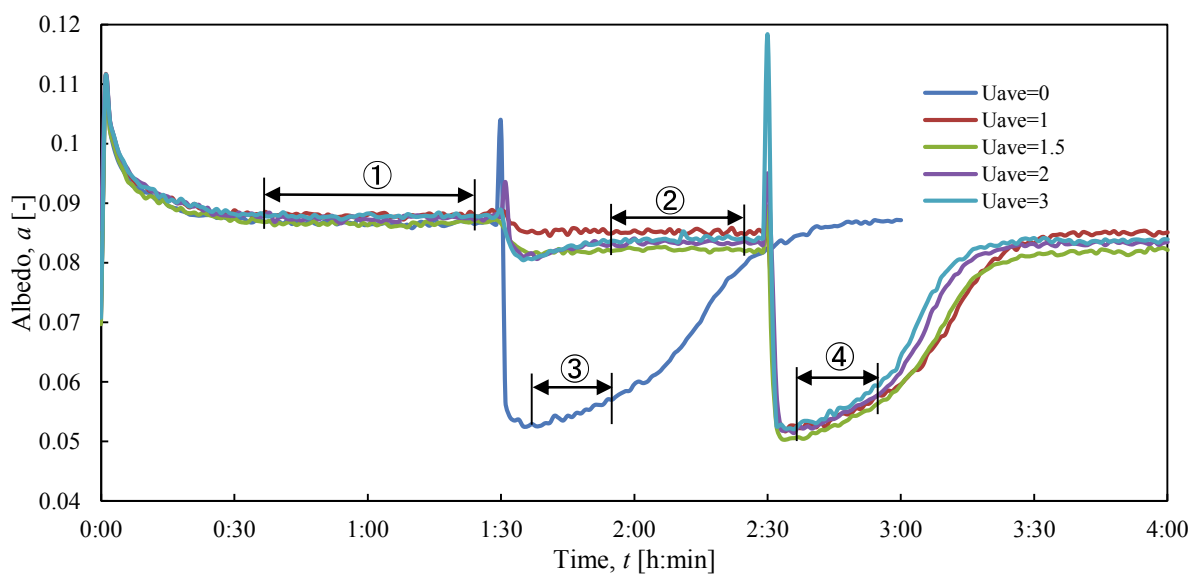
Albedo of Outermost Surfaces

The incoming radiation (i.e. irradiance) were firstly reflected before converted to other forms of heat (refer Fig. 3-1). Accordingly, determining albedo is a crucial assessment in evaluating the thermal performance of the Sunagoke moss green roof. Fig 4-9 (a) shows how the data were analysed and summarized in this dissertation according to different experimental phase. For example, the graph presents the albedo of Sunagoke green panel when irradiance was 600 [W/m²]. Since the experiments were conducted in the first 90 minutes without wind velocity, the next 60 minutes with wind velocity, and the last 90 minutes with both wind velocity and evaporation, therefore the data were broken down according to phases. Only data in steady state were analysed as designated by the number; ①- S3 and C without wind velocity, ②- S3 and C with wind velocity, ③- S3m without wind velocity, and ④- S3m with wind velocity. The average data were taken from each analysis period and the summarized data were presented in graph in Fig. 4-9 (b) and (c). Other results onwards also were treated with the same procedure.

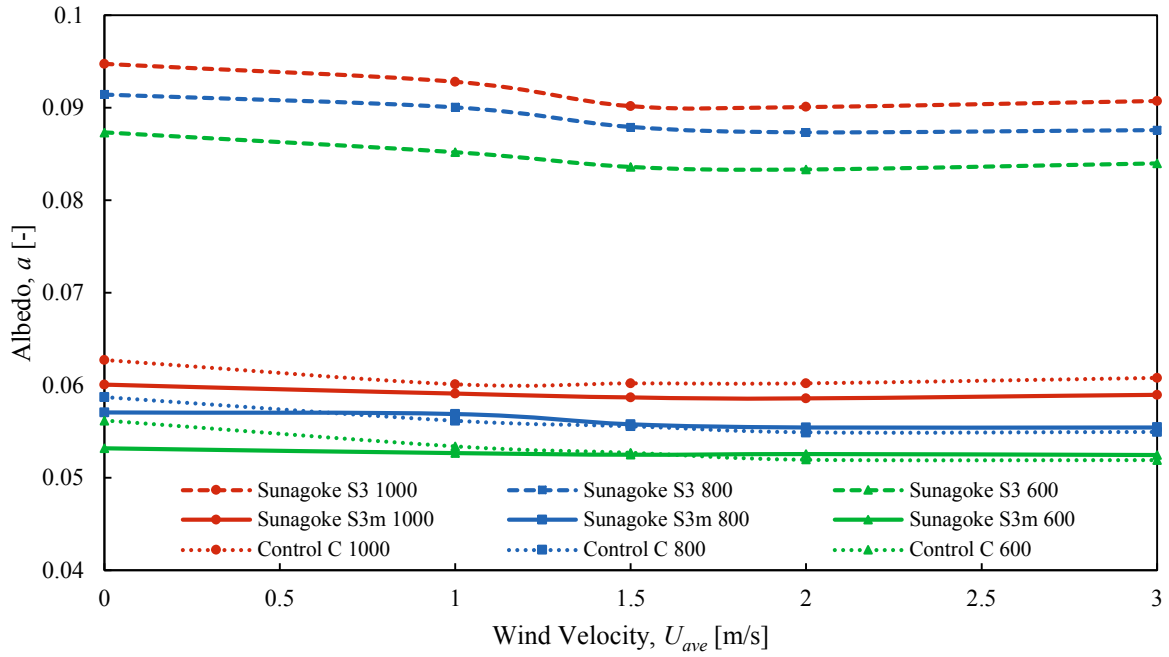
Fig. 4-9 (b) and (c) enlightened that in general, albedo of the dry Sunagoke green panel was in the range of 0.08 to 0.09, which was fairly high compared to the moist Sunagoke moss

and control model house. The moist Sunagoke moss has albedo of 0.05 to 0.06, since the water content reduced the albedo [16]. This occurred as the fact that Sunagoke colour will turn darker when water is applied to it. On the other hand, the control model house was covered by a matte black finishing on the roof surface which resisted the reflected radiation. The documented albedo for model house C was also in range of 0.05 to 0.06. The variation of albedo in each surface condition resulted from the directly proportional relation between irradiance and albedo. However, no significant changes were noticed on the albedo in natural and forced convection region.

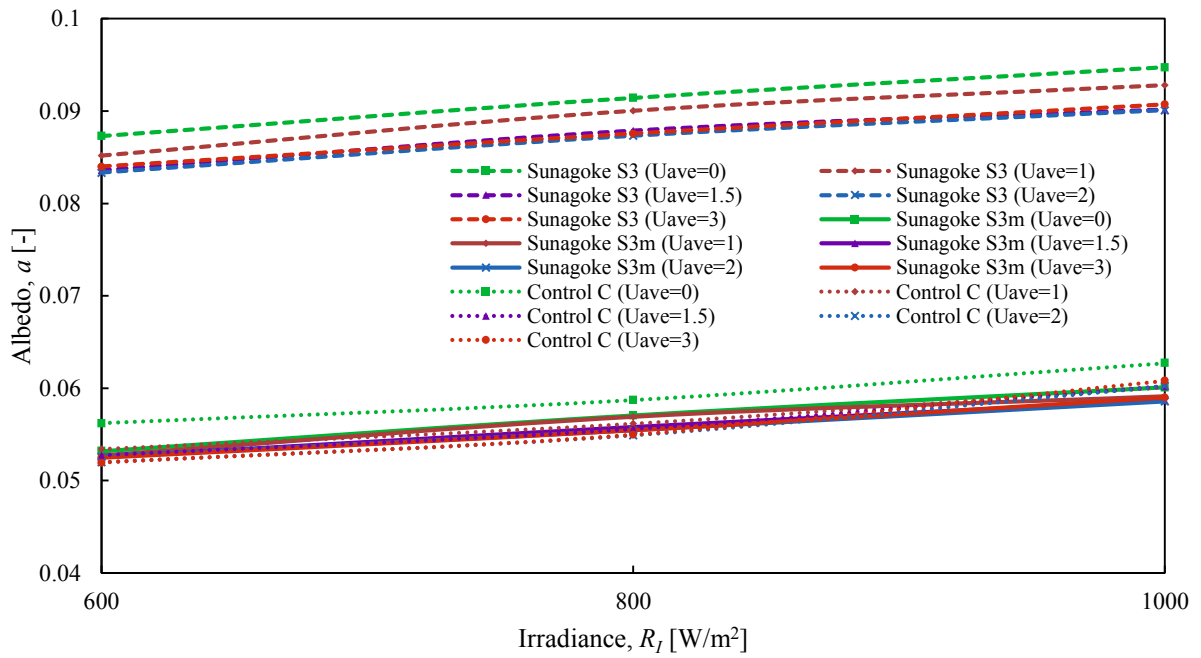
Gaffin et al. [19] suggested that the equivalent albedo for green roofs should be in the range of 0.7-0.85. In addition, Maclvor et al. [58] found that *Carex argyranthra* had an albedo of 0.22 ± 0.007 , which surpassed the other 14 species of plant in a research conducted on top of the Patrick Power Library of Saint Mary's University. However, by referring to the albedo values, the findings in this paper were comparatively lower than the introduced values. The SRID utilised in this paper may not have the ability to produce exactly the same shortwave radiation as the sun. Furthermore, since the measuring environment was in a closed chamber, the radiations from space and the surrounding objects were not or less detected by the albedometer. The outdoor environment as mentioned by Gaffin et al. and Maclvor et al. considered such radiations, thus, the values reported were much higher. For that reason, despite the dissimilarities in the ambient condition, the results obtained in this paper were considered acceptable.



(a) Example of data analysis: Albedo changes respective to experiment phase and time, when irradiance strength was $600 \text{ [W/m}^2\text{]}$.



(b) Albedo according to wind velocity.



(c) Albedo according to irradiance.

Fig. 4-9. Albedo of model houses Sunagoke S3, moist Sunagoke S3m, and control C.

Convection heat flux

Convection heat flux is usually the dominant form of heat energy in the presence of fluid as the heat transfer medium. The convection heat flux is also recognised to be close to the pre-set irradiance especially for the bare roof or dry Sunagoke green panel surface. As illustrated in Fig. 4-10, the convection heat flux increased linearly with the increment of irradiance. This showed that more proportions of irradiance were transported via convection process. However, only a small increment of convection heat flux was detected with the increased of wind velocity for model houses S3 and C. On the contrary, the convection heat flux of the Sunagoke S3m green panel during the evaporation activation period was consistently lower and started to decrease gradually with the increment of wind velocity. This phenomenon is believed to occur because the latent heat formed has consumed most of the heat coming from the SRID, resulting less heat to be transferred by the wind. Increasing the wind velocity has also helped the water to evaporated more rapidly, thus, decreasing the convection heat flux conversely.

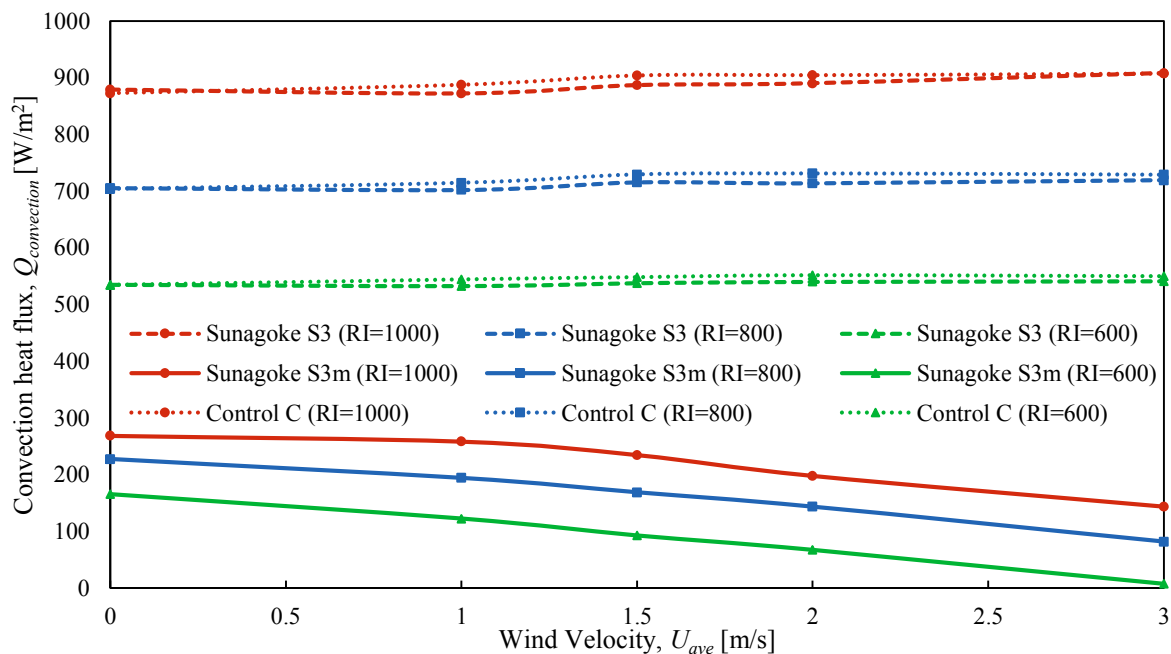


Fig. 4-10. Convection heat flux for all model house.

Latent heat flux

Applying water on the Sunagoke green panel has given an additional cooling effect on the model house. Fig. 4-11 demonstrates the average latent heat flux for 100 ml of water sprayed on the Sunagoke moss green panel. The latent heat flux generally follows the increment of both irradiance and wind velocity. Providing the green panel with extra heat energy has encouraged the evaporation process as the heat increases water temperature and molecular kinetic energy (temperature driving factor). On the other hand, wind velocity will sweep away the water particle just above the green panel surface and at the same time reduce humidity which prevents the water molecules from going back into the liquid. Therefore, it can be said that increasing the wind velocity will help the humidity driving factor to promote evaporation.

Although the experiments conducted only supplied 100 ml of water to the Sunagoke moss green panel surface in a steady temperature and humidity environment, adding more water on the surface will only prolong the evaporation period without elevating the latent heat flux further. The maximum values of latent heat flux documented were all at wind velocity of 3 m/s; 561, 668, and 766 W/m² with respect to irradiances of 600, 800, and 1000 W/m². The results reported in this paper were only limited to wind velocity of 3 m/s. Increasing the wind velocity further beyond 3 m/s is expected to raise the latent heat flux accordingly, however, the maximum magnitude shall be reached at some points near the total radiation value.

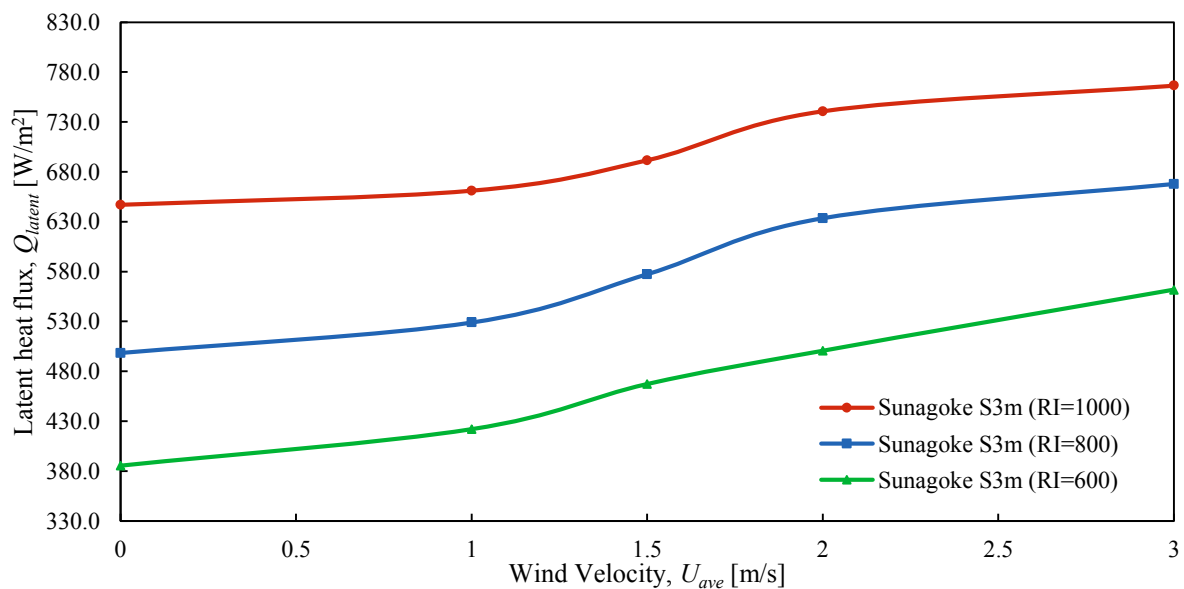


Fig. 4-11. Average latent heat flux of Sunagoke S3m during steady evaporation period.

Conduction heat flux

The mitigation of surface temperature is very important in deciding the tendency of conducting heat flux to penetrate the roof part and enter the model house interior cavity. It is also the by-product of the heat intercepted by reflected radiation, convection heat, and latent heat. In this dissertation, conduction heat was believed to be responsible in warming the interior temperature of the model house. Fig. 4-12 illustrates the conduction heat flux for each model house in the respective experimental conditions. From the results of surface temperature, the conduction heat flux was expected to follow a similar development. The conduction heat flux in static wind was fairly high compared to when wind velocity existed. Furthermore, as a consequence of the reduction of temperature difference between surface and ceiling temperature, the higher wind velocity resulted in the reduction of heat flux. Especially for the moist condition, the conduction heat flux for Sunagoke moss inclined towards 0 axis since the two points temperature differences were almost diminished in the higher wind velocity. The conduction heat fluxes were found to be constant beyond 2 m/s of wind velocity as the temperature between the two surfaces remained the same in high wind velocity including the other model houses (S3 and C) as well.

Sunagoke green panel, either in dry or moist condition, successfully regulated the conduction heat flux as it was significantly lower than that of the control model house. For the static wind, the average conduction heat flux for model houses S3 and S3m ranged from 8.8 to 13.3 W/m² and 3.9 to 6.3 W/m², correspondingly. Meanwhile, the conduction heat flux for model house C ranged between 27.2 and 42.5 W/m² for the same wind state. On the other hand, the dynamic wind velocity reduced the range to 4.3 to 7.1 W/m², 1.5 to 2.9 W/m², and 13.7 to 24.0 W/m² for model houses S3, S3m, and C, respectively, which made the reduction percentages to be 48.4 ±1.8%, 58.7 ±3.2%, and 47.3 ±2.8%, accordingly. In other words, the moist Sunagoke green panel was affected the most by the wind velocity since it provided aid in enhancing the evaporation cooling. However, the variations of irradiance did not affect the conduction heat flux in moist model house S3 when confronted with wind velocity beyond 2 m/s.

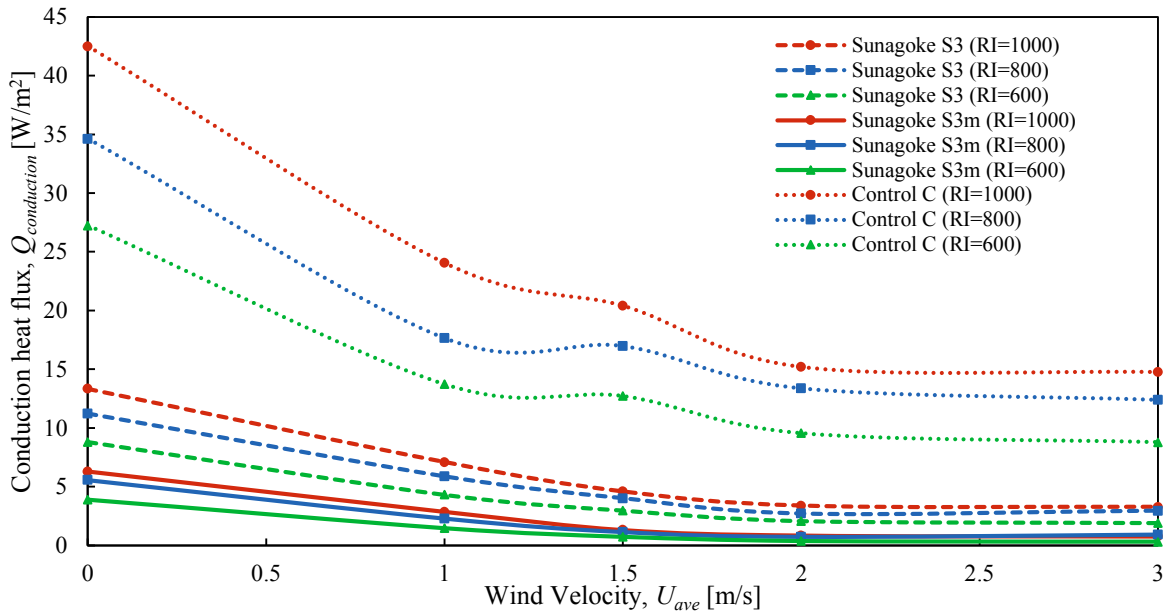


Fig. 4-12. Conduction heat flux for each model house respective to experimental conditions.

Heat Energy Proportions on Each Model House

Based on the heat balance equation (refer Eq. (3-2)), the proportion of each heat fraction transferred on the model houses can be determined by dividing the fractions with total radiation R_T . Total radiation is equal to irradiance minus the reflected radiation flux as explained in Eq. (3-3). The results for each heat fraction were summarised in Fig. 4-13. It was noted that the latent heat fluxes for dry surfaces (model houses S3 and C) were neglected since they were assumed minute and difficult to measure. Thus only latent heat flux proportion for moist model house S3m was presented on the graph. Since the dry surfaces of model houses S3 and C lack evaporation, the convection heat flux dominated the whole heat balance, thus the convection heat proportion was really close to 100% throughout the wind velocity. Convection heat proportion of dry Sunagoke surface was slightly higher than that of the control roof, thus the clarified Sunagoke moss allowed better cooling in dry condition. At the same time less conduction heat flux was entering the interior cavity of the model house.

On the contrary, applying water on the Sunagoke green panel has given an additional cooling effect on the model house S3m. The latent heat flux generally follows the increment of both irradiance and wind velocity. Providing the green panel with extra irradiance has encouraged the evaporation process as the radiation increases water temperature and molecular kinetic energy (temperature driving factor). On the other hand, wind velocity will sweep away the water particle just above the green panel surface and at the same time reduce humidity

which prevents the water molecules from going back into the liquid. Therefore, it can be said that increasing the wind velocity will help the humidity driving factor to promote evaporation.

The latent heat played a major role in partially controlling the other fractions of heat by means of evaporation. The latent heat was found to individually divert about 70% in natural, and 91% from the whole heat transfer process in forced convection. Here, the moist Sunagoke moss clearly demonstrated the significance of evaporation cooling by diminishing the conduction heat of dry Sunagoke moss and control roof by a factor of 2 and 7, respectively. Interestingly, the latent heat and convection heat were found to be inversely related to each other and the diversion rose upon the increment of wind velocity. Two accurate approximation equations were proposed to estimate the contribution of latent and convection heat on the moist Sunagoke moss, as shown on the graph (Fig. 4-13). The latent heat dominated in moist condition but varied approximately $\pm 8\%$ from the mean proportion due to irradiance strength, making the convection heat fluctuated up to $\pm 64\%$.

In addition, the detailed average heat proportions were presented in Table 4-3 along with the data published by Tabares-Velasco et. al [52] that were obtained in a similar laboratory experiment. The conduction heat proportions acquired in this experiment were found to be comparatively lower than the previous data. This may due to the heat in the interior cavity of the well-insulated model house had achieved a saturated state. Tabares-Velasco on the other hand, used an open setup with roof only, without building.

Table 4-3. Heat fluxes relative to total radiation flux R_T in natural and forced convection.

| Model house | Reflected radiation [%] | Convection heat [%] | Latent heat [%] | Conduction heat [%] |
|---|--------------------------------------|--------------------------------------|--------------------------------------|------------------------------------|
| Sunagoke S3 | 10.0 \pm 0.37 (9.7 \pm 0.36)* | 98.4 \pm 0.05 (99.6 \pm 0.03) | - | 1.6 \pm 0.05 (0.4 \pm 0.02) |
| Sunagoke S3m | 7.5 \pm 0.44 (7.4 \pm 0.58) | 30.4 \pm 0.77 (9.2 \pm 5.90) | 70.1 \pm 1.03 (91.0 \pm 7.24) | 0.7 \pm 0.03 (0.1 \pm 0.02) |
| Control C | 6.3 \pm 0.32 (6.0 \pm 0.41) | 95.3 \pm 0.09 (98.4 \pm 0.04) | - | 4.7 \pm 0.09 (1.6 \pm 0.04) |
| Tabares-Velasco et. al (<i>Sedum spurium</i>) | 11 | 16 | 82 | 15 |

*the value written in bracket is for forced convection

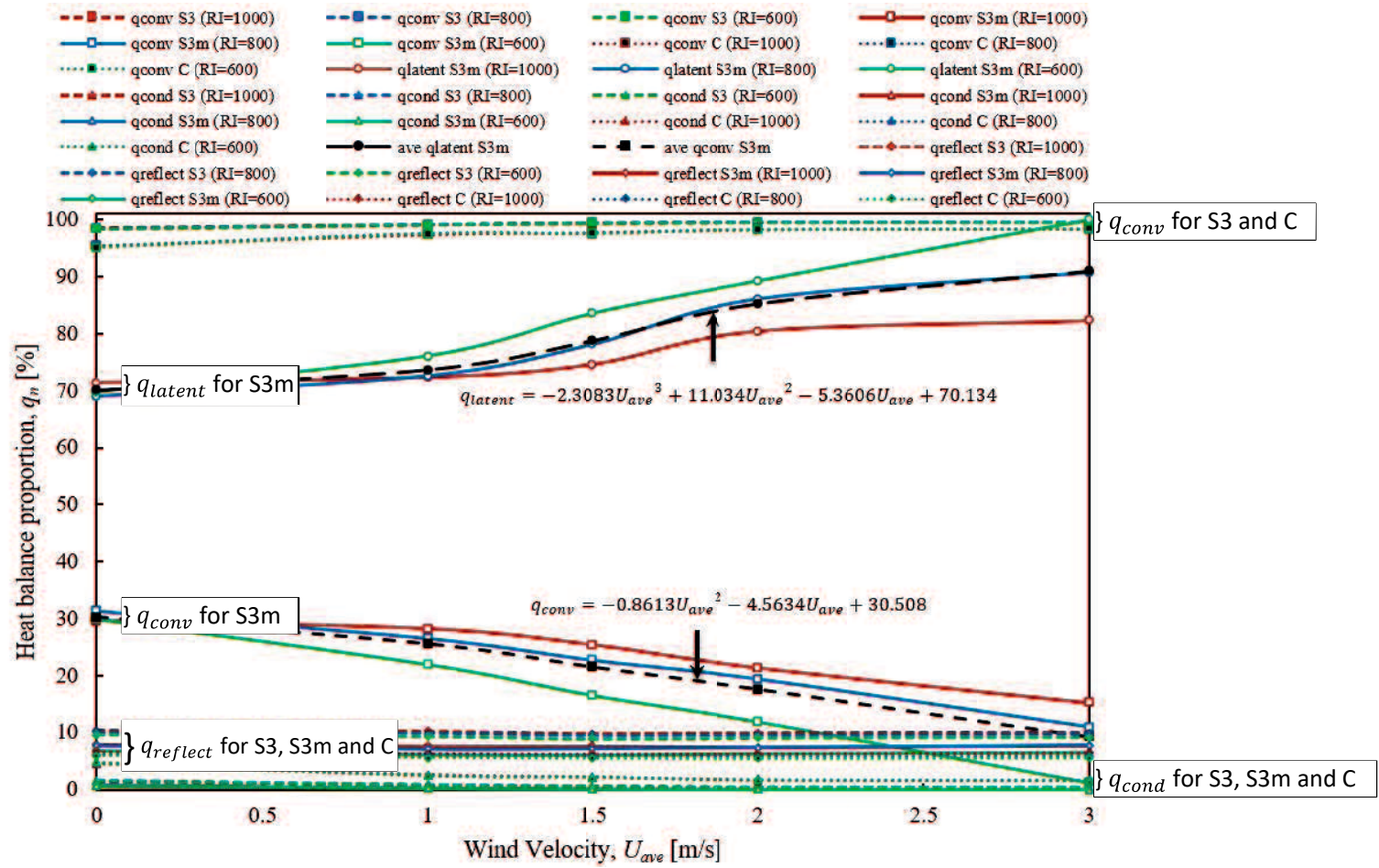


Fig. 4-13. Heat proportions on each model house with the estimation equations for the case of moist Sunagoke moss.

At the same time, the Bowen ratio was determined to compare the different processes of surface cooling that occurred especially on the moist Sunagoke moss green panel. Since the ratio was constructed as the proportion of convection heat to latent heat, the association between these two heat fluxes can be characterised (refer Eq. (3-15)). If the ratio is lower than 1, a larger proportion of the energy on the green panel surface will be delivered to the atmosphere as latent heat instead of convection heat, and vice versa. As explained before, the latent heat dominated the cooling process instead of the convection heat in model house S3m. The results of the Bowen ratio were demonstrated in Fig. 4-14. Despite the fact that a normal plant will evapotranspirated to live, the evaporation on dry Sunagoke moss green panel was too minute that the latent heat flux of the green panel was unable to be determined. Thus, the Bowen ratio for dry Sunagoke was assumed to be greater than 1 by considering that the convection heat was dominating instead of the latent heat.

In natural convection, the Bowen ratio for moist green panel showed the maximum value since the value of latent heat was the least at this condition but double the value of convection heat. Despite the changes of irradiance intensities, the Bowen ratio at this point was approximately 0.42. On the other hand, as the latent heat gradually developed and overshadowed convection heat, the Bowen ratio shrank near 0. The Bowen ratio of 0.02 was the lowest recorded value in the investigations done. Gaffin et al. [19, 21] in their reports explained the comparison results for the effectiveness of green roofs with other vegetated surfaces. The Bowen ratios for other vegetated areas were as follows; wheat field (summer) 0.60, forest in Indiana (annual average) 0.59, soybean field (summer) 0.30, irrigated field (August) 0.20-0.25, tropical ocean 0.10, and Huaihe River Basin (paddy) 0.06. Therefore, the results were considered as reasonable for the Sunagoke moss Bowen ratio which ranged from 0.02 to 0.18 in forced convection, fluctuated due to irradiance, but constantly at 0.42 in natural convection.

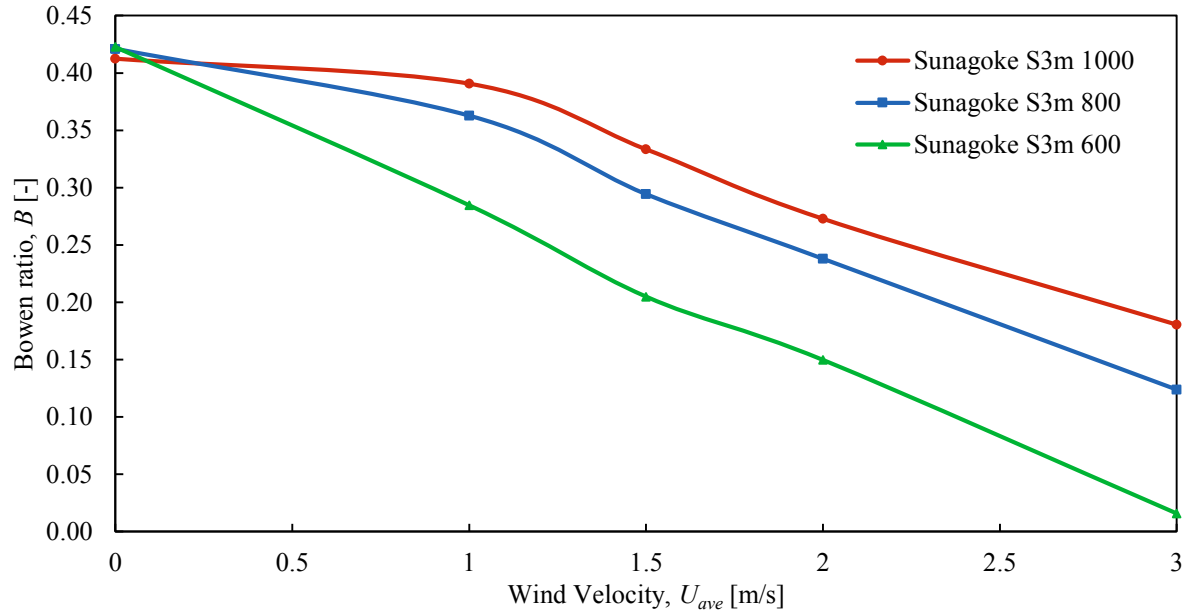


Fig. 4-14. Bowen ratio for moist Sunagoke moss green panel.

4-4-3 Relation of Wind Velocity and Temperature Profile

Surface temperature

Surface temperature is significantly dependent on the environmental condition, which has to be faced by the outermost layer of each model house. All changes of such irradiance, convection characteristic, and presence of water will drastically influence the fluctuation of surface temperature. Fig. 4-15 establishes the surface temperature for each outermost layer of the model houses under every experimental condition. In natural convection, the surface temperature varied from 51.5 to 66.4 °C for model house S3, 40.0 to 48.5 °C for moist model house S3m, and 67.5 to 89.5 °C for control model house C. Based on the figure, even a small presence of wind initiated a significant reduction in surface temperature by comparing temperature gradient for wind velocity of 0 and 1 m/s. Changing the convection phase from natural to forced convection reduced the surface temperature 37.4 ± 4.0% for model house d-A, 25.0 ± 3.8% for model house m-A and 36.4 ± 2.0% for control model house d-B. The fluctuations were affected by irradiance intensities. However, the surface temperature reduction percentages were decreasing with the increment of wind velocity. Besides, with sufficient wind velocity, it can be clarified that the surface temperature of moist Sunagoke moss gravitated near the pre-set ambient temperature (30 °C).

The Sunagoke green panel was way cooler than the control roof surface due to the shading and evaporation cooling effects. A report made by Niachou et al. [18] in year 2001,

explained that in an outdoor environment (ambient temperature 28 °C and relative humidity 57%), the surface temperature of a green roof on a non-insulated building ranged from 28 to 40 °C, whereas the surface temperature of a non-insulated building was warmer, which ranged between 42 and 48 °C. In another remarkable article by Suzuki et al. [34], they confirmed the surface temperatures of Sunagoke were recorded the highest at 31 and 33 °C for a rainy and a clear day, compared to the surface temperatures of slab at 35 and 37 °C, correspondingly. As a record, the average wind velocity values for the two days were 2.7 and 2.6 m/s, respectively. In addition, results by Anderson et al. [43] demonstrated similar findings where the maximum temperature of Sunagoke surface recorded in August was 49.2 °C in contrast to medium only roof at 51.0 °C. Hence, the effect of applying green roof especially the Sunagoke moss green roof was proven to give beneficial impact on the building, and the energy savings are certainly anticipated.

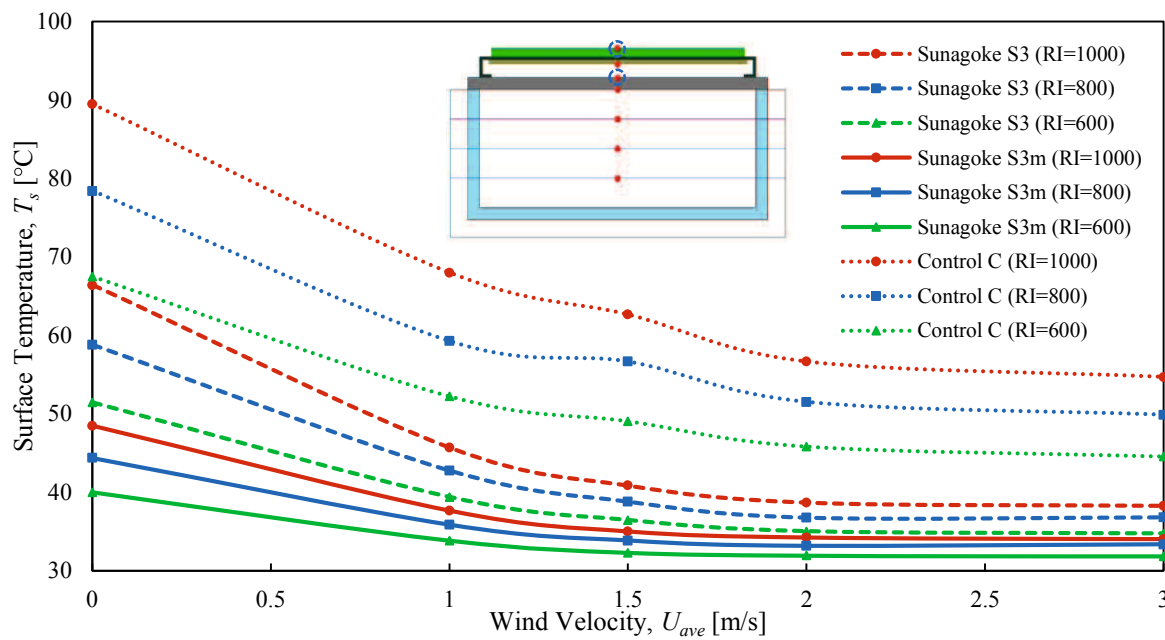


Fig. 4-15. Outermost surface temperature for all model houses. Temperature measuring point for model house S3 and S3m was on the green panel surface, while for model house C was on the roof plate surface.

Interior temperature

The interior temperature was investigated to display the best thermal performance of Sunagoke moss green roof. As a result of net inflow and outflow of heat through the roof part (conduction heat flux), the interior temperature fluctuated through time. The average interior temperature values from the three thermocouples inside the model houses were compiled in Fig. 4-16. Based on the graph, the interior temperature increased with the increment of irradiance but decreased with the increment of wind velocity. Trailing the similar inclination with surface temperature, the higher wind velocity helped the interior temperature to decrease to a level comparable to the ambient temperature.

The interior temperature varied broadly associated with the irradiance strength. For instance, the interior temperature ranged from 38.6 to 45.8 °C and 35.3 to 40.0 °C for model houses S3 and S3m, respectively, while for model house C it ranged from 46.2 to 56.1 °C in natural convection. Later, the generation of wind velocity to create forced convection heat transfer reduced the variation $20.8 \pm 3.9\%$, $13.0 \pm 2.9\%$ and $23.6 \pm 2.6\%$ in the same order. There were no significant temperature reductions at wind velocity above 1.5 m/s. However, the lowest interior temperature for model house S3m was 32.0 °C, which was just 2 °C above the ambient temperature. Any additional temperature reduction below the ambient temperature was assumed to be impossible since the conduction heat fluxes (refer Fig. 4-12 and 4-13) were all in positive proportions and the heat flowed inwards the interior cavity irrespective of the state of the model houses. If the conduction heat flux shows any negative value, then the reverse phenomena may occur.

A fascinating study investigated by Halwatura [59] established the indoor air temperature of a three-story house which used three type of roofs; tile, bare, and Buffalo grass green roofs. The highest indoor temperatures obtained were 34.5 °C, 35.9 °C and 32.7 °C for tile, bare, and green roofs, respectively. From the findings, the Buffalo grass green roof was able to reduce the indoor temperature at 1.8 and 3.2 °C topmost. Although the interior temperature differences between the control roof and the Sunagoke green roof in this paper were relatively high, the results of the application of Sunagoke green roof were expected to be comparable with that of the reference, considering a proper ventilation of a real building.

By comparing the results for model houses C and S3, the dry Sunagoke green panel clearly showed that the insulation effect suppressed the interior temperature. Plus, moisture in the moist Sunagoke green panel further provided additional evaporation cooling effect to the model house. Thus, the moist model house S3m had the lowest interior temperature than the other

two. The idea of applying water on green roof was to effectively divert the incoming radiation to latent heat. By doing so, the heat energy which warmed the interior cavity of a building can be reduced hence, lessening the temperature load as encouraged by Clements et al. [15] and Wang et al. [60] in their publications. In the real application, applying water on the green roof on peak warm hours (e.g. afternoon) can help to regulate the interior temperature efficiently. Nevertheless, supplementary studies are needed to verify the extent of temperature reduction by applying water in the low ambient temperature environment such as night time and winter days since overcooling may happen in such situations.

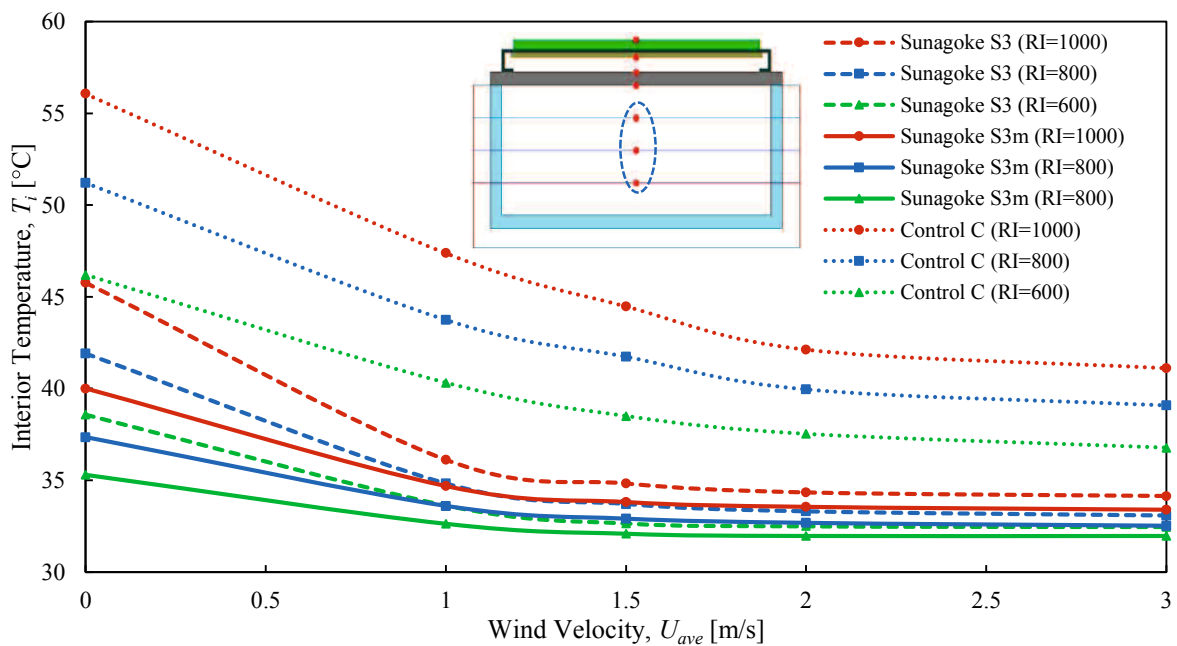


Fig. 4-16. Interior temperature of each model houses associated to each experimental condition.

Dimensionless temperature

To further analyse the cooling characteristic that occurred in the model houses, a dimensionless temperature ratio was proposed to determine the normalised temperature difference. The temperature ratio was constructed by taking the differences in temperature between surface and interior temperatures, relative to differences in temperature between interior and ambient temperatures. High ratio in Fig. 4-17 specifies more influence from the roof surface condition, affecting the rise of interior temperature. On the other hand, low ratio meant there was more heat transferred to the atmosphere and less heat penetration into the interior cavity. Both temperature driving forces were balanced on dry Sunagoke moss in forced convection region as the temperature ratios were close to 1. Though, a dissimilar finding was seen on moist Sunagoke moss. Since the evaporation consumed most of the heat on moist Sunagoke moss, the temperature ratio was lower as compared to the other two model houses, and the ratio further diminished near the 0-axis in forced convection region. Therefore, to reduce the cooling load of a building, the heat facing roof surface need, in the first place, to be mitigated. This kind of temperature ratio may be a base line to compare the thermal performance of other green roof plants.

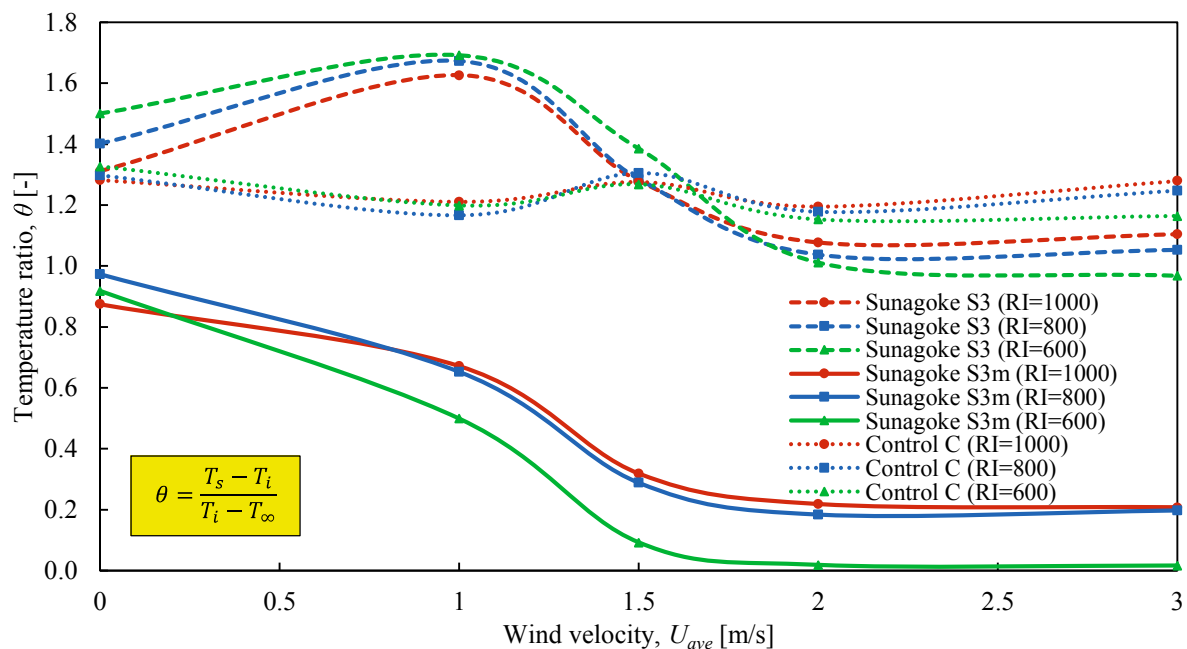


Fig. 4-17. Normalised temperature difference associated with interior temperature, surface temperature and ambient temperature.

4-5 Chapter Summary

The outcomes demonstrated in this chapter clarified the effects of wind velocity and irradiance on the thermal performance of the Sunagoke moss green roof. Despite being a nearly maintenance-free green roof plant, both dry and moist Sunagoke green roofs showed a decent shading and evaporation cooling performance in regulating the heat balance that occurred on the roof. Through finding the heat balance proportion, the convection heat was found to dominate the whole heat transfer in dry Sunagoke moss and control roof surfaces which lack of evaporation. In contrast, the latent heat of moist Sunagoke green roof governed and diverted 70% from the whole heat transfer process in natural, and 91% in forced convection region. The latent heat and convection heat were inversely related to each other, verified by the Bowen ratio. Besides moist Sunagoke moss in combined and forced convection, there were no correlation between irradiance and convection heat transfer coefficient. Meanwhile, the albedo of Sunagoke moss green panel was influenced by irradiance strength, not the wind velocity. Nevertheless, the effects of wind velocity on Sunagoke moss green roof above 2 m/s were clarified identical since no significant changes were found in the convection heat transfer coefficient, surface temperature, conduction heat flux, and interior temperature afterwards. The results displayed can be used further in examining the system by a 3-dimensional thermal fluid numerical simulation to establish a Sunagoke green roof control system.

The results in this dissertation applies to locations which have similar environment with the Artificial Climate Chamber. Conclusions drawn may not fully describe the heat transfer in a whole day, but only at a certain part of time, for example at noon where the peak ambient temperature is usually present. In the actual application, the environmental parameters would likely change through time, especially the wind velocity. Wind velocity fluctuations may disrupt the thermal inertia and time constant of the system. Either in a warmer or cooler climate, the heat balance proportions and normalised temperature differences would remain similar throughout the day. Future exploration should focus on utilising other parameters for the laboratory approach such as variation of ambient temperature and humidity. Besides, altering the thickness of the Sunagoke moss to investigate the evaporation behaviour should be taken into account as well.

4-6 Equipment List in Chapter 4

1. Artificial Climate Chamber
 - Manufacturer : Marui Co., Ltd.
 - Model : MC-402
 - Temperature fluctuation error : ± 0.5 [°C]
 - Humidity fluctuation error : ± 3 [%]
 - Temperature gradient : 10 [°C / hr]
 - Irradiance intensity : 0 ~ 1000 [kcal / hm²] (specimen surface)
 - Irradiance indication system : 1 [kcal / hm²]
 - Irradiance distribution system : ± 20 [%]
 - Temperature control range : -20 [°C] ~ 50 [°C]
 - Humidity control range : 30 [% RH] ~ 90 [% RH]

2. Portable data logger
 - Manufacturer : Yokogawa Electric Co., Ltd.
 - Model : Datum-Y XL100
 - Temperature range : 0 ~ 350 [°C]

3. Temperature and humidity loggers
 - Manufacturer : T & D Co., Ltd.
 - Model : RTR-53A
 - Temperature measurement accuracy : 0 ~ 50 [°C]
 - Humidity measurements accuracy : 10 ~ 95 [%]

4. Temperature and humidity sensor
 - Manufacturer : Hioki Co., Ltd.
 - Model : 3641 Type
 - Number of channels : 2ch
 - Highest decomposition : 0.1 [°C]

5. Electronic balance
 - Manufacturer : A&D Co., Ltd.
 - Model : EK-6100i
 - Measuring range : 0.1 ~ 6000 [g]

6. Lightweight data logger for electronic balance

| | |
|-------------------|-----------------|
| Manufacturer | : A&D Co., Ltd. |
| Model | : AD-1688 |
| Measurement range | : 0.1~6000 [g] |

7. Pyranometer

| | |
|---------------------|-------------------------------------|
| Manufacturer | : Eko Instruments Co., Ltd. |
| Model | : MS-402 |
| Instrument constant | : 6.99 [mV / kW · m ⁻²] |
| Internal resistance | : 500 [Ω] |
| Wavelength range | : 285-2800 [nm] |

8. Albedometer

| | |
|---------------------|--|
| Manufacturer | : Delta Ohm |
| Model | : LP-PYRA-06 |
| Instrument constant | : 15.15 [mV / kW · m ⁻²] for up 15.55 [mV / kW · m ⁻²] for down |
| Internal resistance | : 37.6 [Ω] for up 36.9 [Ω] for down |
| Wavelength range | : 305-2800 [nm] |

9. Environment Recorder (Vane-type anemometer)

| | |
|--------------------------|-----------------------|
| Manufacturer | : Sato Shouji Inc. |
| Model | : EM-SD |
| Wind velocity range | : 0.4~25.0 [m/s] |
| Wind velocity resolution | : 0.1 [m/s] |
| Wind velocity accuracy | : ± (2 % + 0.2 [m/s]) |
| Temperature range | : 0~50 [°C] |
| Temperature resolution | : 0.1 [°C] |
| Temperature accuracy | : ± 0.8 [°C] |

10. Blower fan

| | |
|-------------------|------------------------------|
| Manufacturer | : SIS |
| Model | : SHT-250 |
| Voltage rating | : 100V 50/60 [Hz] |
| Power consumption | : 337 [W] |
| Wind velocity | : 500 [cm ³ /min] |

| | |
|--------------------------------------|--------------------------------------|
| Rotation speed | : 3323 [RPM] |
| Number of wings | : 7 |
| 11. Blower fan inverter | |
| Manufacturer | : Mitsubishi Electric Corporation |
| Model | : FR-FS2-0.4K |
| Input voltage, frequency | : Single phase 100 [V], 50/60 [Hz] |
| Operating frequency changeable range | : 22~60Hz |
| 12. Honey-comb funnel | |
| Manufacturer | : Shin Nippon Feather Core Co., Ltd. |
| Model | : V-13-100 |
| Cell size | : 13 [mm] |
| Film thickness | : 100 [μm] |
| Density | : 26 [kg/m^3] |
| 13. Infrared dryer bulb | |
| Manufacturer | : TOKI |
| Model | : IR200/220V125WRHK |
| Radiation efficiency | : Above 62% |
| Power consumption | : 125 [W] |
| Life | : 5000 [h] |

Chapter 5 - Indoor Experiment: Effects of Irradiance Angle on Sunagoke Moss Green Roof

5-1 Experiment Introduction

In this chapter, the author conducted indoor laboratory experiment by utilizing controllable parameter to fix the experiment conditions. As the experiment location, the author carried out the experiment inside an Artificial Climate Chamber (ACC) in Yamaguchi Prefectural Industrial Technology Institute. As described in Fig. 5-1, in ACC, the total radiation, ambient temperature and humidity could be technically controlled by the illustrated devices. Here, the ambient temperature and humidity refers to the temperature and humidity inside the ACC.

The total radiation source was radiated by the infrared dryer bulb in Solar Radiation Irradiation Device. Differs with chapter 4, in this chapter, the total radiation in Eq. (3-3) was only considered as irradiance solely without the subtraction of reflected radiation flux since on the time these experiments were conducted, there was no usage of albedometer yet. Since the simulating outdoor conditions inside ACC, the comparison of solar radiation spectral distribution and infrared dryer bulb irradiation spectral distribution is shown in Fig. 5-2 and Fig. 5-3. The infrared dryer bulb irradiation spectral distribution graph was taken from the manufacturer; Iwasaki Electric Co., Ltd.. From the graph, it can be seen that the radiation radiated by the infrared dryer bulb is similar to solar radiation properties of wavelength and specific energy. In addition, the author controlled the angle of Solar Radiation Irradiation Device (SRID) to imitate the movement of sun. By means of imitating sun movements in day time, the author set the SRID angle to 30°, 45°, 60° and 90°.

Based from National Astronomical Observatory of Japan website, summer season in Yamaguchi Japan located on latitude 34.1833°, longitude 131.4667°, altitude 0.0 m, and time UT+9h regularly encounter sunrise on about 5:00 AM while sunset on 7:30 PM. Winter season on the other hand encounter sunrise around 7:20 AM and sunset on 5:20 PM. By marking the sunrise on 0° and sunset on 180°, hence if the period of time from sunrise to sunset is divided

by 180°, the time for each angle can be known. The details of time of day according to the sun angle and season are shown in Table 5-1. By changing the irradiance angle as shown in Fig 5-4, the author simulated the sun movements to quantitatively evaluate the effects of green roof according to time.

The evaluation subject mainly focussed on the changes of each heat quantity in the heat balance equation. In this chapter, the author evaluated the changes of conduction heat, convection heat and latent heat that exerts on model houses of dry Sunagoke S3, moist Sunagoke S3m and Control C when different irradiance angles and irradiances are inflicted on the model houses. The appearance of S3, S3m and C, together with evaluation classification are shown in Fig. 5-5. These model houses were placed under SRID to evaluate the changes of conduction heat, convection heat and latent heat of each model houses.

Table 5-1. Sun Angle and Time.

| Sun Angle | Summer 2015 July | Winter 2015 January |
|---------------|------------------|---------------------|
| 0° (Sunrise) | 05:00 | 07:20 |
| 30° | 07:25 | 09:00 |
| 45° | 08:38 | 09:50 |
| 60° | 09:50 | 10:40 |
| 90° | 12:15 | 12:20 |
| 120° | 14:40 | 14:00 |
| 135° | 15:53 | 14:50 |
| 150° | 17:05 | 15:40 |
| 180° (Sunset) | 19:30 | 17:20 |

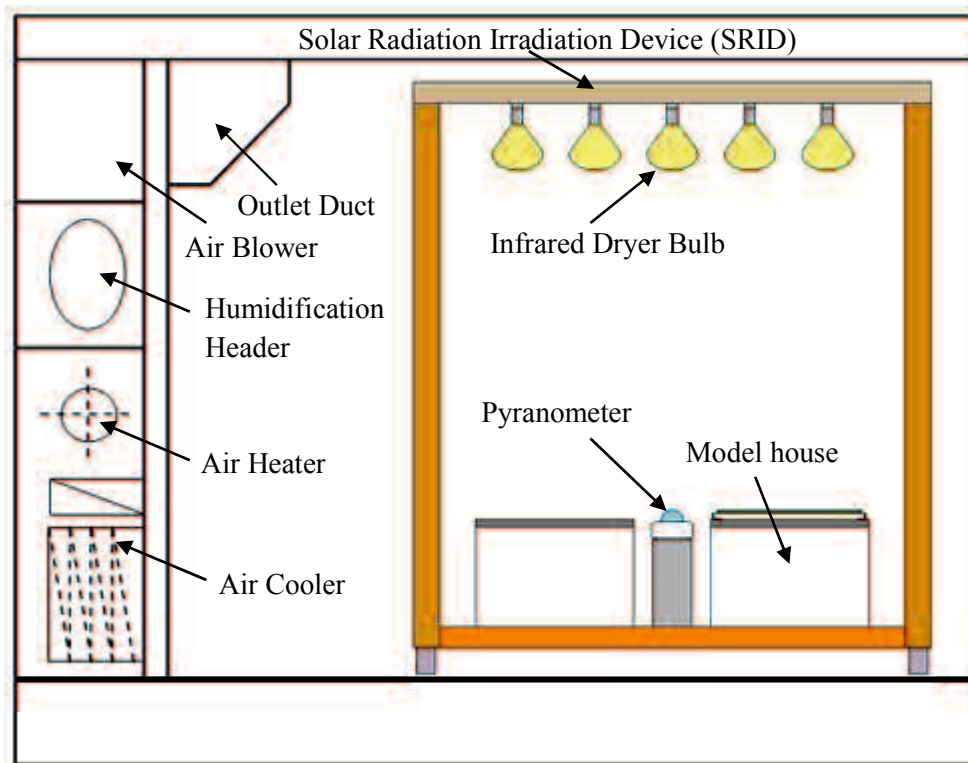


Fig. 5-1. Equipment in Artificial Climate Chamber.

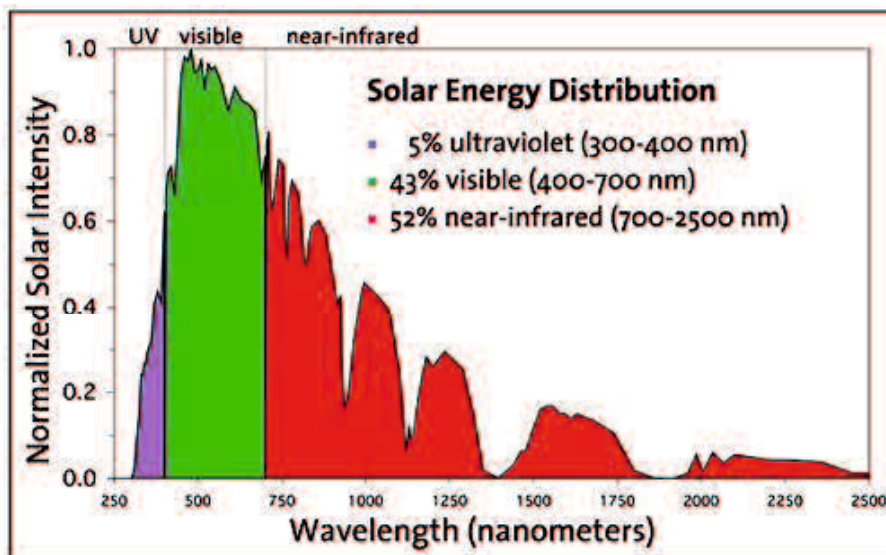


Fig. 5-2. Solar Radiation Spectral Distribution.

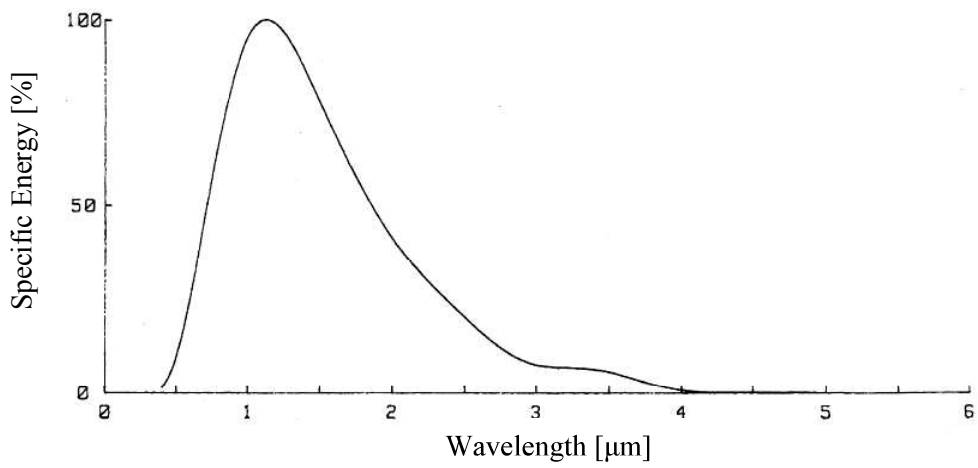


Fig. 5-3. Infrared Dryer Bulb Irradiation Spectral Distribution.

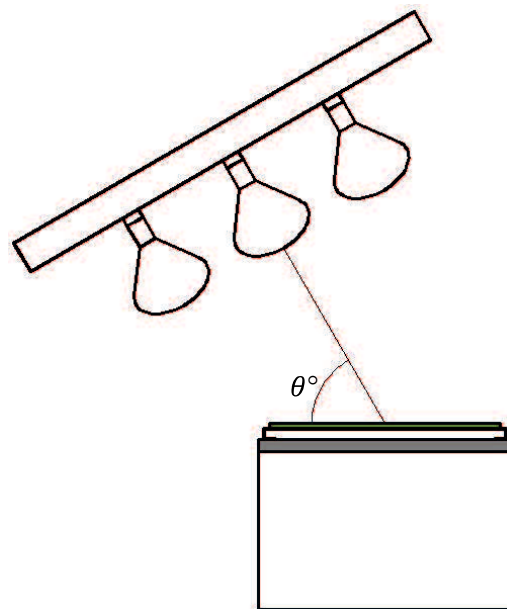


Fig. 5-4. Solar Radiation Irradiation Device irradiance angle (side view).

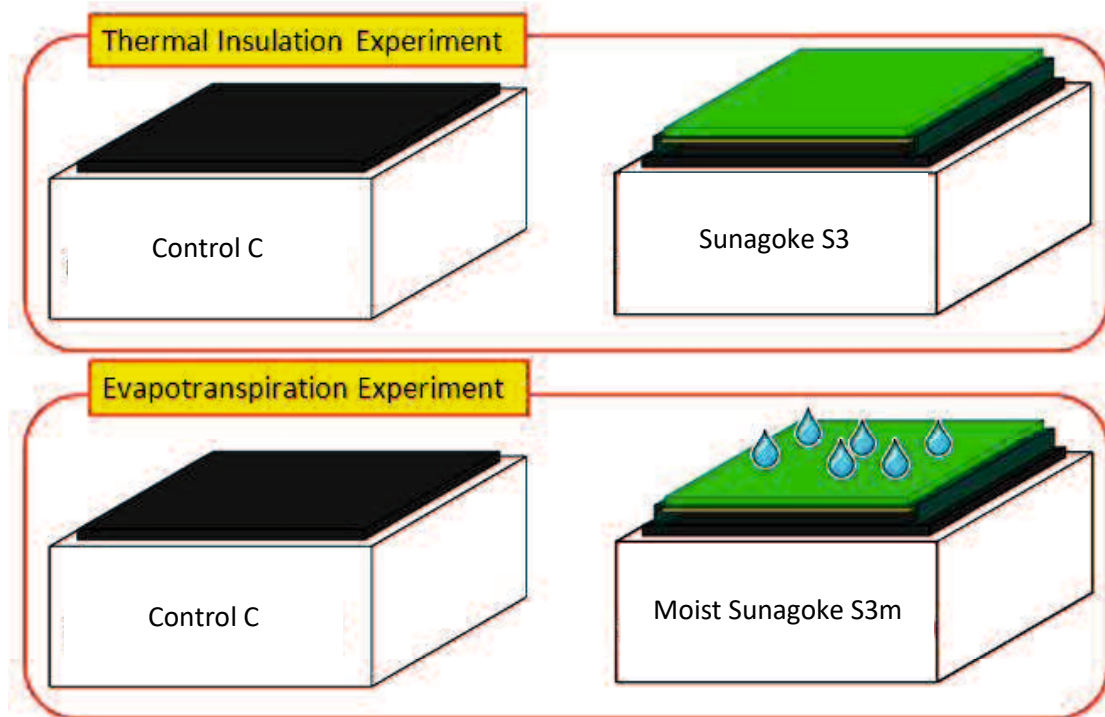


Fig. 5-5. Appearance of model houses Sunagoke S3, Moist Sunagoke S3m and Control C.

5-2 Experimental Conditions

Laboratory based indoor experiments were conducted inside the Artificial Climate Chamber according to experimental conditions in Table 5-2. The graphs for ambient temperature T_{∞} and ambient humidity RH , and total radiation R_T were shown in Fig. 5-6 and Fig. 5-7 respectively. Here, the ambient temperature and humidity were measured by T-type thermocouple and humidity sensor placed inside an instrument shelter positioned 1200 mm above ACC's floor. In ACC, as there is no artificial wind applied on model house, forced convection are not considered, while only natural convection was assumed to occur. Besides, the total radiation was measured by pyranometer positioned 800 mm below SRID, at same level with model houses roof level.

Table 5-2. Artificial Climate Chamber conditions.

| Parameter | Value |
|--|--|
| Ambient Temperature, T_{∞} [°C] | 30 |
| Ambient Humidity, RH [%RH] | 70 |
| Wind Velocity, U_{ave} [ms^{-1}] | 0 |
| Hydration Water Volume of S3m [mL] | 100 |
| Irradiance, R_T [W/m^2] | 200, 400, 600, 800, 1000 |
| Irradiance angle, φ [°] | 30, 45, 60, 90 |
| Model houses | Sunagoke S3, Moist Sunagoke S3m, Control C |

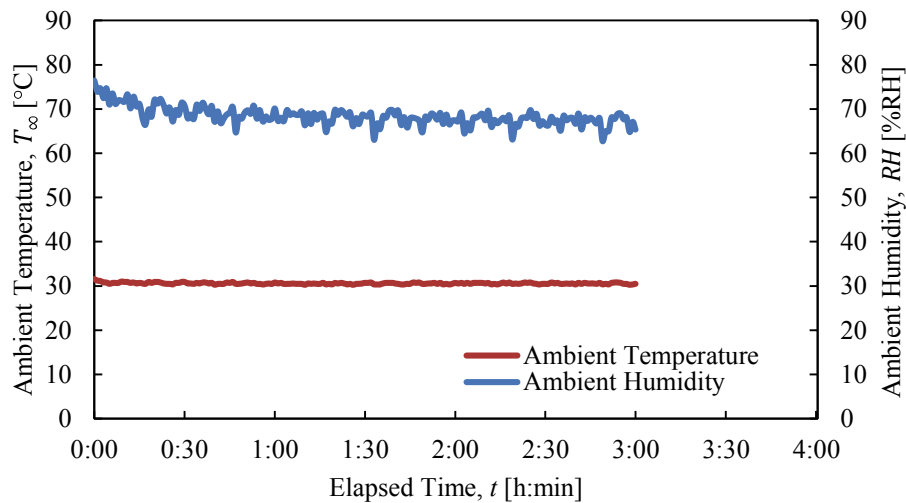


Fig. 5-6. Ambient conditions.

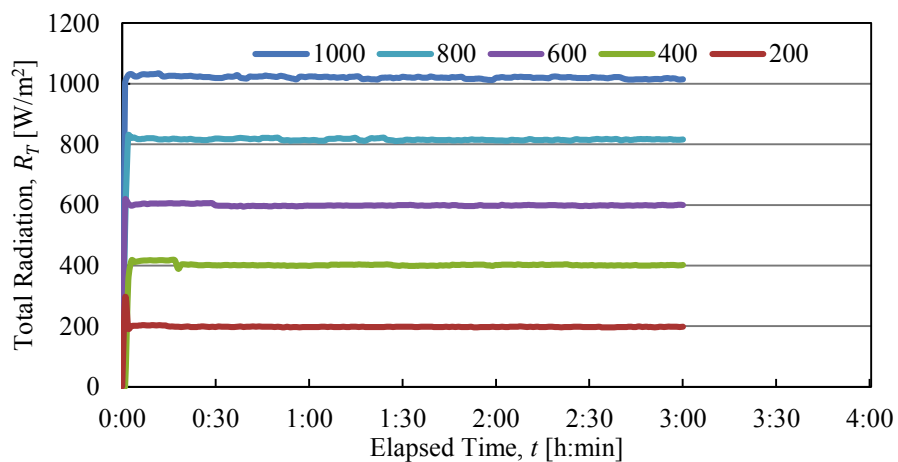


Fig. 5-7. Total radiation measured by pyranometer.

5-3 Experimental Methodology

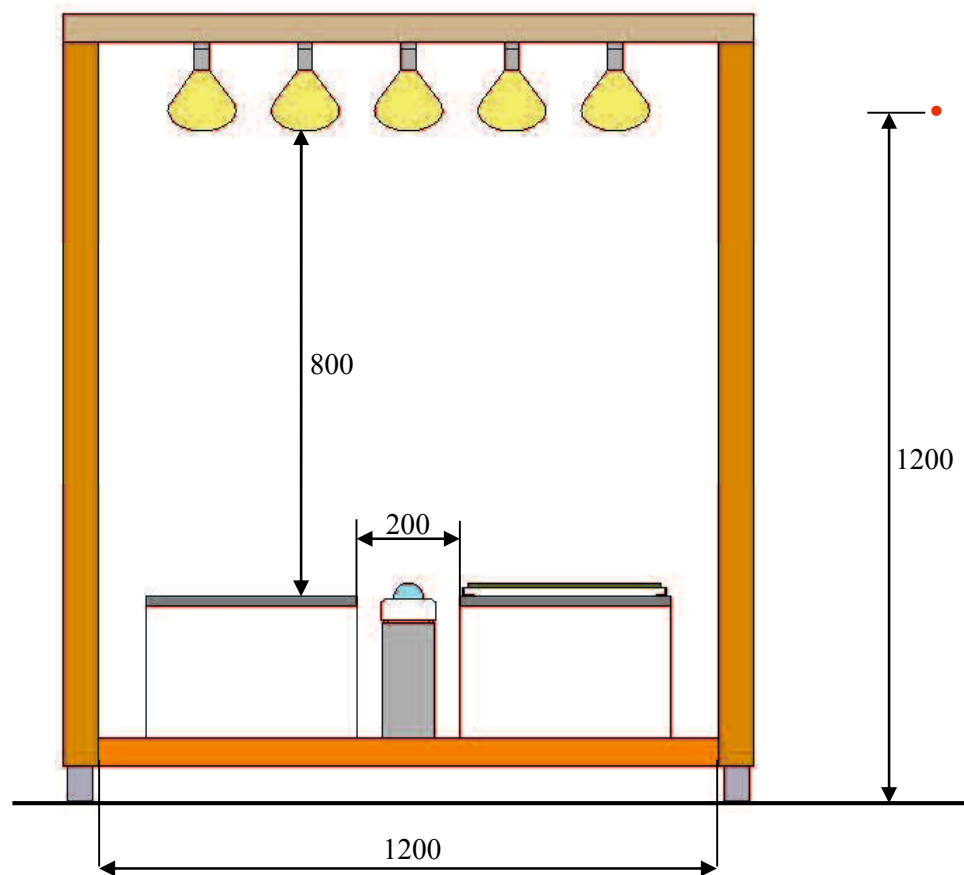
In these indoor experiments, 3 different types of model houses; S3, S3m and C were used to evaluate the effect of irradiance angle on the green panel. An overview of the experimental apparatus in indoor laboratory experiment was shown in Fig. 5-8. The model houses were placed under SRID with environment conditions set by ACC. The model houses were positioned 200 [mm] from each other to allow wind circulate around model houses.

Temperature measurement was taken at each temperature measuring points within 1 minute intervals for 4 hours as 1 cycle and recorded in a portable data logger. Similar with experiments in chapter 4, the ambient temperature and humidity sensor were placed inside an instrument shelter positioned 1.2 m above floor and recorded by a data logger. Meanwhile, the weight of S3m was measured by electronic balance, placed below S3m and recorded in a lightweight data logger within 1 minute interval to measure the evaporation amount. The SRID was positioned 800 mm directly above roof part of model house to simulate sun at 90° position. The SRID angle is adjusted to 30°, 45°, 60°, and 90° according to experiment repetition. 2 pyranometers were placed in parallel between the model houses; one for controlling the irradiance amount from infrared dryer bulb (control system), and the other one was for measuring the total radiation received by the model house. This time, the total radiation received by model houses was considered as equal to the SRID irradiance amount, without considering the reflected radiation, since the albedometer was not available during the experiments.

The indoor experiments in this chapter were conducted according to the following procedures:

- 1) Prepare the model houses (S3, S3m or C,) according to experiment conditions.
- 2) Set SRID angle to 30° according to experiment condition.
- 3) Operate the Artificial Climate Chamber to control the interior conditions match to experiment conditions. Set the ambient temperature to 30°C and humidity to 70 %RH.
- 4) Allow the interior conditions of ACC to reach steady state before starting the experiment.
- 5) Start logging readings for every data logger. For evaporation experiment, start logging the weight of S3m via lightweight logger.

- 6) Operate the SRID irradiance from 200 W/m^2 to 1000 W/m^2 according to experiment condition. On the same time, apply 100 ml of water thoroughly on S3m green panel by water sprayer for evaporation experiment.
- 7) Stop every data logger when 3 hour elapsed and turn off SRID irradiance. Here the experiment may be stopped earlier, because there is a possibility that model house roof plate may be damaged when SRID irradiance angle is low and the irradiance is high.
- 8) Repeat the procedures from 1) to 7) for all SRID irradiance angles; 45° , 60° and 90° .
- 9) Repeat experiment for each experiment conditions 2 or 3 times to get reliable data.



• : Location for ambient temperature and humidity sensor

Fig. 5-8. Schematic indoor experiment apparatus diagram.

5-4 Results and Discussions

5-4-1 Effects of Irradiance Angle on Heat Balance

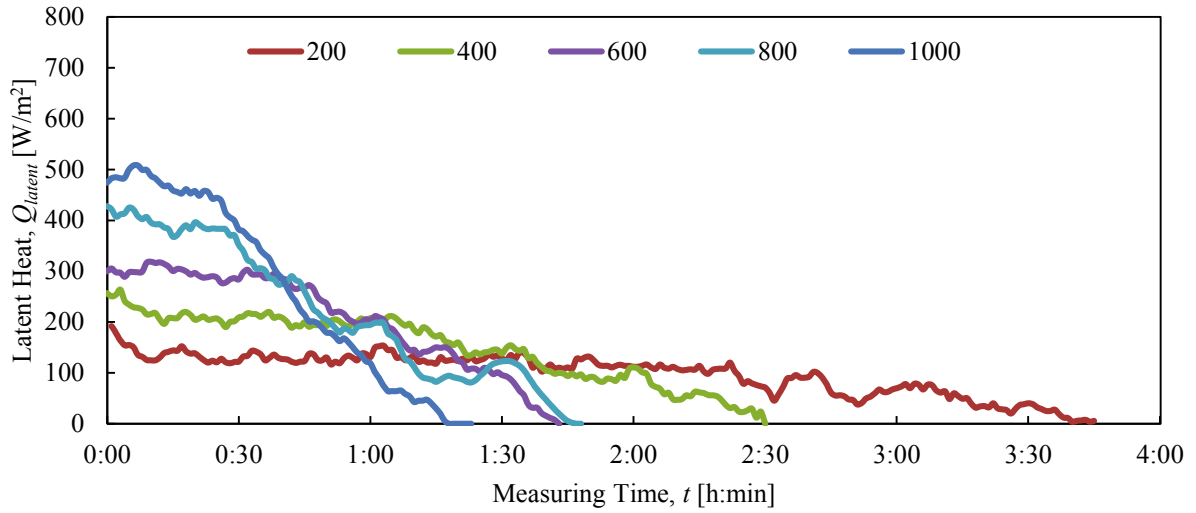
By measuring each temperature measuring points in model house as described in Chapter 3, the heat quantities exerted on each model house can be determined. By referring on heat balance equation Eq. (3-2), the author determined each heat quantity; conduction heat $Q_{conduction}$, convection heat $Q_{convection}$, and latent heat Q_{latent} for each model house. Note that only S3m was applied with water, and by considering only S3m releases latent heat, only latent heat for S3m was calculated. Based on experiment conditions where the total radiation was set for 200, 400, 600, 800 and 1000 W/m² and SRID irradiance angle φ at 30°, 45°, 60° and 90°, 20 data results were collected for evaluation. However, during the experiments for φ at 45°, because there were problems with the ACC, the experimental conditions were not stable like other angles experiments, thus the results for φ at 45° experiments will not be shown in this dissertation as they were kept only as the reference data. Therefore, the calculation results for each heat quantity when SRID irradiance angle φ at 30°, 60° and 90° will be explained in the subsequent paragraphs.

Latent Heat on S3m

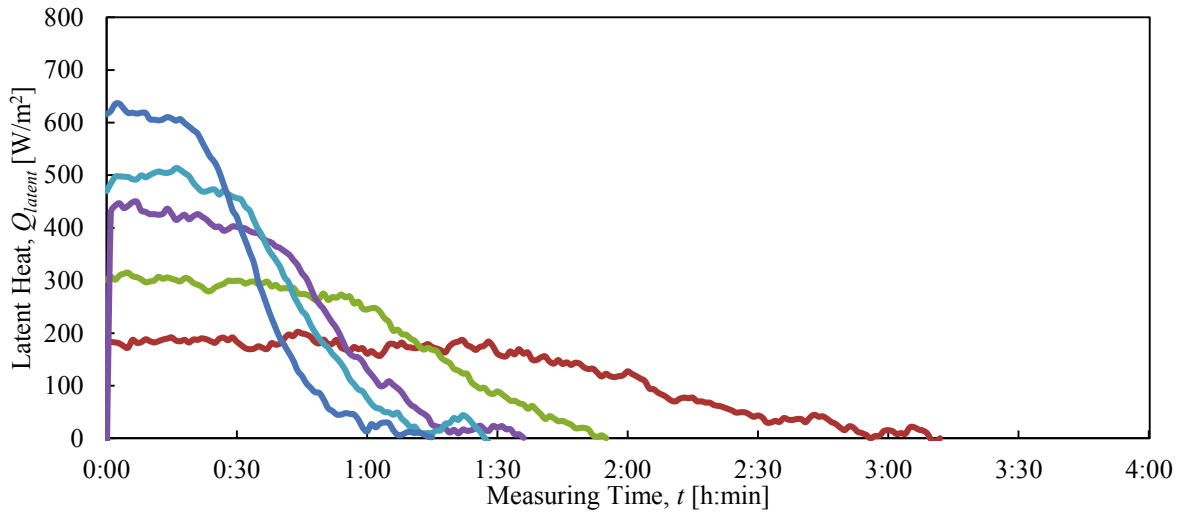
Differed from model houses C and S3, S3m was hydrated with 100 mL of water thoroughly on the green surface in order to allow the heat transport of latent heat by evaporation process. By substituting evaporation amount into Eq. (3-11), the latent heat Q_{latent} of S3m according to each total radiation R_T and SRID irradiance angle φ could be derived. Latent heat amount depends on evaporation amount, ambient temperature, humidity, total radiation and wind velocity encountered on the Sunagoke green panel surface. The calculation results were plotted in graphs as shown in Fig. 5-9 (a) to (c).

By referring Fig. 5-9 (a) to (c), the form of latent heat Q_{latent} could be seen when total radiation and SRID irradiance angle changed. From the starting point of experiment where the water was applied on S3m, the evaporation started to activate and latent heat started to generate. At some point where the latent heat has reached steady state, the amount of latent heat became constant along some period. This form of latent heat can be seen due to steady environment parameters of ambient temperature, humidity and total radiation. Nevertheless, the period of constant latent heat decreases upon increment of total radiation. Higher amount of total radiation leads to higher evaporation amount, which then increase the latent heat amount. However, because of the water content was fixed, higher latent heat will consume all the water content and approaches dry state faster. Further, when the water content of Sunagoke is insufficient to maintain the latent heat, the latent heat started to decrease and finally dissipates completely as the green panel dried up.

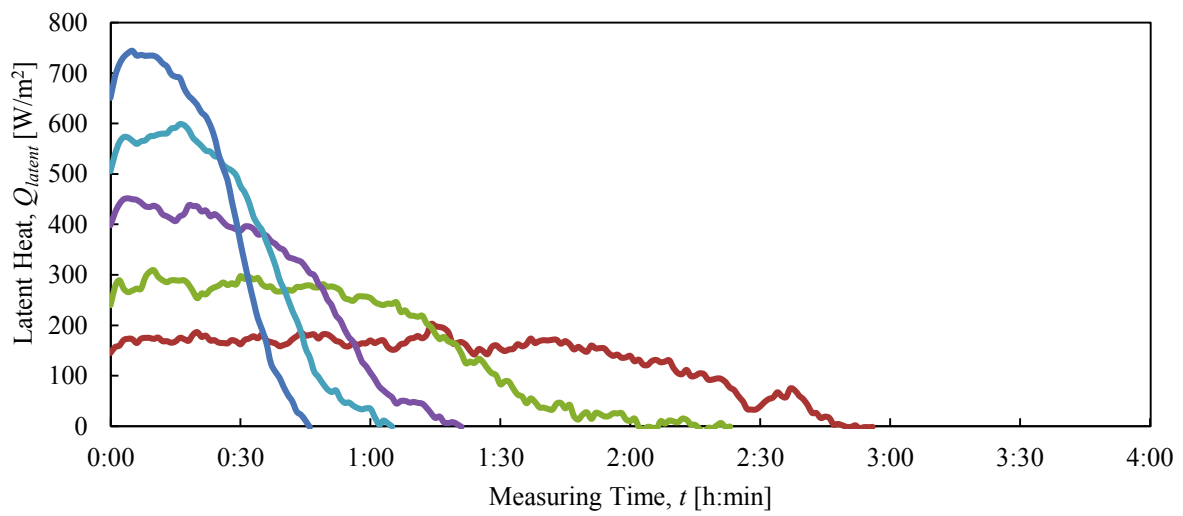
From Fig. 5-9, the steady state average latent heats in each parameter conditions were calculated and the results were plotted in graph as depicted in Fig. 5-10. By referring to the graph, the relationship of latent heat with SRID irradiance angle and total radiation had become cleared. Overall, the latent heat increases when both SRID irradiance angle and total radiation increases. Therefore, the evaporation latent heat was clarified to be the highest when φ is set at 90° . Furthermore, based on the gradient shown in the graph, the projection of latent heat when certain amount of total radiation is radiated on moist green panel, at certain irradiance angle corresponds to sun location, can also be estimated.



(a) $\varphi = 30^\circ$



(b) $\varphi = 60^\circ$



(c) $\varphi = 90^\circ$

Fig. 5-9. Latent heat E according to R_T and φ in moist green panel condition.

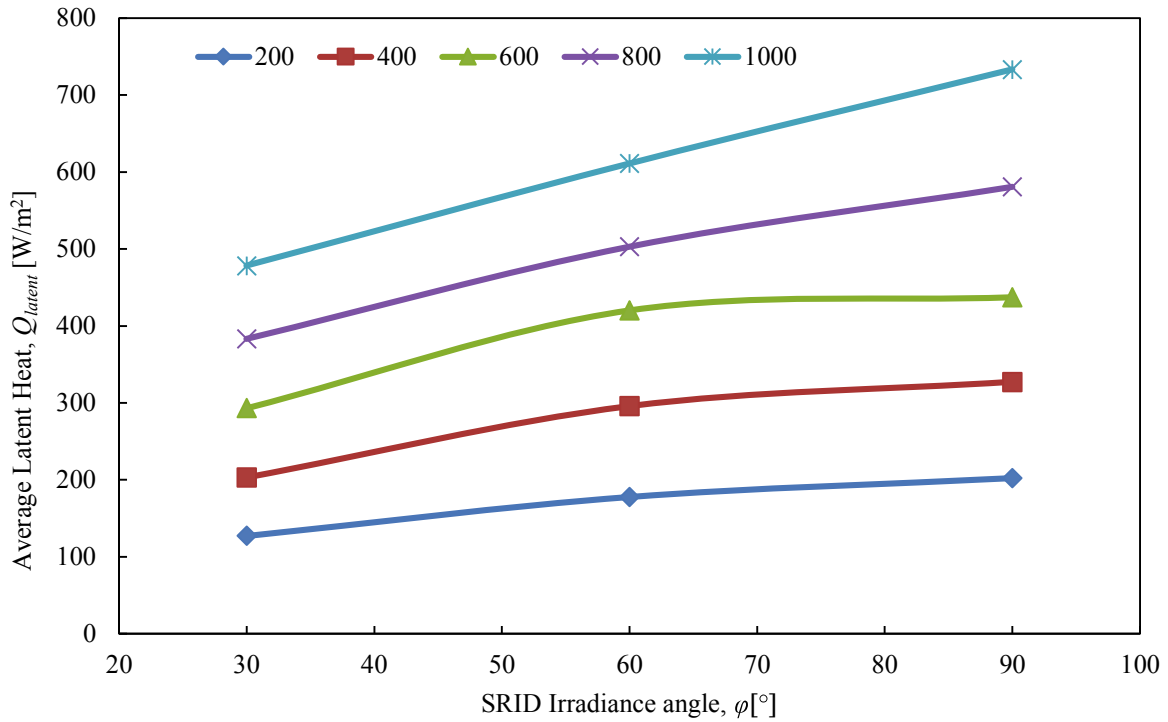


Fig. 5-10. Average steady-state latent heat Q_{latent} according to ϕ and R_T .

Evaporation Efficiency of S3m

From the derivation of convection heat $Q_{convection_S3m}$ and evaporation amount e , the average steady-state evaporation ratio n to evaluate the evaporation characteristics of green panel is calculated by using Eq. (3-18). The calculation results are depicted in Fig. 5-11 (a) and (b). Note that the x-axis for Fig. 5-11 (a) is the total radiation R_T while Fig. 5-11 (b) is the modified x-axis graph of SRID irradiance angle ϕ . Now, since the evaporation ratio only cover from 0 to 1, the y-axis for both graphs have been adjusted to upper limit of 1.0 and lower limit of 0.0.

Base on Fig. 5-11 (a), the relationship of evaporation ratio with total radiation can be seen constant through the total radiation. Although there are small changes of evaporation ratio when the total radiation increases, but overall, the evaporation ratio can be concluded as constant and irrespective with the total radiation. However, the evaporation ratio seems to be increasing with the increment of SRID irradiance angle as shown in Fig. 5-11 (b). Here, the evaporation ratio shows highest amount when SRID irradiance angle is set at 90° , while the lowest value is shown at SRID irradiance angle of 30° . In average, when SRID irradiance angle is set at 30° , 60° , and 90° , the evaporation ratio is 0.08, 0.29, and 0.37 respectively.

As the evaporation ratio is a dimensionless quantity, it can be compared with other object's evaporation ratio. For reference, paddy has recorded 0.5~0.8 [61] of evaporation ratio, while 0.2~0.4 for grassland, 0.15 [62] for Hedera helix, and 0.21 for Euonymus fortunei. Compared to other greening method, the green panel in this study showed a comparable value. For example, Ishida [51] has reported the evaporation ratio of 0.22 by conducting the evaluation experiment in outdoor summer environment. Thus the evaporation ratio calculated in this indoor experiment shows a similar value with the outdoor experiment by simulating the summer environment parameters. Nevertheless, as reported by Okamoto [49] the evaporation ratio of Sunagoke green panel was recorded as 0.57 in winter outdoor environment. From the above, the evaporation ratio is Sunagoke green panel is confirmed to be highly dependent on environmental conditions such as temperature, humidity, and wind velocity.

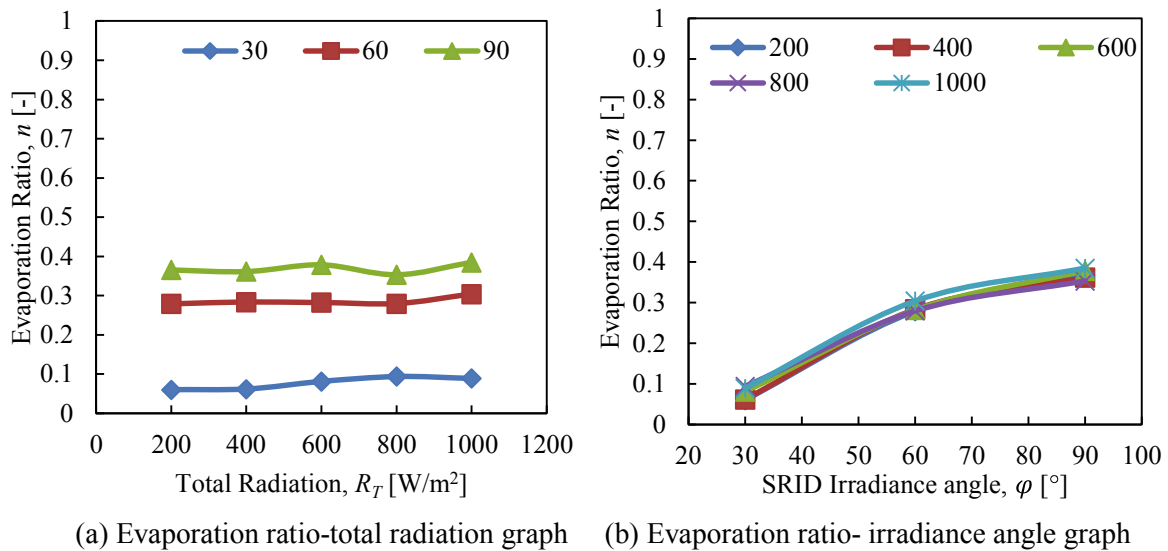


Fig. 5-11. Evaporation ratio n [-] according to each conditions.

Convection Heat on Model Houses S3, S3m and C

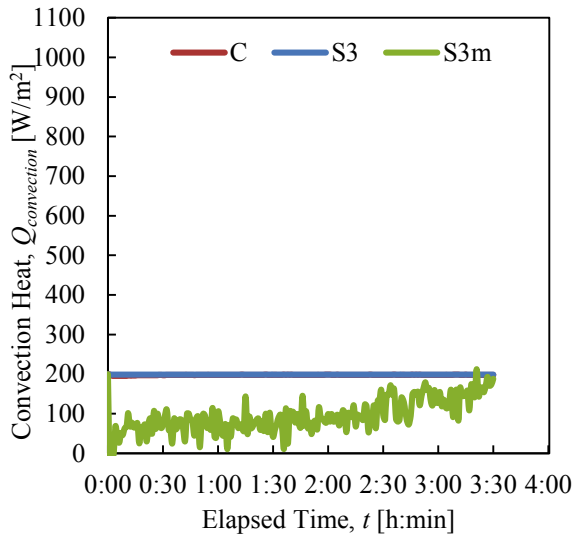
As well as conduction heat, convection heat is also a crucial heat quantity that has to be contained in the process of mitigating heat island phenomenon. In this study, the convection heat of C, S3 and S3m; $Q_{convection_C}$, $Q_{convection_S3}$ and $Q_{convection_S3m}$ were determined by Eq. (3-13) by taking the revenue minus of conduction heat $Q_{conduction}$ and latent heat Q_{latent} from total radiation R_T . Hence, the calculation results of convection heat are depicted in Fig. 5-12, Fig. 5-13 and Fig. 5-14 according to each total radiation R_T and SRID irradiance angle φ .

Through Fig. 5-12, Fig. 5-13 to Fig. 5-14, the changes of convection heat $Q_{convection}$ according to green panel condition (dry or moist) can be seen. If these graphs are observed carefully, the $Q_{convection_{S3}}$ shows slightly higher value than $Q_{convection_C}$ although the convection heat in dry green panel condition $Q_{convection_{S3}}$ shows almost similar amount with $Q_{convection_C}$ as the graph for these two convection heats are overlapping with each other. This matter occurs because the green panel on S3 had slightly higher convection heat than C, which do not installed with any green panel. Thus, it can be said that the dry Sunagoke moss green panel is able to release heat better than the control roof. On the other hand, the evaporation effect shows a really great effectiveness in reducing convection heat. Convection heat of moist green panel $Q_{convection_{S3m}}$ is relatively lower than $Q_{convection_{S3}}$ and $Q_{convection_C}$ because the latent heat produced in evaporation process snatched a huge portion of convection heat and small portion of conduction heat at the same time.

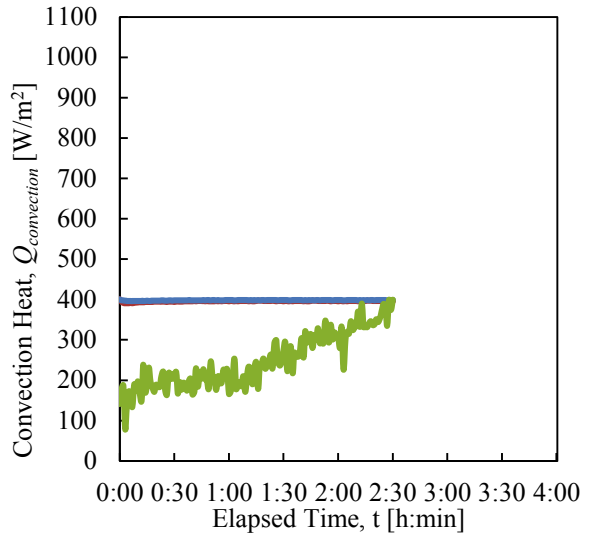
By increasing the total radiation and SRID irradiance angle, the convection heat increases as more heat energy received by roof part of C or green panels of S3 and S3m. Here, the convection heat for model house S3m also increases, but it also reduces more, when the green panel received more heat energy. Also, the reduction period of $Q_{convection_{S3m}}$ reduces as latent heat used the evaporation amount, more evaporation amount leads to more latent heat produced. Also, the longer the period of evaporation, the cooling period by latent heat also turns longer. Next, by subtracting average value in steady state between $Q_{convection_C}$ with $Q_{convection_{S3m}}$, the reduction value of convection heat in each condition can be recognized as shown in Table 5-3. In moist green panel condition, averagely, regardless the total radiation amount, convection heat can be improved approximately 286 [W/m²] at 30°, 390 [W/m²] at 60°, and 423 [W/m²] at 90°.

Table 5-3. Average convection heat reduction amount.

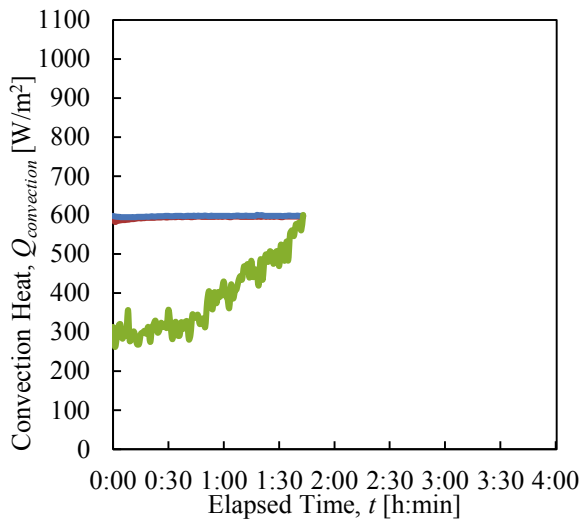
| Total Radiation, R_T [W/m ²] | Average Convection Heat Reduction $ Q_{convection_C} - Q_{convection_{S3m}} $ [W/m ²] | | |
|---|--|--------------------|--------------------|
| | $\varphi=30^\circ$ | $\varphi=60^\circ$ | $\varphi=90^\circ$ |
| 200 | 123.77 | 169.49 | 202.91 |
| 400 | 196.69 | 283.01 | 294.66 |
| 600 | 284.82 | 339.67 | 396.75 |
| 800 | 370.32 | 485.28 | 542.41 |
| 1000 | 456.72 | 670.14 | 675.87 |
| Average | 286.46 | 389.52 | 422.52 |



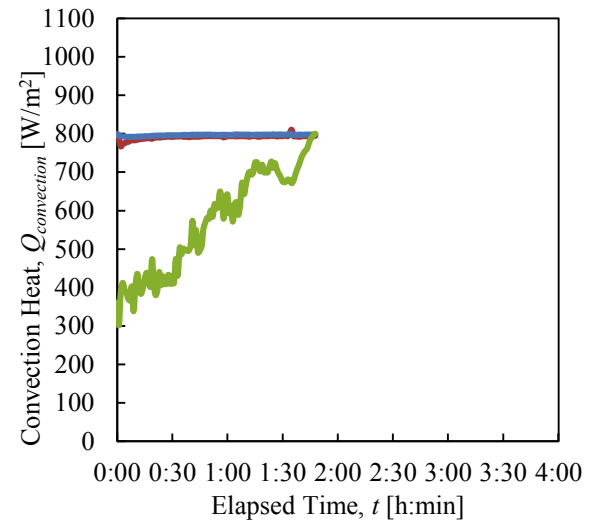
(a) $\varphi = 30^\circ$, $R_n = 200$ [W/m²]



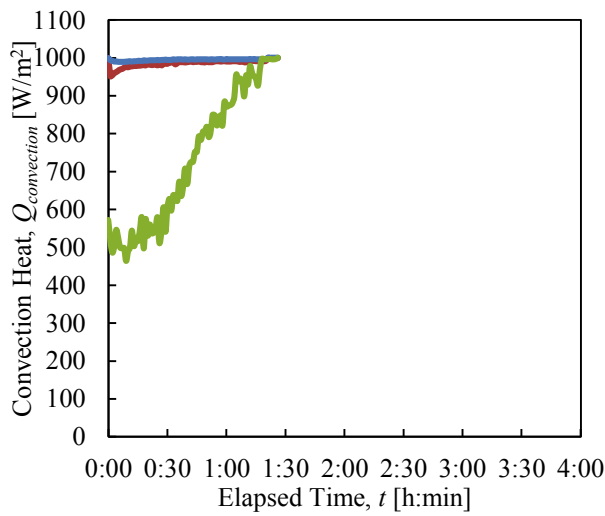
(b) $\varphi = 30^\circ$, $R_n = 400$ [W/m²]



(c) $\varphi = 30^\circ$, $R_n = 600$ [W/m²]

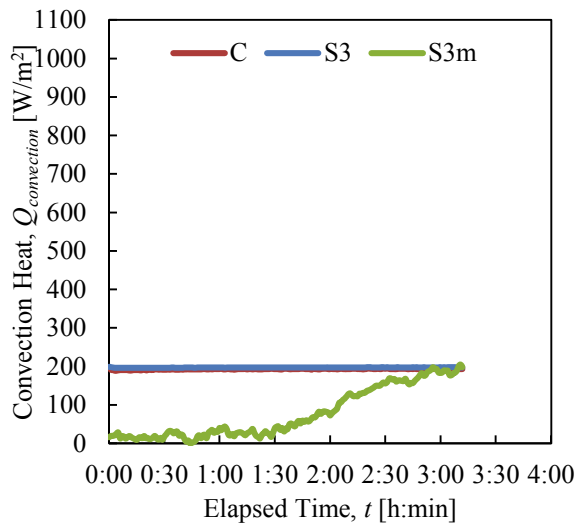


(d) $\varphi = 30^\circ$, $R_n = 800$ [W/m²]

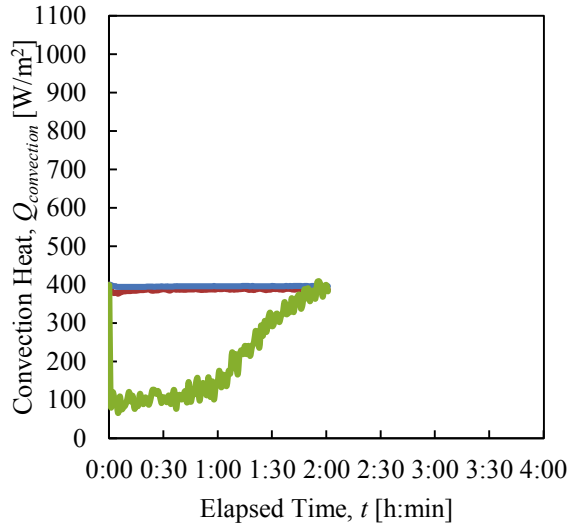


(e) $\varphi = 30^\circ$, $R_n = 1000$ [W/m²]

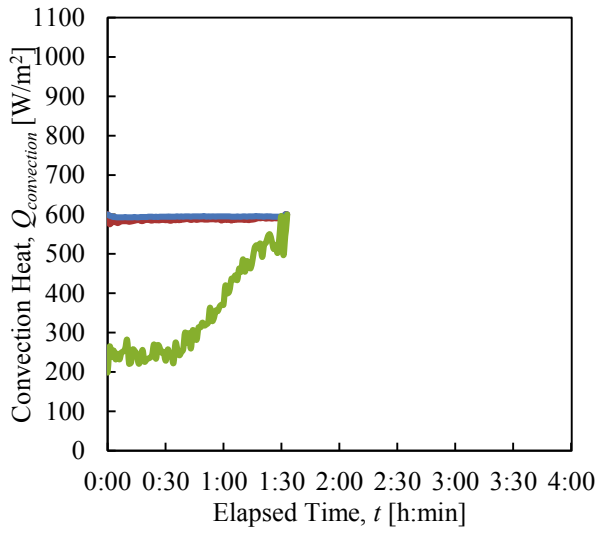
Fig. 5-12. Convection Heat of C, S3 and S3m when $\varphi = 30^\circ$.



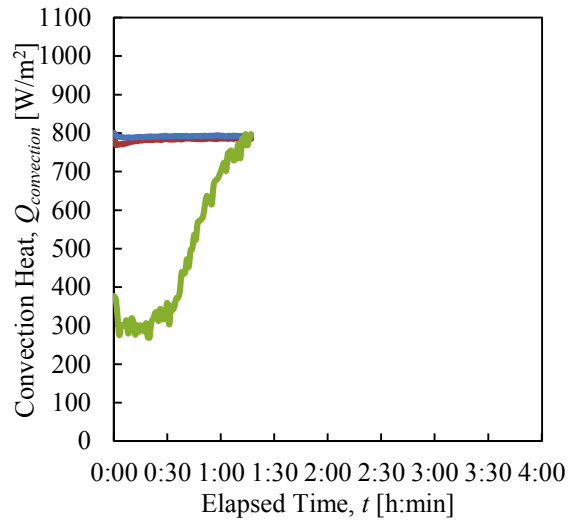
(a) $\varphi = 60^\circ$, $R_n = 200$ [W/m²]



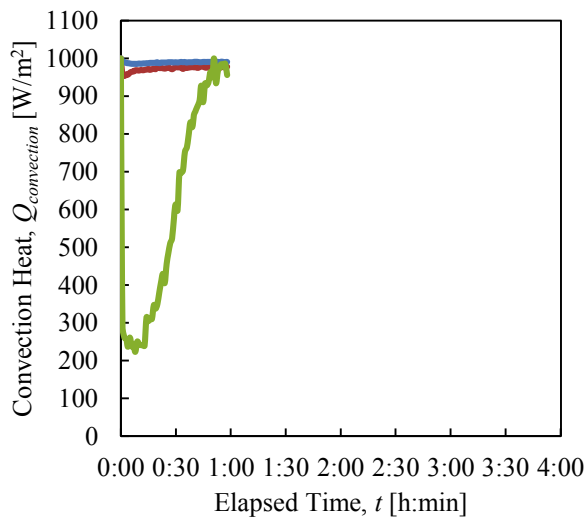
(b) $\varphi = 60^\circ$, $R_n = 400$ [W/m²]



(c) $\varphi = 60^\circ$, $R_n = 600$ [W/m²]

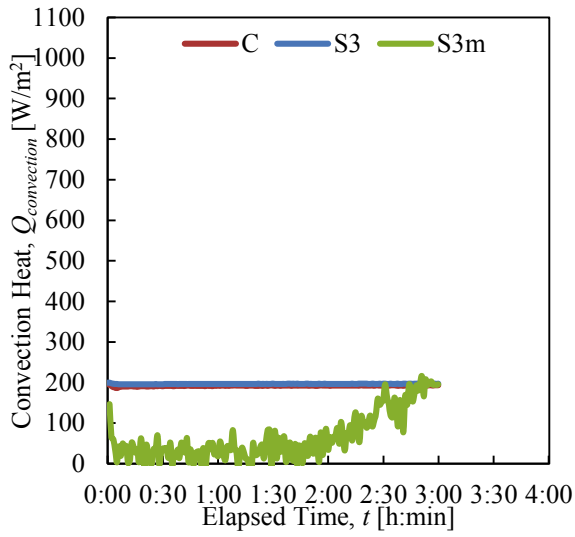


(d) $\varphi = 60^\circ$, $R_n = 800$ [W/m²]

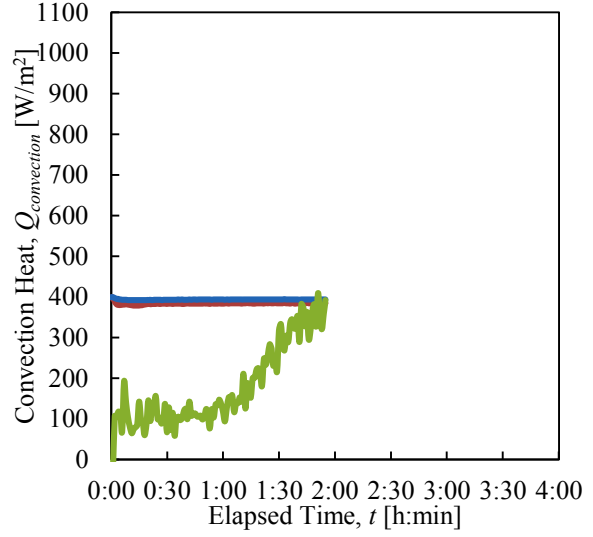


(e) $\varphi = 60^\circ$, $R_n = 1000$ [W/m²]

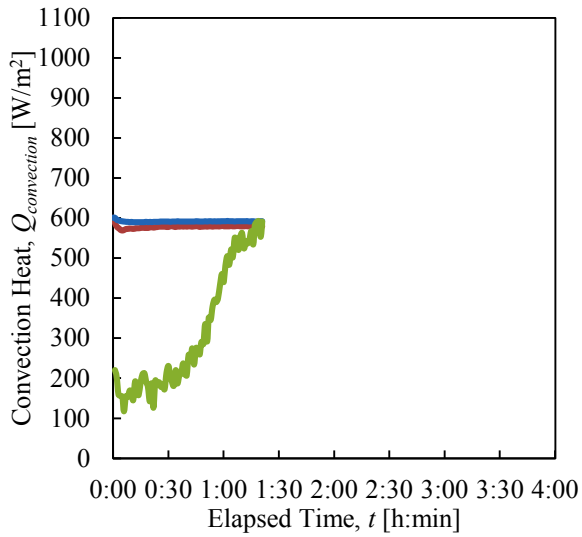
Fig. 5-13. Convection Heat of C, S3 and S3m when $\varphi = 60^\circ$.



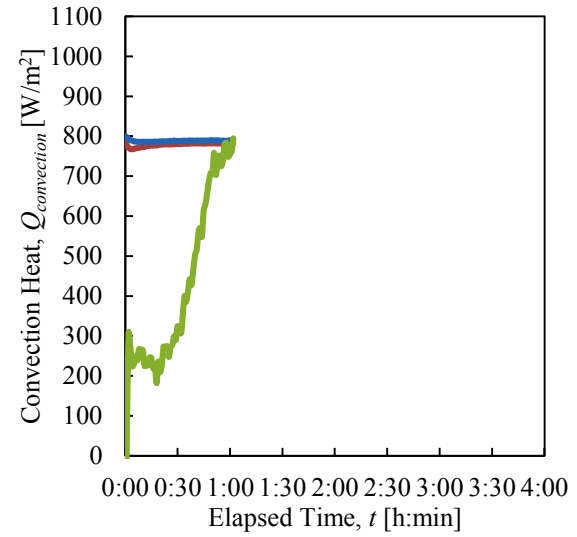
(a) $\varphi = 90^\circ$, $R_n = 200$ [W/m²]



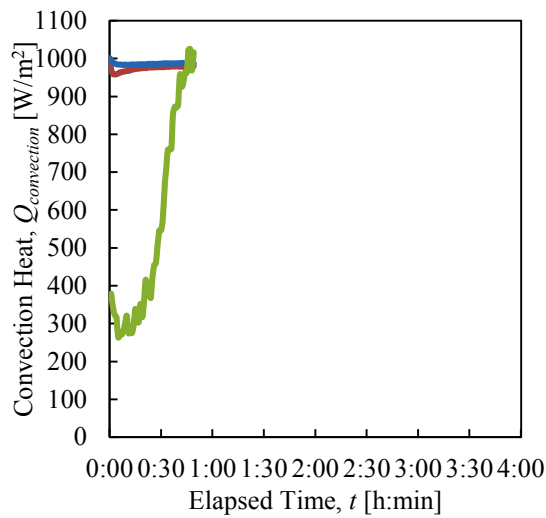
(b) $\varphi = 90^\circ$, $R_n = 400$ [W/m²]



(c) $\varphi = 90^\circ$, $R_n = 600$ [W/m²]



(d) $\varphi = 90^\circ$, $R_n = 800$ [W/m²]



(e) $\varphi = 90^\circ$, $R_n = 1000$ [W/m²]

Fig. 5-14. Convection Heat of C, S3 and S3m when $\varphi = 90^\circ$.

Conduction Heat on S3, S3m, and C

Conduction heat that pass through each model houses' green panel and roof part were calculated via Eq. (3-8). The conduction heat is defined as $Q_{conduction_C}$ for C, $Q_{conduction_S3}$ for S3, and $Q_{conduction_S3m}$ for S3m. By setting the ambient temperature T_{∞} to 30°C, relative humidity RH to 70%, total radiation R_T from 200 W/m² to 1000 W/m², and SRID irradiance angle φ at 30°, 60° and 90°, the calculation results of conduction heat for each model house was explained as follows.

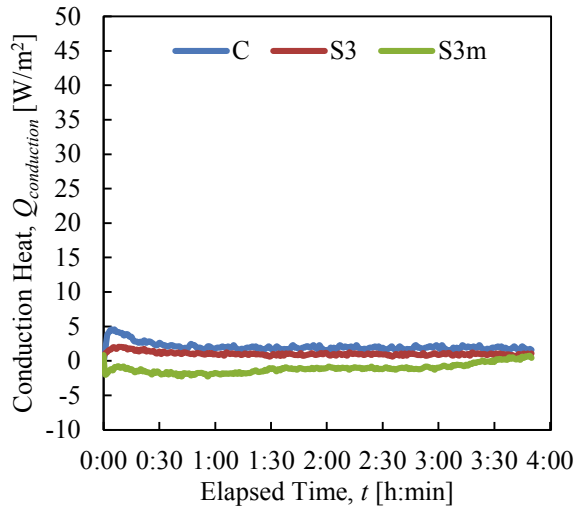
Fig. 5-15 to Fig. 5-17 depicted the calculation results of conduction heat $Q_{conduction_C}$, $Q_{conduction_S3}$ and $Q_{conduction_S3m}$ respective to each total radiation R_T and SRID irradiance angle φ . From these graphs, the conduction heat $Q_{conduction_C}$ can be seen as the highest conduction heat among the three model houses. $Q_{conduction_S3}$ showed second highest readings and lastly followed by $Q_{conduction_S3m}$ in each conditions. Here, the suppression of the conduction heat which entering the model house, by placing the green panel was confirmed. Since the conduction heat depends on the temperature differences between outermost surface and ceiling, higher surface temperature leads to higher amount of conduction heat passing through the roof part and enter the interior of model house. As the ambient temperature during the experiment was constantly at 30°C, the outermost surface temperature of C and S3 did not changed after several minutes from experiment starting time, and this makes the $Q_{conduction_C}$ and $Q_{conduction_S3}$ values constant throughout the experiments. Here, when the heat exchange between ambient air and outermost surface reach equilibrium, the temperature distribution on the roof disappeared when the roof temperature reaches certain temperature. The outermost surface of S3 and S3m which covered by Sunagoke green panel has much lower temperature if compared with C as a result of the thermal insulation effect by Sunagoke that suppressed the entrance of conduction heat.

Besides, with comparing the conduction heat between dry and moist Sunagoke moss, $Q_{conduction_S3m}$ shows lower reading than $Q_{conduction_S3}$. This occurred because S3m was hydrated with water which leads to lower green panel surface temperature when evaporation was active. When water was applied on S3m green panel, the green panel surface temperature of S3m dropped and leads to the reduction of conduction heat because once the green panel is hydrated, latent heat started to form as a result of evaporation and intercepted the incoming heat (total radiation). However, when all the hydrated water was evaporated completely and

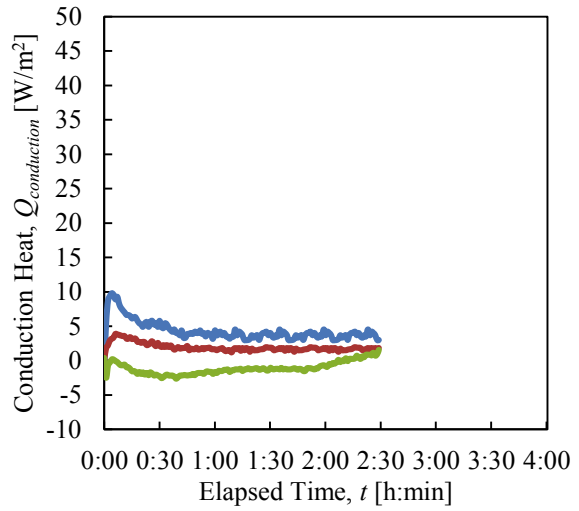
the moist green panel dried, $Q_{conduction_S3m}$ begins to rise and converge with $Q_{conduction_S3}$ line, indicating the end of evaporation.

In addition, by increasing the total radiation R_T leads to the increase of model house roof surface temperature, consequently rising the inflow of conduction heat. For example, through Fig. 5-16(a) to (e) of $\varphi=60^\circ$, when total radiation R_T increases, the conduction heat magnitude of every model houses increase, and the gap between the three conduction heat enlarged. Besides, the reduction period of $Q_{conduction_S3m}$ turns shorter since more latent heat produced during liquation in evaporation process when more total radiation R_T received by the green panel.

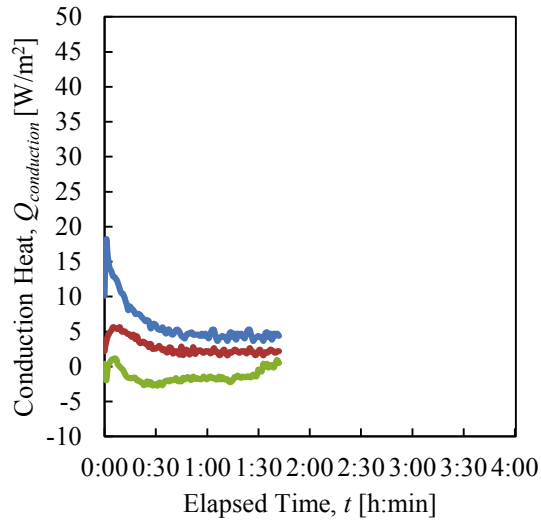
Furthermore, by determining the temperature difference of average values for each conduction heat in steady state, the reduction of conduction heat in dry and moist state of green panel can be investigated. Fig. 5-18 shows the conduction heat differences $|Q_{conduction_C} - Q_{conduction_S3}|$ in dry state while Fig. 5-19 shows the conduction heat differences $|Q_{conduction_S3} - Q_{conduction_S3m}|$ between dry and moist Sunagoke moss. Based on both graphs, the conduction heat differences in both conditions increase when total radiation and SRID irradiance angle increase. In details, when SRID irradiance angle was set at 30° , 60° and 90° the conduction heat can be reduced 1.01~7.08 [W/m²], 2.73~11.98[W/m²] and 6.19~18.92 [W/m²] in dry green panel condition, and further 3.41~10.23 [W/m²], 4.09~10.98[W/m²] and 4.62~12.19 [W/m²] respectively in moist green panel condition. Furthermore, in average the reduction of conduction heat according to each irradiance angle is 3.31[W/m²], 7.54[W/m²], and 12.51[W/m²] in dry, with additional 6.70[W/m²], 7.38[W/m²] and 8.33[W/m²] in moist green panel condition. Hence, by looking at these numbers, SRID irradiance angle at 90° shows the most conduction heat reduction effect, consequently the thermal insulation effect and evaporation effect of Sunagoke green panel in green roof application is highly anticipated during hot noon time.



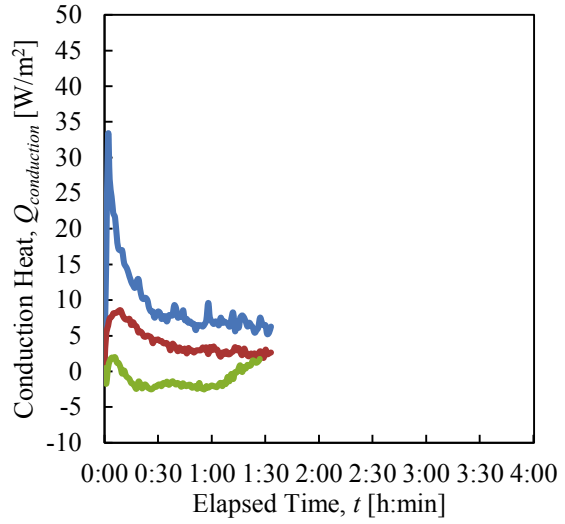
(a) $\varphi = 30^\circ$, $R_n = 200$ [W/m²]



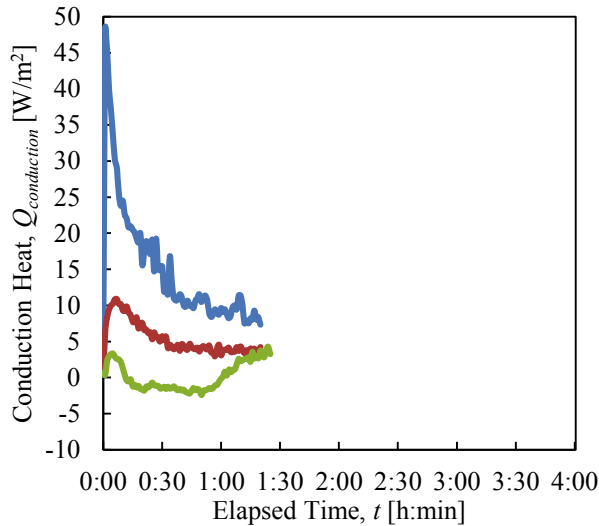
(b) $\varphi = 30^\circ$, $R_n = 400$ [W/m²]



(c) $\varphi = 30^\circ$, $R_n = 600$ [W/m²]

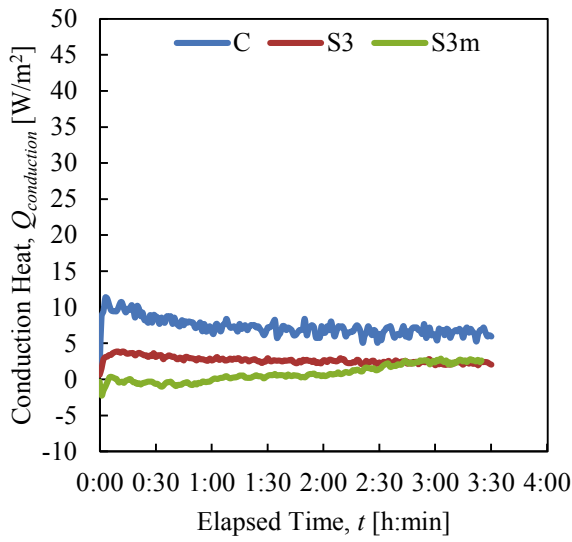


(d) $\varphi = 30^\circ$, $R_n = 800$ [W/m²]

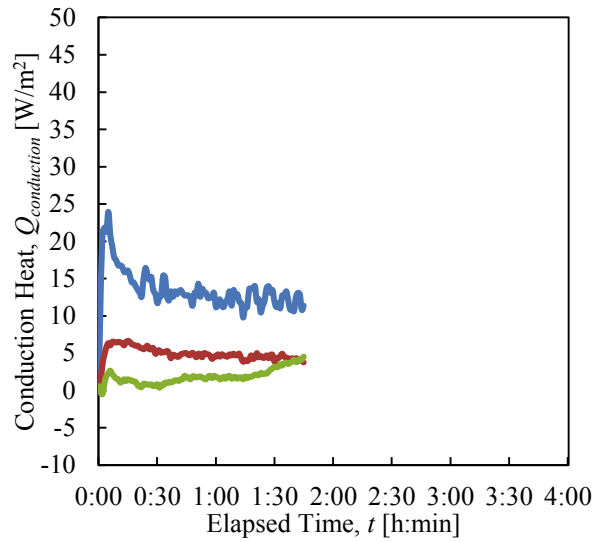


(e) $\varphi = 30^\circ$, $R_n = 1000$ [W/m²]

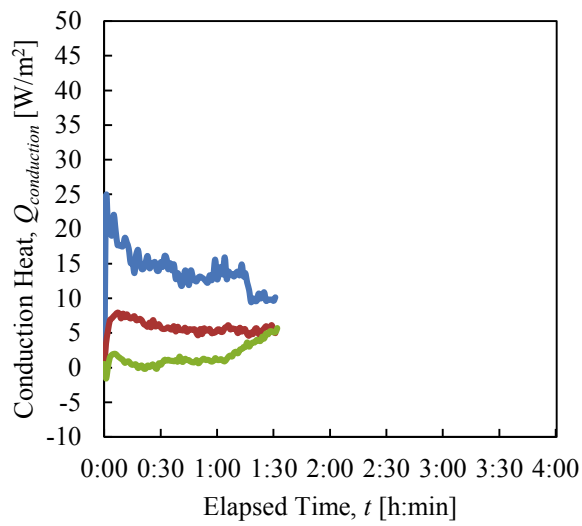
Fig. 5-15. Conduction Heat of C, S3 and S3m when $\varphi = 30^\circ$.



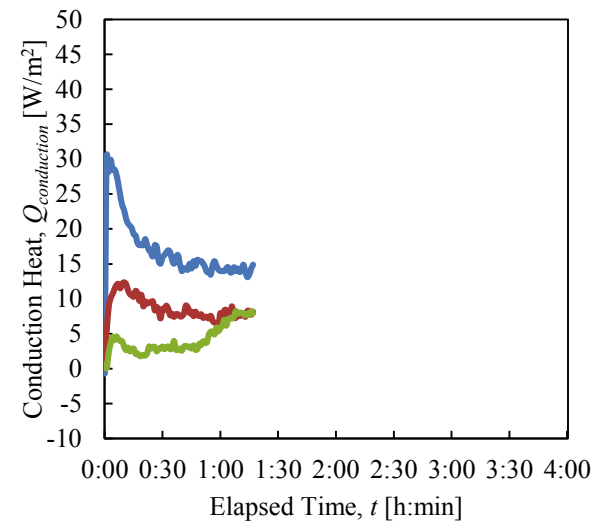
(a) $\varphi = 60^\circ$, $R_n = 200$ [W/m²]



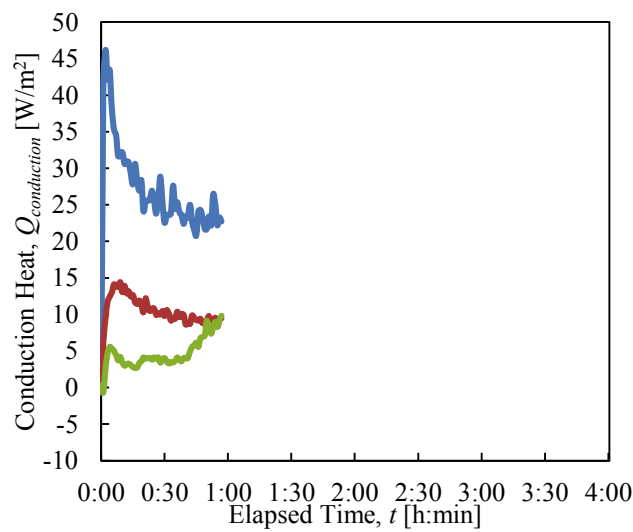
(b) $\varphi = 60^\circ$, $R_n = 400$ [W/m²]



(c) $\varphi = 60^\circ$, $R_n = 600$ [W/m²]

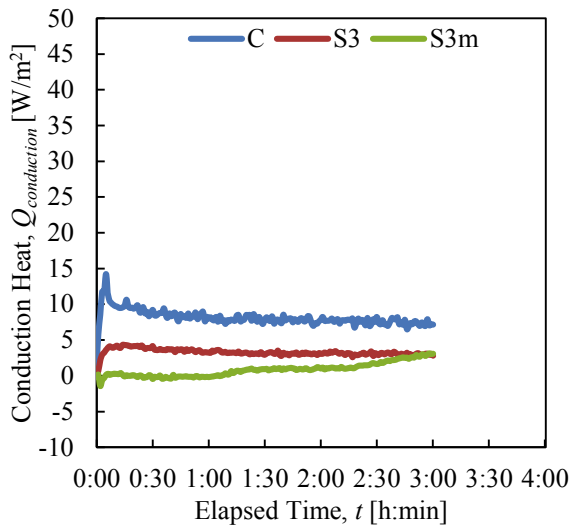


(d) $\varphi = 60^\circ$, $R_n = 800$ [W/m²]

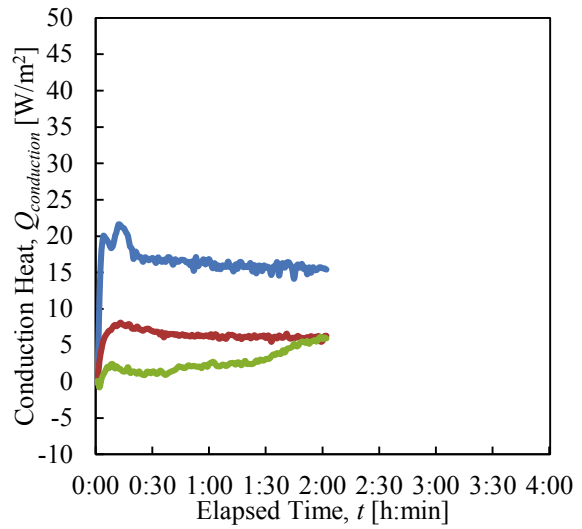


(e) $\varphi = 60^\circ$, $R_n = 1000$ [W/m²]

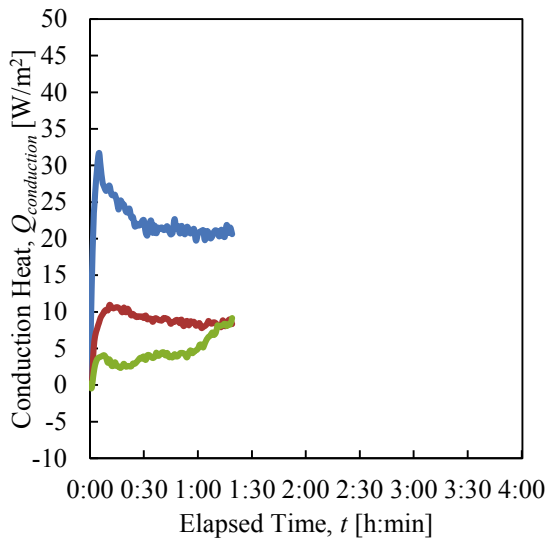
Fig. 5-16. Conduction Heat of C, S3 and S3m when $\varphi = 60^\circ$.



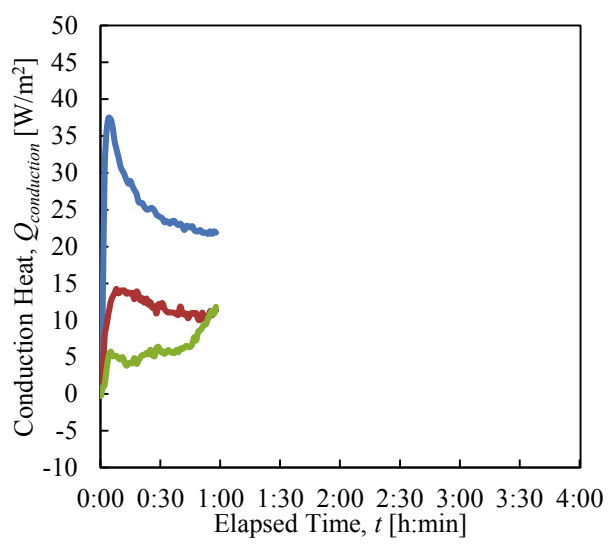
(a) $\varphi = 90^\circ$, $R_n = 200$ [W/m²]



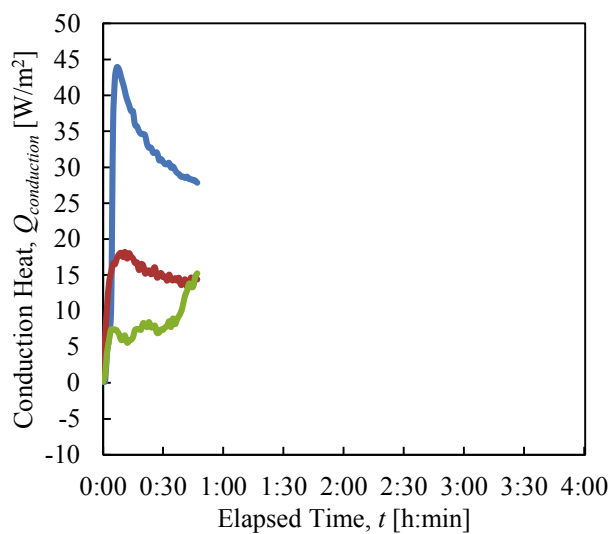
(b) $\varphi = 90^\circ$, $R_n = 400$ [W/m²]



(c) $\varphi = 90^\circ$, $R_n = 600$ [W/m²]



(d) $\varphi = 90^\circ$, $R_n = 800$ [W/m²]



(e) $\varphi = 90^\circ$, $R_n = 1000$ [W/m²]

Fig. 5-17. Conduction Heat of C, S3 and S3m when $\varphi = 90^\circ$.

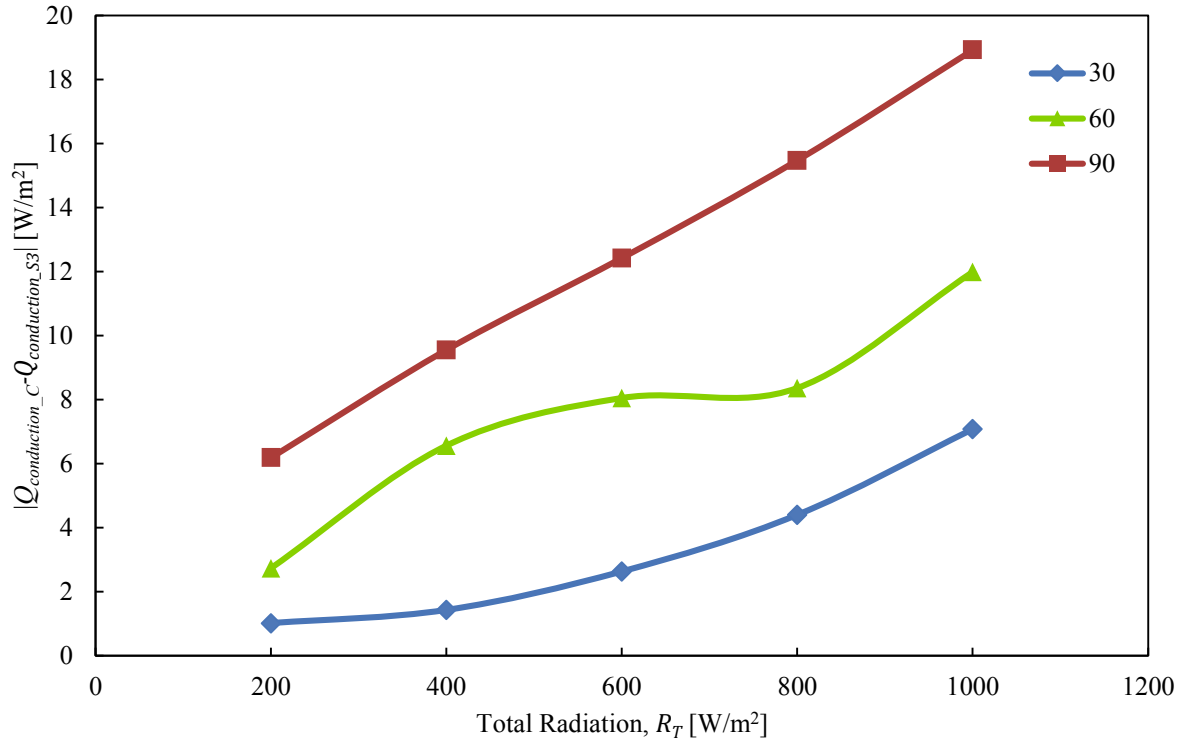


Fig. 5-18. Conduction Heat Difference $|Q_{conduction_c} - Q_{conduction_s3}|$.

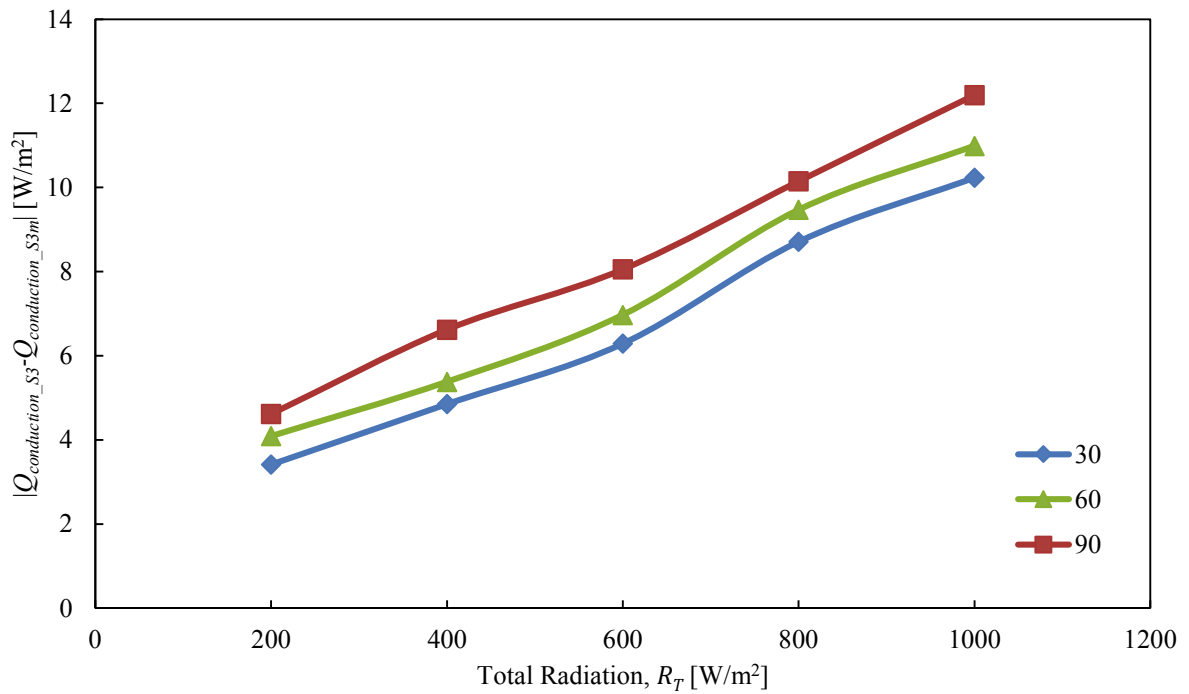


Fig. 5-19. Conduction Heat Difference $|Q_{conduction_s3} - Q_{conduction_s3m}|$.

5-4-2 Model Houses Interior Temperature Differences

As the consequence of inflow of conduction heat into the model houses, the author determined the reduction of average interior temperature difference, ΔT_i that human may feel in daily life by conducting green roof. Fig. 5-20 illustrates the results of the average model houses interior temperature differences in dry ($T_{i_C} - T_{i_{S3}}$) and moist ($T_{i_C} - T_{i_{S3m}}$) green panel condition for each SRID irradiance angle φ and total radiation R_T . Note that the interior temperature of each model houses was calculated as the average value from the three temperature measuring points. (Refer Fig. 3-1 for details).

Form the graph, when SRID irradiance angle was set at 30° , the interior temperature differences did not showed a great improvements but increases at 60° and reached maximum values at 90° . At 30° of SRID irradiance angle, the average interior temperature difference in dry green panel condition is almost 0 as a result of low entrance of conduction heat. As the conduction heat itself is too small in physical unit, the suppressed conduction heat does not affect the interior temperature of S3m and C. Generally, the average interior temperature differences ΔT_i increase upon increment of total radiation and SRID irradiance angle. The maximum interior temperature difference is recorded at 90° on $1000[\text{W}/\text{m}^2]$ of radiation amount which is 8.5°C in dry condition while 13.3°C in moist condition. As explained above, the performance of Sunagoke green panel in green roof application in reducing interior temperature of model house is clarified in this study. Hence, in the real application of this system, the Sunagoke green panel is expected to have the similar ability in reducing the house or building interior temperature which further helps in mitigating urban heat island effect.

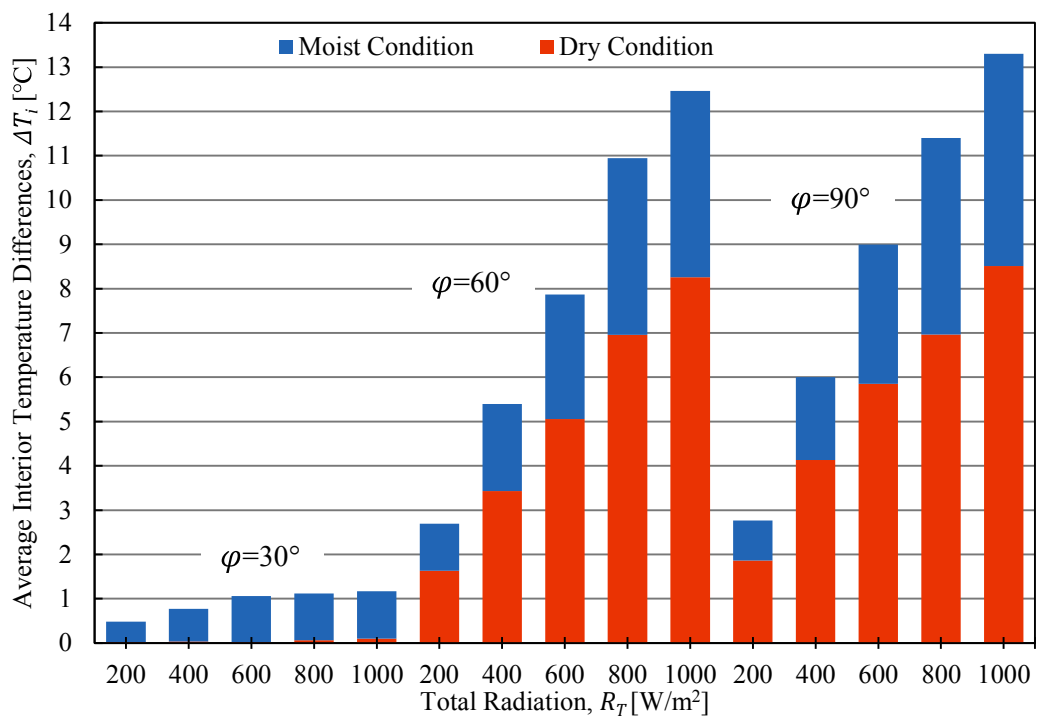


Fig. 5-20. Average Interior Temperature Differences reduced by Sunagoke green panel.

5-5 Chapter Summary

In Chapter 5, we have discussed about the effects of irradiance angle and irradiance amount on the dry and moist Sunagoke moss green roofs. From indoor experiment conducted inside the Artificial Climate Chamber under simulated solar angle in summer environment, the findings are summarized as below:

- From the gradient shown in the average steady-state latent heat graph, the projection of latent heat when certain amount of total radiation is radiated on moist green panel at certain irradiance angles correspond to sun positions can be estimated.
- Via simulating summer environment inside ACC, the evaporation rate of Sunagoke moss did not depends on total radiation but increases upon increment of SRID irradiance angle. By overall average, the evaporation rate calculated in indoor experiment is recorded in the range of 0.08 to 0.37 which shows similarity with the value calculated in outdoor environment.
- By simulating the SRID irradiance angle with sun position time, the time necessary and not necessary to apply water on green panel to improve thermal insulation effect is recognized. Applying water on the afternoon is the most efficient way to intercept the incoming heat.
- The average interior temperature differences ΔT_i increase upon increment of total radiation and SRID irradiance angle. The maximum interior temperature difference is recorded at 90° on 1000[W/m²] of irradiance which is 8.5°C in dry condition while 13.3°C in moist condition.

5-6 Equipment List in Chapter 5

1. Artificial Climate Chamber
 - Manufacturer : Marui Co., Ltd.
 - Model : MC-402
 - Temperature fluctuation error : ± 0.5 [°C]
 - Humidity fluctuation error : ± 3 [%]
 - Temperature gradient : 10 [°C / hr]
 - Irradiance intensity : 0 ~ 1000 [kcal / hm²] (specimen surface)
 - Irradiance indication system : 1 [kcal / hm²]
 - Irradiance distribution system : ± 20 [%]
 - Temperature control range : -20 [°C] ~ 50 [°C]
 - Humidity control range : 30 [% RH] ~ 90 [% RH]

2. Portable data logger
 - Manufacturer : Yokogawa Electric Co., Ltd.
 - Model : Datum-Y XL100
 - Temperature range : 0 ~ 350 [°C]

3. Temperature and humidity loggers
 - Manufacturer : T & D Co., Ltd.
 - Model : RTR-53A
 - Temperature measurement accuracy : 0 ~ 50 [°C]
 - Humidity measurements accuracy : 10 ~ 95 [%]

4. Temperature and humidity sensor
 - Manufacturer : Hioki Co., Ltd.
 - Model : 3641 Type
 - Number of channels : 2ch
 - Highest decomposition : 0.1 [°C]

5. Electronic balance
 - Manufacturer : A&D Co., Ltd.
 - Model : EK-6100i
 - Measuring range : 0.1 ~ 6000 [g]

6. Lightweight data logger for electronic balance

| | |
|-------------------|-----------------|
| Manufacturer | : A&D Co., Ltd. |
| Model | : AD-1688 |
| Measurement range | : 0.1~6000 [g] |

7. Pyranometer

| | |
|---------------------|-------------------------------------|
| Manufacturer | : Eko Instruments Co., Ltd. |
| Model | : MS-402 |
| Instrument constant | : 6.99 [mV / kW · m ⁻²] |
| Internal resistance | : 500 [Ω] |
| Wavelength range | : 285-2800 [nm] |

8. Infrared dryer bulb

| | |
|----------------------|---------------------|
| Manufacturer | : TOKI |
| Model | : IR200/220V125WRHK |
| Radiation efficiency | : Above 62% |
| Power consumption | : 125 [W] |
| Life | : 5000 [h] |

Chapter 6 - Outdoor Experiment and Relationship with Indoor Experiment

6-1 Experiment Introduction

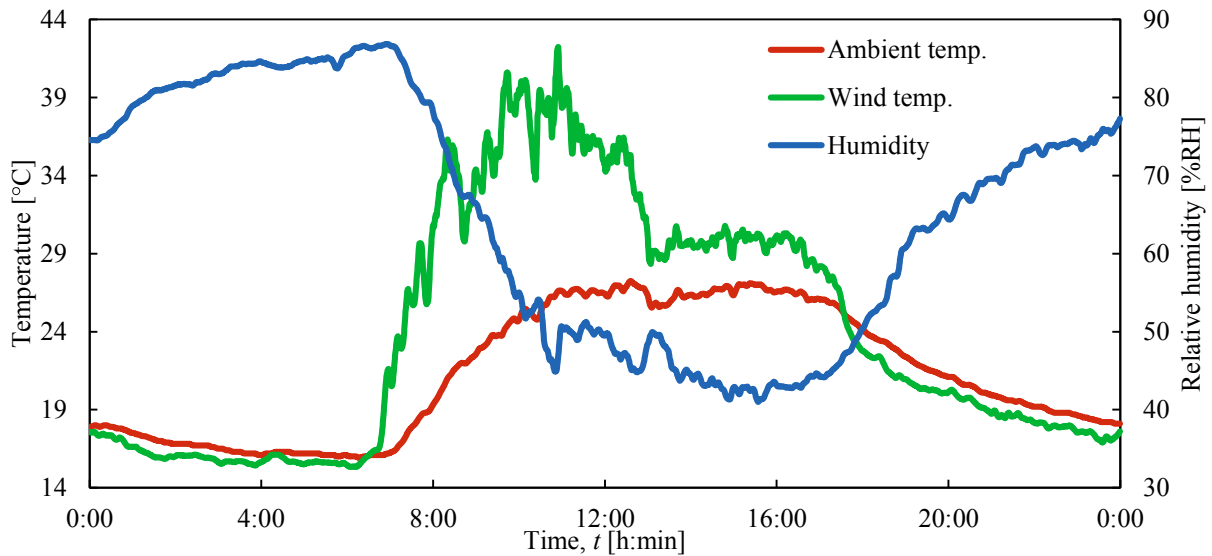
Outdoor experiments were piloted to observe the Sunagoke moss green roof capability in regulating thermal load of a model house in actual environments. Experiments were conducted throughout the year in selective days, but were more focus during summer to express full effectiveness. Besides, a hot summer environment can also be interpreted to other warm climates encountered by south-east Asian countries throughout the year, for example. The Main Office Building Rooftop of Yamaguchi University Engineering Campus (33.956171, 131.272037) was chosen as the experimental site to avoid human accessibility and unintentional shadow. The Main Office Building is a typical 4-storey office building. Model houses were aligned north-west of each other. Data were recorded throughout the day from 0:00 to 23:59, with 1 minute recording interval. The same measuring instruments were used as in the indoor experimental setup. A clear day of 30 September in 2017 was chosen as the representative experimental data.



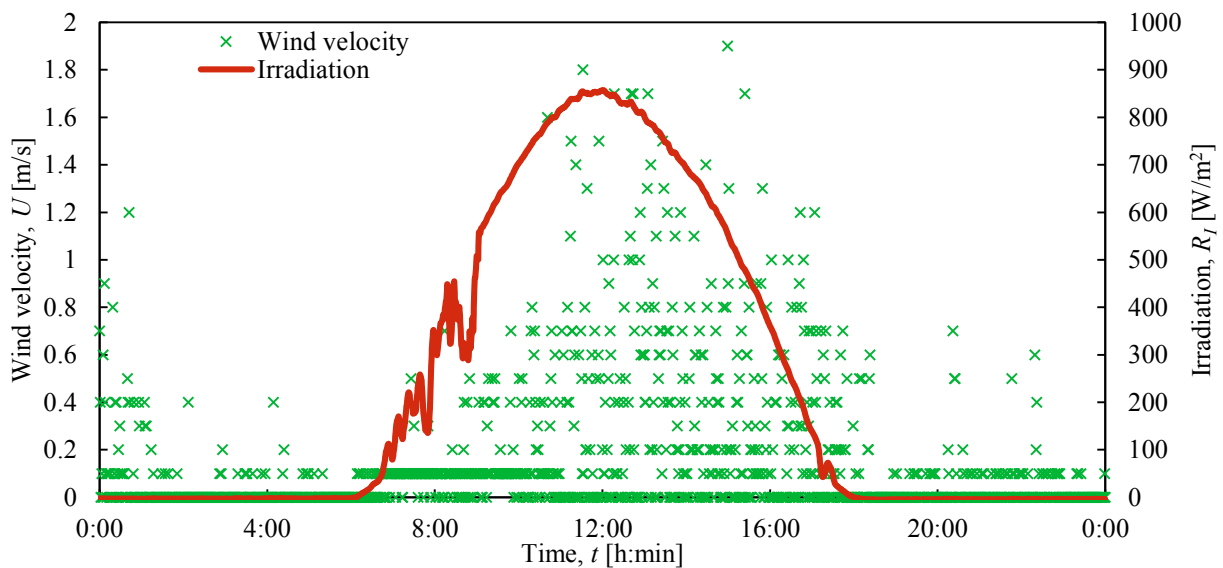
Fig. 6-1. Outdoor experimental setup on The Main Office Building Rooftop of Yamaguchi University Engineering Campus.

6-2 Experimental Conditions

The parameter conditions in outdoor experiment on 30th September 2017 are presented in Fig. 6-2 (a) and (b). Existence of cloud was minimal throughout the experiment except during morning. Usually wind movements were calmer during night-time, but varied during day-time. Also, notice that the humidity decreased with the rise of wind velocity because the movement of wind swept away the water molecules at the experiment location. Since wind was rapidly changing during day-time, the data in period of 9:40 to 16:00 had been took as the evaluation subject.



(a) Ambient temperature and relative humidity were recorded inside an instrument shelter, whereas wind temperature was recorded at near of green panel. During daytime, maximum ambient and wind temperature, and humidity were 27.3 °C, 44.0 °C and 60.1 %RH, respectively.



(b) Wind velocity and irradiance. During daytime, maximum wind velocity and irradiance were 1.9 m/s and 858.9 W/m², respectively.

Fig. 6-2. Important parameter conditions in outdoor experiment on 30th September 2017.

6-3 Experimental Methodology

To evaluate the thermal performance of multiple green roofs, four identical model houses (three with green panels) made from house-shaped Polystyrene foams were prepared. Table 6-1 indicates the model houses used, associated with their respective green panels' specifications. A model house, named C, was used as the control house; i.e., a representative of a conventional dry and untreated roof. All green panels (S3, S30 and G) were assumed to be in a naturally dry condition because no irrigation was made since day 1 prior to the experimental. A green panel with grass mat (G) was equipped with 5 mm thickness of soil layer. On the other hand, there were no substrate layer on both Sunagoke moss green panels (S3 and S30) since Sunagoke does not require them to cultivate. Except for model house S3, Sunagoke moss was mixed with organic adhesives to fix it on top of the galvalume steel plate. Additionally, the back of the galvalume steel plate was adhered with Styrofoam, acting as a heat insulator. Meanwhile, the roof plate was painted with matte black finishing to reduce radiation reflectivity. All sensors including thermocouples were logged within 1 minute intervals for 24 hours.

6-4 Results and Discussion

6-4-1 Convection Heat Transfer Characteristics in Outdoor Environment

Wind existence is an important parameter in the experiment, therefore it is crucial to learn the behaviour of the wind flow as it will give the basic understanding on how the wind responds and affects the heat transfer system of the whole model house. Fig. 6-3 illustrates the derived ratio of the Grashof number and the square of Reynolds number from Eq. (3-23) to (3-25). Only for indoor experiments, the results shown are associated with the irradiance irradiated in the experiment.

The ratio of Grashof number and square of Reynolds number specified a natural convection if the value was larger than 10, combination of forced and natural convection in between 0.1 and 10, and forced convection if the value was less than 0.1. At static wind of 0 m/s, the ratio extended to infinity, thus the natural convection was assumed to dominate the heat transfer on all model houses. The region of $0 < U_{ave} < 2$ m/s was considered as the transition region where the combined convection took place. Although the maximum wind velocity in outdoor experiment was 1.9 m/s, the ratios for S3, S30, G and C were assumed to follow the same curvature beyond 2 m/s of wind velocity. Hence, wind velocity of 2 m/s ($Re=74,500$) was considered as the critical point where the forced convection started to dominate the heat

transfer on all model houses. Gaffin et al. [19] achieved similar finding where wind velocity of 1.75 m/s was verified to be the indicator of forced convection in their investigation.

Results for model houses S3 and C shows great agreement between indoor and outdoor data, however outdoor data were detected with some fluctuation due to irradiance strength variation. Generally, the ratios for model houses with green panel (S3, S30 and G) were lower compared to the ratio for untreated model house C. This occurred because the surface and ambient temperature differences of model houses with green panels were much lower. In indoor experiment, the same concept also applies to higher irradiance condition where a higher irradiance will elevate the surface temperature and the temperature differences as well. Thus, the ratio increases in higher irradiance.

Disparate the ratio of Grashof number and square of Reynolds number, the increased wind velocity had reduced the surface temperature along with the temperature differences with ambient temperature, causing the convection heat transfer coefficient derived from Eq. (3-16), to increase in laboratory experiments, as depicted in Fig. 6-4. Generally, there were no correlations between the irradiance and the convection coefficient since only $\pm 1\%$ variations were found for model house S3 and C. At the time when the wind velocity was getting faster, the surface temperature remained almost constant which caused the heat transfer coefficient to remain similar with the wind velocity of 2 m/s onwards (forced convection region).

In a natural convection region, the resulting average convection heat transfer coefficients were $24.5 \pm 0.31 \text{ W/m}^2\text{K}$, and $14.5 \pm 0.16 \text{ W/m}^2\text{K}$ for model house S3 and C, respectively. Meanwhile, in a forced convection region, the obtained convection heat transfer coefficients were $116.1 \pm 0.99 \text{ W/m}^2\text{K}$, and $37.8 \pm 0.24 \text{ W/m}^2\text{K}$ in the same model houses order. Therefore, the application of Sunagoke moss green roof was clarified to improve the convection heat transfer ability of the model houses by a factor of 1.6 in natural convection and 2.9 in forced convection.

As a comparison with common plants, Kumar et al. [57] reported that the maximum convection heat transfer coefficient in natural convection was $26.8 \text{ W/m}^2\text{K}$ for peperomia, $10.1 \text{ W/m}^2\text{K}$ for egg-plant, and $23.5 \text{ W/m}^2\text{K}$ for wax-bean, as acquired in experiments conducted in a wind tunnel. The convection heat transfer coefficient increased to $59.5 \text{ W/m}^2\text{K}$ for peperomia and egg-plant, and $42.7 \text{ W/m}^2\text{K}$ for wax-bean in forced convection. The convection heat transfer coefficients for Sunagoke moss, especially in the forced convection, were 2 times higher than the reference, and may result from the different heating intensities to the subject plant. Therefore the data presented in this paper were considered valid.

Nevertheless, the convection heat transfer coefficient taken in outdoor experiment shows huge fluctuations during the day as demonstrated in Fig. 6-5. Fascinatingly, the increment of wind velocity did not guaranteed high convection coefficient because the temperature differences between surface and ambient air were uneven, irrespective to the wind velocity. Clearly the solar radiation flux fluctuations also contributed to the irregularity. The three green panels displayed better convection coefficient than the control roof, however, the thinnest S3 had the best ability to release heat compared to other competitors. Also, thicker S30 was not necessarily better than S3 since thicker plant mat has higher heat capacity which makes temperature reduction less effective.

Besides that, there were extreme fluctuations detected during early morning and late evening where the temperature differences were the greatest during those times. However, the temperature differences were steadier during noon, and almost 0 during night. For the representation, in average the convection heat transfer coefficients for model houses S3, S30, G and C were 78.7 ± 26.5 , 38.1 ± 10.7 , 52.4 ± 12.2 , and 33.5 ± 7.5 [W/m²K], respectively, while the average wind velocity was 0.33 ± 0.41 [m/s]. Compared to the indoor experiment, the result for model house C were similar, however the result for model house S3 shows variance in the two environments. The average value in outdoor experiment was lower than the indoor experiment in forced convection region, however, if the upper limit is taken, the both values are very similar, where 105.2 [W/m²K] for outdoor, and 116.1 [W/m²K] for indoor measurement.

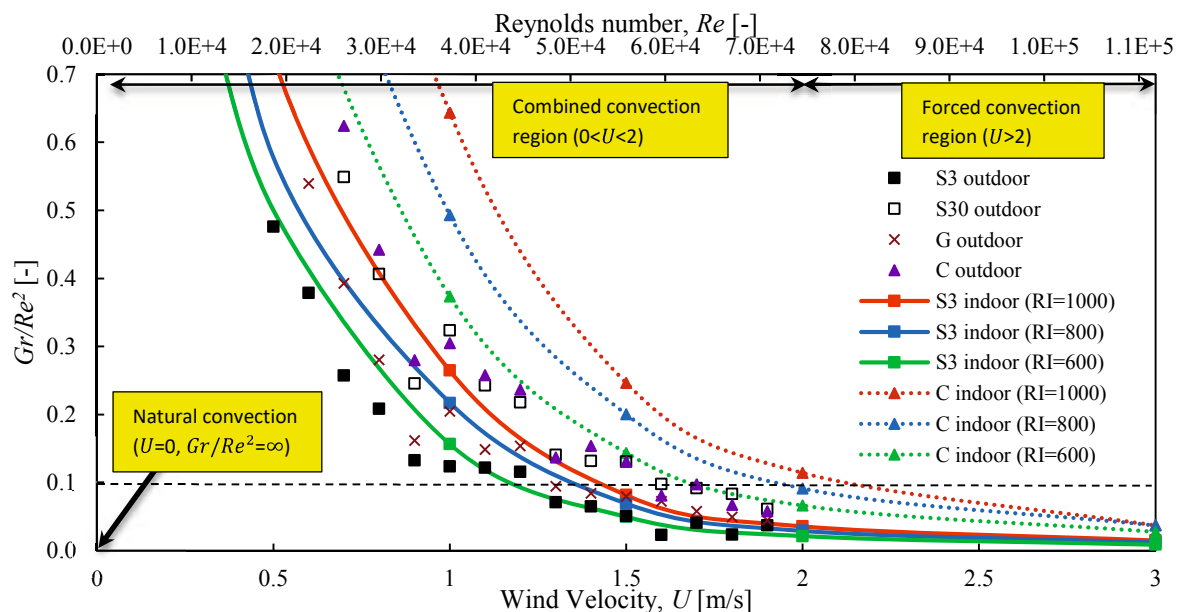


Fig. 6-3. Ratio of Grashof number and square of Reynolds number. Indoor data were displayed according to the irradiance and wind velocity, while outdoor data were sorted and displayed only according to the wind velocity, regardless the irradiance.

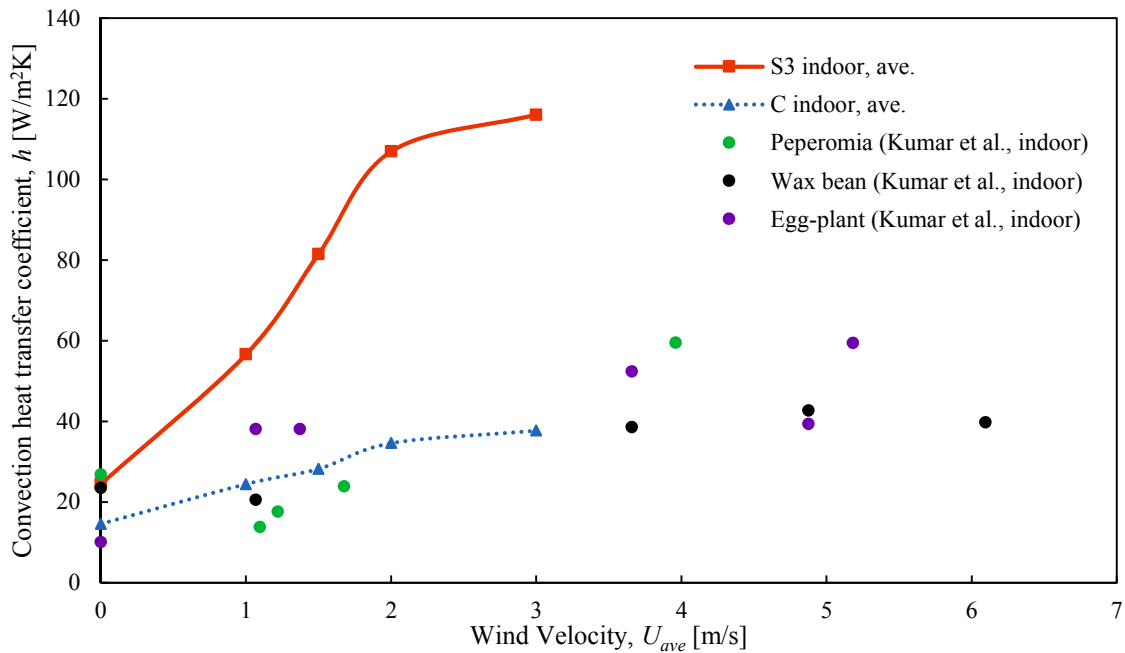


Fig. 6-4. Convection heat transfer coefficient for each model house in indoor experiment with different wind velocity. Since there were no positive correlation between irradiance and convection heat transfer coefficient, only averaged data were displayed. Reference data by Kumar et al. shows some other typical plants' convection heat transfer coefficient.

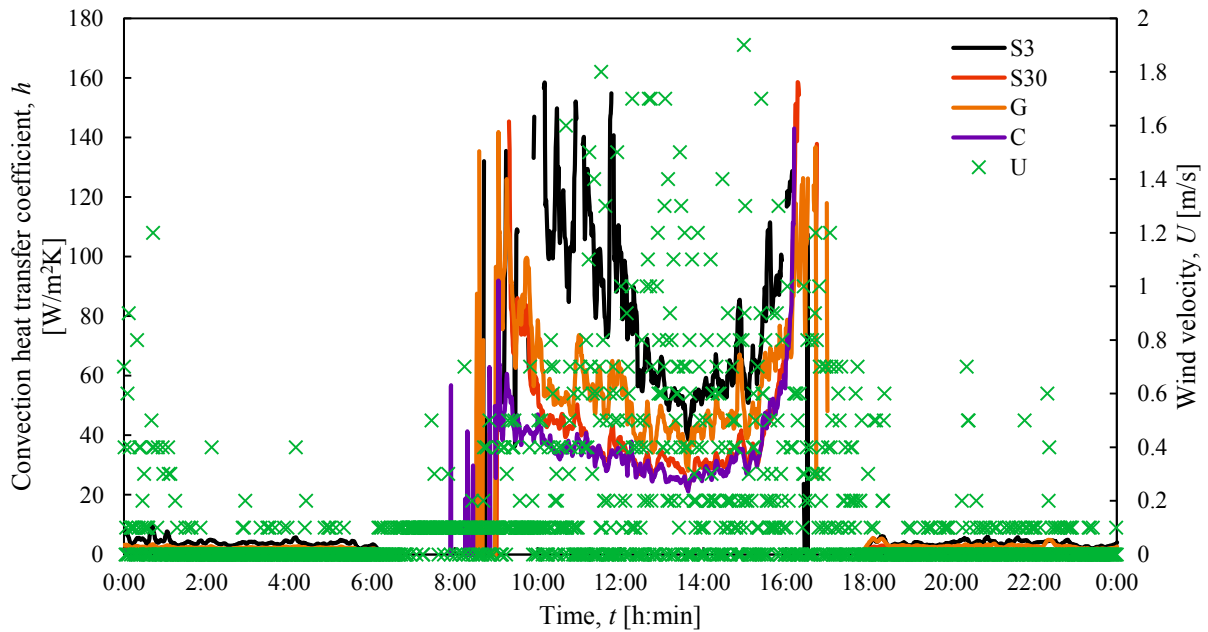


Fig. 6-5. Convection heat transfer coefficient for each model house in outdoor experiment, according to elapsed time. Results were analysed by taking moving average of 5 data.

6-4-2 Heat Balance on Model Houses

The incoming radiation (i.e. irradiance) were initially reflected before converted to other forms of heat (refer Fig. 3-1). Accordingly, determining albedo from Eq. (3-5) is a crucial assessment in evaluating the thermal performance of the Sunagoke moss green roof. In general, either in indoor or outdoor experiments, albedo was not affected by wind velocity, but slightly affected by the irradiance as depicted in Fig. 6-6. An average albedo gap of 0.03 differentiated the model houses S3 (ave. 0.09 ± 0.003) and C (ave. 0.06 ± 0.003). On the other hand, the albedo of outdoor experiments were comparatively higher than indoor experiments. As the outdoor environment also provide high atmospheric and surrounding radiation, model houses reflected more radiation accordingly. In contrast, indoor environment did not consist of such radiations, thus the albedo differences between the two environments were significant. Therefore, the indoor albedo of S3 should be corrected by adding 0.16 to 0.18 to match with the outdoor experimental outcomes.

It is also worth to mention that in outdoor environment, the surface roughness aspect played a key role in determining the albedo in model house C. Although model house C was purposely painted with matte black finishing to reduce the albedo, the flat and smooth surface of roof plate still inevitably reflected a huge portion of the irradiance. While Gaffin et al. [19] suggested that the equivalent albedo for green roofs should be in the range of 0.7-0.85, the average albedo found in outdoor experiments were 0.25 ± 0.004 , 0.22 ± 0.004 , 0.22 ± 0.006 , and 0.24 ± 0.001 for model houses S3, S30, G and C, individually. However, the results obtained in this paper were very similar to *Carex argyranthra* of 0.22 ± 0.007 which reported by MacIvor et al. [58] in a research conducted on top of the Patrick Power Library of Saint Mary's University.

Based on the heat balance equation (refer Eq. (3-2)), the proportion of each heat fraction transferred on the model houses can be determined by dividing the fractions with total radiation. Total radiation is equal to irradiance minus the reflected radiation flux as explained in Eq. (3-3). Conduction and convection heat proportions were obtained from Eq. (3-10) and (3-14), respectively. The results of the calculations were compiled in Fig. 6-7 and Table 6-1. It was noted that regardless of indoor and outdoor experiment cases, the latent heat fluxes for all dry model houses were neglected since they were assumed minute and difficult to measure. Since the dry surfaces of model houses lack evaporation, the convection heat flux dominated the whole heat balance, thus the convection heat proportion was really close to 100% throughout the wind velocity for both experiment category. Although the increments were insignificant

and not affected by irradiance strength, the convection proportion reach maximum and unchanged beyond 2m/s of wind velocity in indoor environment. Also, convection heat proportion of green roof surfaces were slightly higher than that of the control roof, thus clarified the green roofs moss allowed better cooling even in dry condition.

Convection heat proportion of model houses Sunagoke S3 and control C have great discrepancy in steady environment of Artificial Climate Chamber. In contrast, the convection proportions in outdoor experiments, when sorted according to wind velocity, did not displayed major variance for model houses S3, S30, G and C. But still, all green panels dissipated heat better than control roof especially in natural convection condition. Similar with results of convection heat transfer coefficient, the 30mm thickness Sunagoke moss did not deliver heat as good as 3mm Sunagoke moss and grass. While Sunagoke S3 utilized its thinness, grass G utilized its slenderness in delivering heat to atmosphere.

As the by-product of heat transfer on the system after reflected and delivered to atmosphere, the conduction heat penetrated into interior cavity of the model house. As a result of higher proportion of convection heat on green panels, lesser proportion of conduction heat were noticed in both cases, indoor and outdoor environments. Compared to convection heat, the proportions of conduction heat were extremely small, in some circumstances close to 0. This happened as the heat cannot penetrate anymore on account of interior cavity of well-insulated model house reached saturated state. Nonetheless, it can be concluded that indoor experiments can display a similar outcomes with outdoor experiment in term of heat proportions developed on the model houses.

Table 6-1. Heat fluxes relative to irradiance in natural and forced convection.

| Model house | Convection heat [%] | Conduction heat [%] |
|-----------------------|-------------------------|-----------------------|
| Sunagoke S3, indoor | 98.4 ±0.05 (99.6 ±0.03) | 1.6 ±0.05 (0.4 ±0.02) |
| Sunagoke S3, outdoor | 99.5 ±0.34 | 0.5 ±0.34 |
| Sunagoke S30, outdoor | 99.3 ±0.23 | 0.7 ±0.23 |
| Grass G, outdoor | 99.7 ±0.13 | 0.3 ±0.13 |
| Control C, indoor | 95.3 ±0.09 (98.4 ±0.04) | 4.7 ±0.09 (1.6 ±0.04) |
| Control C, outdoor | 98.6 ±1.03 | 1.4 ±1.03 |

*the value written in bracket is for forced convection

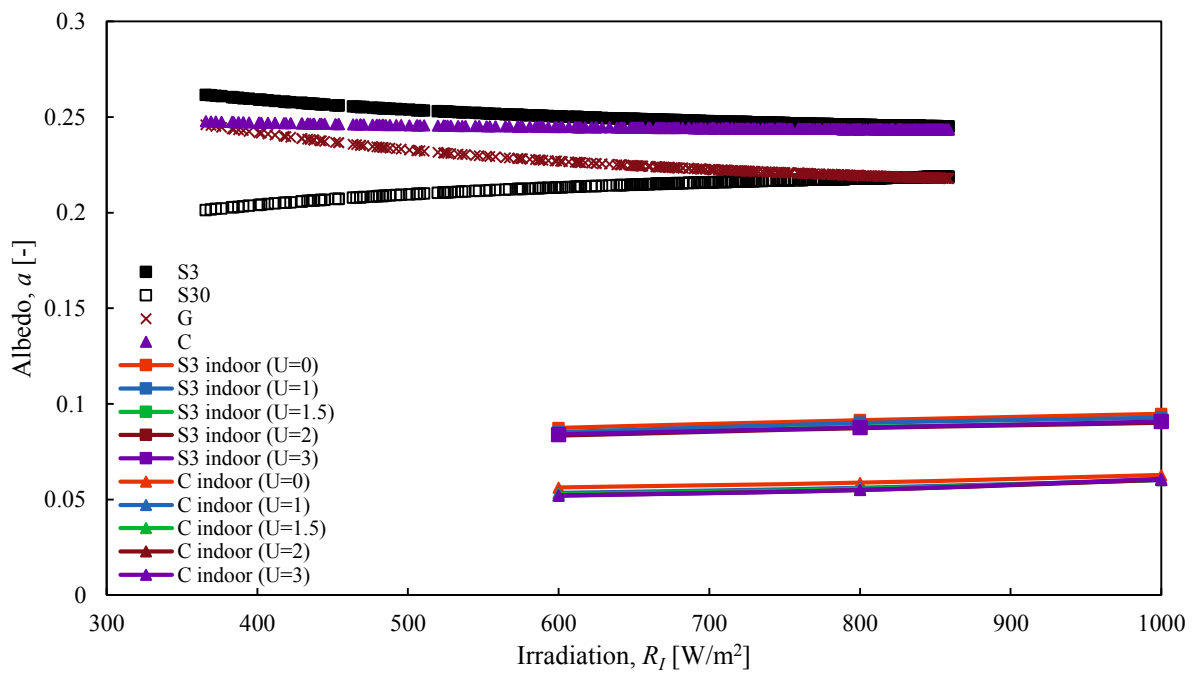


Fig. 6-6. Albedo of model houses S3, S30, G, and C in outdoor experiments, and model houses S3 and C in indoor experiments. The albedo were sorted according to irradiance in both cases. Indoor experimental results were averaged from three experimental data in one plot.

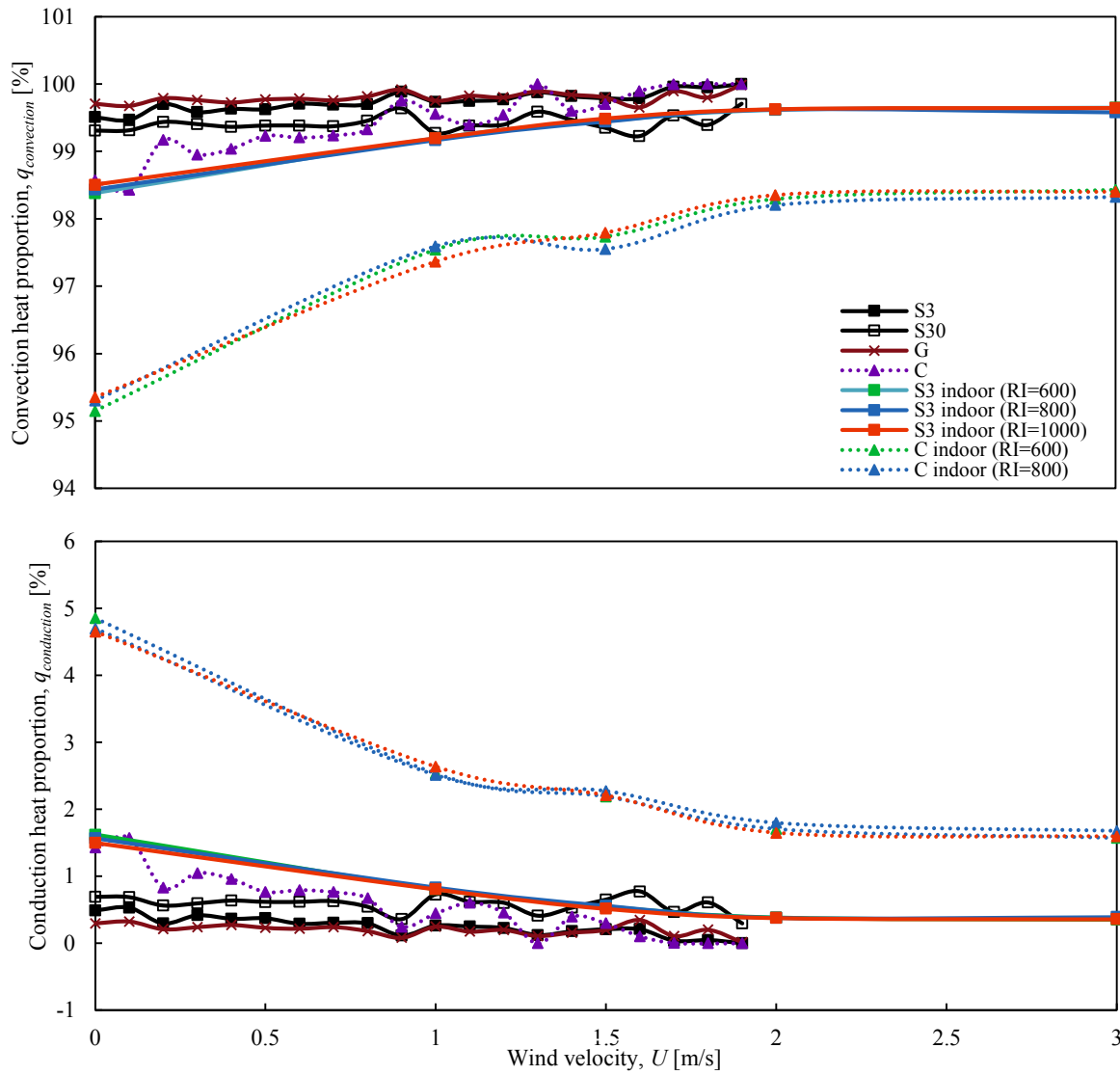


Fig. 6-7. Heat proportions on each model house. Graph was plotted together; indoor and outdoor data.

6-4-3 Temperature Profile

Surface and Interior Temperature

Surface temperature is significantly dependent on the environmental condition, which has to be faced by the outermost layer of each model house. All changes of such irradiance, convection characteristic, and wind velocity will drastically influence the fluctuation of surface temperature. Fig. 6-8 establishes the outermost surface and interior temperature for each model houses under outdoor experimental condition, along with the ambient temperature as reference. Most temperature fluctuations were seen during high irradiance around noon, but greatly calmer at night. During day-time, even though the surface temperature of Sunagoke S30 was the second highest after control roof, the interior temperature was the lowest compared with other candidates. Thicker material i.e., material with higher thermal resistance is more effective in suppressing the rise of interior temperature. Besides, the soil layer in grass green panel also provide additional aid to the temperature suppression. Despite the absence of soil, both Sunagoke moss green panels (S3 and S30) showed decent insulation effect and provide similar thermal comfort with grass. The maximum and average temperatures between 9:30 to 16:00 were outlined in Table 6-2.

Since the ambient temperature and irradiance strength were constant in indoor experiment, it is possible to analyse the surface and interior temperature according to wind velocity as demonstrated by Fig. 6-9. In natural convection, the surface temperature varied from 51.5 to 66.4 °C for model house S3, and 67.5 to 89.5 °C for control model house C. Based on the figure, even a small presence of wind initiated a significant reduction in surface temperature by comparing temperature gradient for wind velocity of 0 and 1 m/s. Changing the convection phase from natural to forced convection reduced the surface temperature $37.4 \pm 4.0\%$ for model house S3, and $36.4 \pm 2.0\%$ for control model house C. The fluctuations occurred due to irradiance intensities. However, the surface temperature reduction percentages were declining with the addition of wind velocity.

The Sunagoke green panel was by far cooler than the control roof surface due to the shading effects. A report made by Niachou et al. [18] in year 2001, highlighted that in an outdoor environment (ambient temperature 28 °C and relative humidity 57%), the surface temperature of a green roof on a non-insulated building ranged from 28 to 40 °C, whereas the surface temperature of a non-insulated building was warmer, which ranged between 42 and 48 °C. In another remarkable article by Suzuki et al. [34], they confirmed the surface temperatures of Sunagoke were recorded the highest at 31 and 33 °C for a rainy and a clear

day, compared to the surface temperatures of slab at 35 and 37 °C, correspondingly. As a record, the average wind velocity values for the two days were 2.7 and 2.6 m/s, respectively. In addition, results by Anderson et al. [43] demonstrated parallel discoveries where the maximum temperature of Sunagoke surface documented in August was 49.2 °C in contrast to medium only roof at 51.0 °C. Hence, the effect of applying green roof especially the Sunagoke moss green roof was proven to give positive effect on the building, and the energy savings are certainly promising.

On the other hand, the interior temperature varied associated with the irradiance strength. For instance, the interior temperature established in indoor experiments ranged from 38.6 to 45.8 °C and 46.2 to 56.1 °C for model houses S3 and C, respectively in natural convection as revealed in Fig. 6-9 (b). Later, the occurrence of forced convection heat transfer reduced the variation $20.8 \pm 3.9\%$ and $23.6 \pm 2.6\%$ in the same order. There were no significant temperature reductions at wind velocity above 1.5 m/s. However, the coolest interior temperature of model house S3 was 32.5 °C, which was cooler by 4.3 °C than the control model house C. Any additional temperature drop below the ambient temperature was assumed to be impossible since the conduction heat fluxes (refer Fig. 6-7) were all in positive proportions and the heat flowed inwards the interior cavity irrespective of the condition of the model houses. If the conduction heat flux displays any negative value, then the reverse phenomena may happen.

A stimulating study investigated by Halwatura [59] documented the indoor air temperature of a three-story house which used three type of roofs; tile, bare, and Buffalo grass green roofs. The highest indoor temperatures obtained were 34.5 °C, 35.9 °C and 32.7 °C for tile, bare, and green roofs, respectively. From the findings, the Buffalo grass green roof was able to suppress the indoor temperature at 1.8 and 3.2 °C topmost. Although the interior temperature differences between the control roof and the Sunagoke green roof in this paper were comparatively high, the results of the application of Sunagoke green roof were likely to be comparable with that of the reference, in view of a proper ventilation of a real building.

Table 6-2. Maximum and average temperature of all model house candidates in outdoor environment, on period of 9:30 to 16:00.

| Model house | Max. surface temperature [°C] | Ave. surface temperature [°C] | Max. interior temperature [°C] | Ave. interior temperature [°C] |
|--------------|-------------------------------|-------------------------------|--------------------------------|--------------------------------|
| Sunagoke S3 | 48.0 (-12.0) | 40.7 (-9.8) | 40.4 (-8.9) | 38.0 (-7.3) |
| Sunagoke S30 | 58.8 (-1.3) | 48.6 (-1.9) | 36.9 (-12.4) | 35.0 (-10.3) |
| Grass G | 53.8 (-6.3) | 44.5 (-6.0) | 38.1 (-11.2) | 36.2 (-9.1) |
| Control C | 60.1 | 50.5 | 49.3 | 45.3 |

*value in bracket is difference with control model house C.

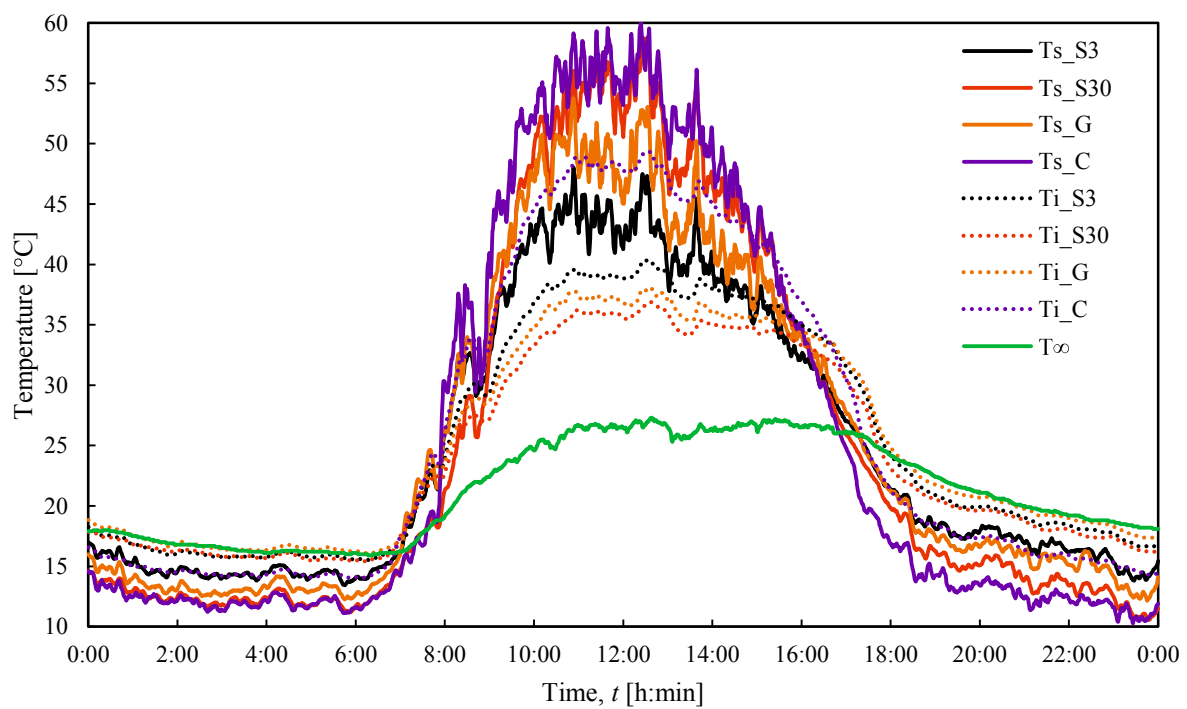
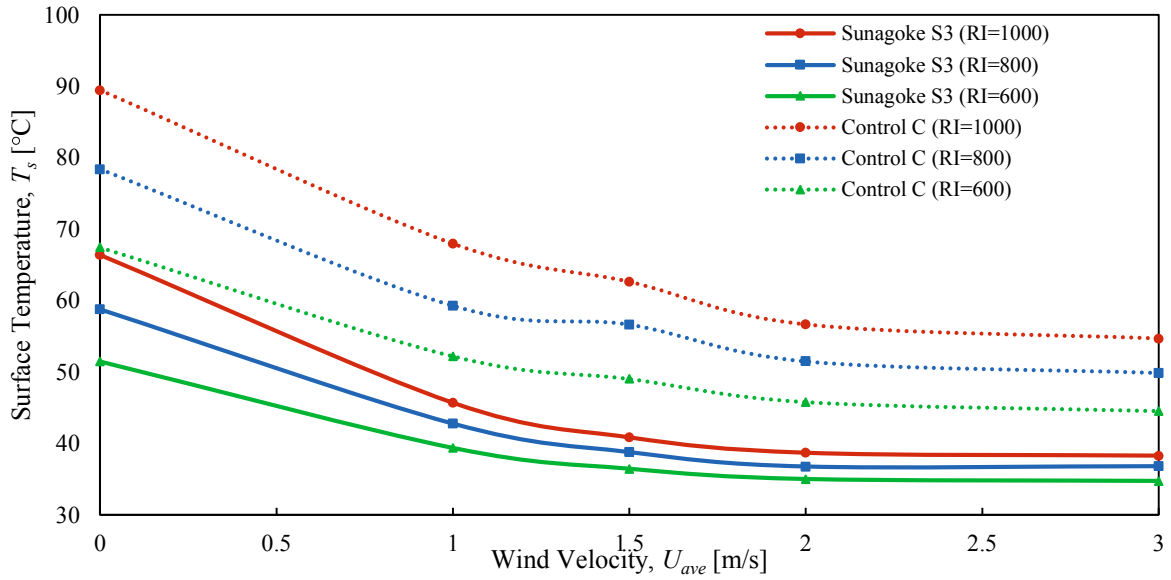
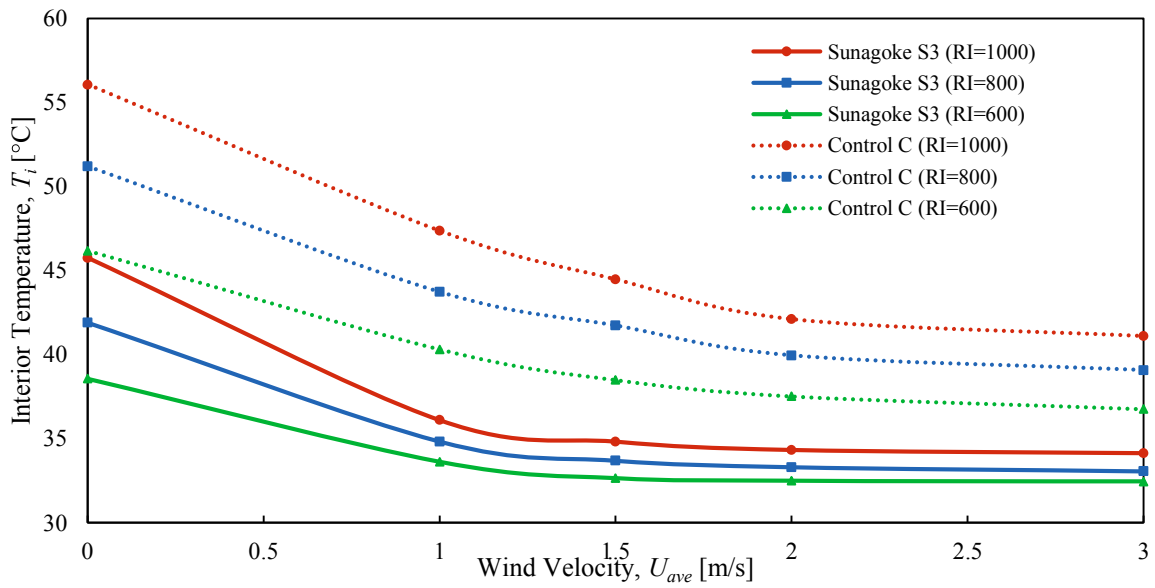


Fig. 6-8. Surface and interior temperature profile in outdoor environment. Outermost temperature is presented with the solid lines, while interior temperature is dotted lines.



(a) Surface Temperature



(b) Interior Temperature

Fig. 6-9. Temperature profile of model houses S3 and C in indoor experiments.

Dimensionless Temperature

To further analyze the cooling characteristic that occurred in the model houses, a dimensionless temperature ratio was proposed to determine the normalised temperature difference. The temperature ratio was constructed by taking the differences in temperature between surface and interior temperatures, relative to differences in temperature between interior and ambient temperatures (refer Eq. (3-1)). High temperature ratio specifies more influence from the roof surface condition, affecting the rise of interior temperature. On the other hand, low ratio meant there was more heat transferred to the atmosphere and less heat penetration into the interior cavity.

In indoor environment, both temperature driving forces were balanced on dry Sunagoke moss in forced convection region as the temperature ratios were close to 1, as presented in Fig. 6-10. Though, a dissimilar finding was seen on dry control roof where they were roughly 1.2 despite the changes of wind velocity. This signifies that the control roof tends to warm the interior cavity with the heat from the roof plate itself. A similar normalized temperature trends were seen on Sunagoke S30 in outdoor environment as depicted in Fig. 6-11, which also reflect the distress to release heat as the air cavity in between Sunagoke moss leafs detain the heat. Therefore, to reduce the cooling load of a building, the heat facing roof surface need, in the first place, to be mitigated.

Captivatingly, the temperature ratios in outdoor environment were mostly steady before afternoon, but starting to decrease until evening, as mostly the heat accumulating the interior cavity of model houses started to be released more to atmosphere. This event may affected by the elevation on convection heat transfer as the fact that wind velocity above 1 m/s were mostly presented after 12:00 pm.

Separately, neither Sunagoke S3 nor Control C have good agreement in the temperature ratio results in indoor and outdoor experiments. While both temperature ratios in indoor experiments were presented above 1, the outdoor experiments displayed ratios of below 1 for both model houses cases. Different environment limitation may be the reason of this contradiction, as the enclosed indoor environment is easily reaches saturated state and allows only limited degree of heat transfer from the model house, considering the heat capacity of the space inside of the Artificial Climate Chamber. Nevertheless, outdoor environment is limitless. Still, this kind of temperature ratio may be a base line to compare the thermal performance of other green roof plants.

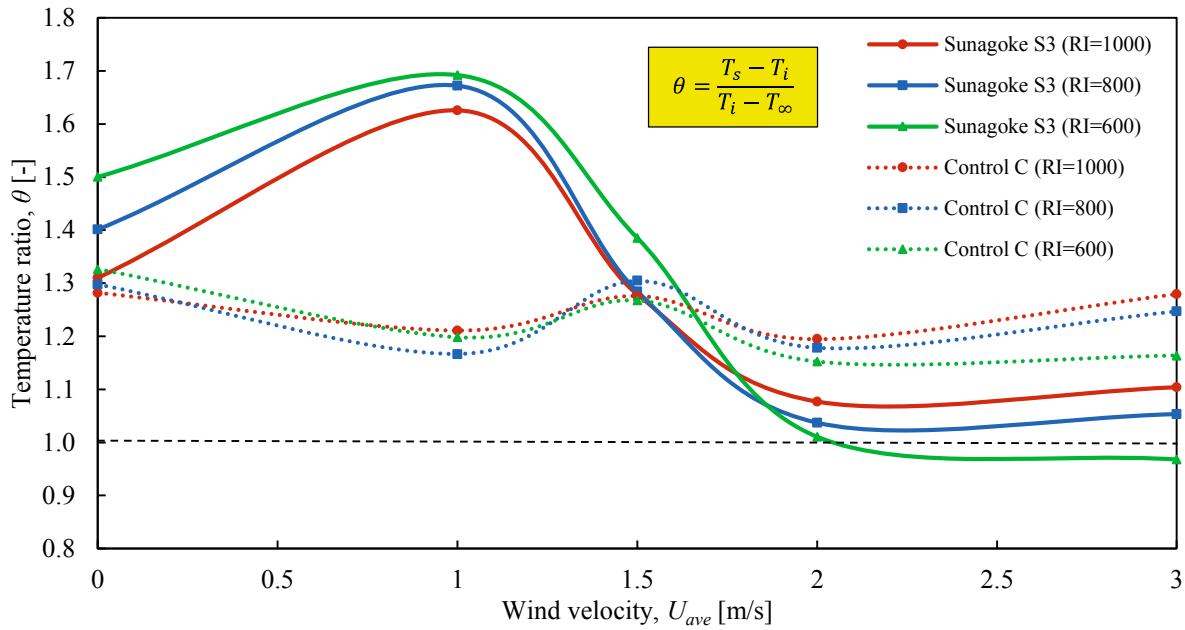


Fig. 6-10. Normalised temperature difference in indoor experiment, associated with interior temperature, surface temperature and ambient temperature.

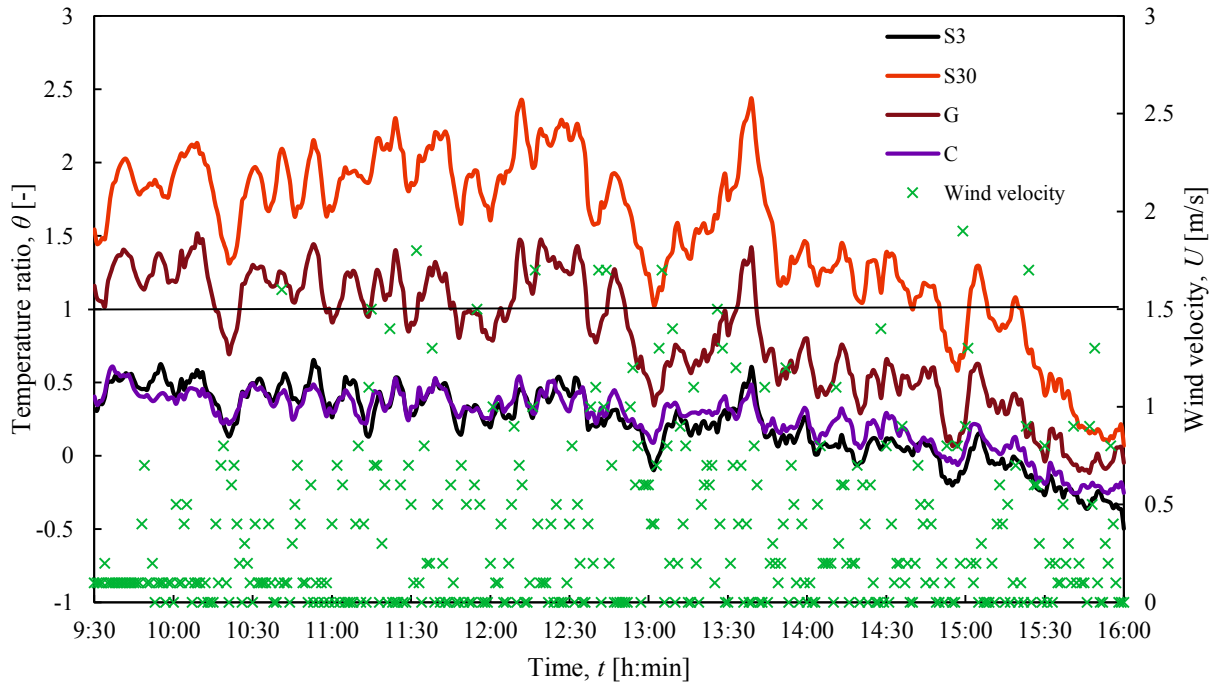


Fig. 6-11. Normalised temperature difference in outdoor experiment. Data were presented base on 5 moving averages.

6-5 Chapter Summary

The findings established in both indoor and outdoor experiments clarified the effects of wind velocity and irradiance on the thermal performance of the Sunagoke moss green roof. Despite being a nearly maintenance-free green roof plant, the Sunagoke green roofs showed a decent shading in regulating the heat balance that occurred on the roof. Through finding the convection heat transfer characteristics, the wind velocity of beyond 2m/s can be classified as the forced convection region acting on green roofs. In outdoor experiments, the three green panels (S3, S30, and G) displayed better convection heat transfer coefficient than the control roof, however, the thinnest S3 had the best ability to release heat compared to other competitors. Meanwhile, the albedo was not affected by wind velocity, but irradiance strength, noting 0.25 ± 0.004 , 0.22 ± 0.004 , 0.22 ± 0.006 , and 0.24 ± 0.001 for model houses S3, S30, G and C, individually in outdoor environment. The 30mm thickness Sunagoke moss did not deliver heat as good as 3mm Sunagoke moss and 25mm grass in term of convection heat, but the suppression of interior temperature was the most superior. Despite the absence of soil, both Sunagoke moss green panels (S3 and S30) showed decent insulation effect and provide thermal comfort comparable to grass.

There were results in some extent, the indoor experiments can reflect the outdoor outcomes, for example the ratio of Grashof number and square of Reynolds number and heat proportions developed on model houses. However, there were still many outcomes from outdoor experiment which disagreed with the indoors' due to the metamorphosis of measuring environment. Nevertheless, since the environment can be controlled, results from indoor experiment was capable to be analysed in details, which outdoor experiment could not provide the opportunity. The outcomes discussed in this paper may contribute to the understanding on the benefit of implementing Sunagoke moss green roof to the practitioners as an effort to build a healthy interior environment and enhance energy efficiency in a building, as encouraged by Ghani [63]. The changes start from us.

6-6 Equipment List in Chapter 6

1. Portable data logger
 - Manufacturer : Yokogawa Electric Co., Ltd.
 - Model : Datum-Y XL100
 - Temperature range : 0 ~ 350 [°C]

2. Temperature and humidity loggers
 - Manufacturer : T & D Co., Ltd.
 - Model : RTR-53A
 - Temperature measurement accuracy : 0 ~ 50 [°C]
 - Humidity measurements accuracy : 10 ~ 95 [%]

3. Temperature and humidity sensor
 - Manufacturer : Hioki Co., Ltd.
 - Model : 3641 Type
 - Number of channels : 2ch
 - Highest decomposition : 0.1 [°C]

4. Electronic balance
 - Manufacturer : A&D Co., Ltd.
 - Model : EK-6100i
 - Measuring range : 0.1 ~ 6000 [g]

5. Lightweight data logger for electronic balance
 - Manufacturer : A&D Co., Ltd.
 - Model : AD-1688
 - Measurement range : 0.1~6000 [g]

6. Pyranometer
 - Manufacturer : Eko Instruments Co., Ltd.
 - Model : MS-402
 - Instrument constant : 6.99 [mV / kW · m⁻²]
 - Internal resistance : 500 [Ω]
 - Wavelength range : 285-2800 [nm]

7. Albedometer
- | | |
|---------------------|--|
| Manufacturer | : Delta Ohm |
| Model | : LP-PYRA-06 |
| Instrument constant | : 15.15 [mV / kW · m ⁻²] for up 15.55 [mV / kW · m ⁻²] for down |
| Internal resistance | : 37.6 [Ω] for up 36.9 [Ω] for down |
| Wavelength range | : 305-2800 [nm] |
8. Environment Recorder (Vane-type anemometer)
- | | |
|--------------------------|-----------------------|
| Manufacturer | : Sato Shouji Inc. |
| Model | : EM-SD |
| Wind velocity range | : 0.4~25.0 [m/s] |
| Wind velocity resolution | : 0.1 [m/s] |
| Wind velocity accuracy | : ± (2 % + 0.2 [m/s]) |
| Temperature range | : 0~50 [°C] |
| Temperature resolution | : 0.1 [°C] |
| Temperature accuracy | : ± 0.8 [°C] |

Chapter 7 - General Conclusion

7-1 Relation between Indoor and Outdoor Experiments

From the findings obtained in indoor (Chapter 4 & 5), and outdoor (Chapter 6) experiments, the overall conclusion can be drawn. With a certain degree, the corresponding results in outdoor environments can be interpreted in detail by referring to the results of forced and complex convection in indoor experiments. Subjects that had good agreement either in indoor and outdoor environments were:

- 1- Wind velocity region where the natural, forced, and combined convection take place. —For both cases, the wind velocity of 2 [m/s] was found to be the critical wind velocity where the forced convection started to act on all model houses, including the control roof. For some cases of model houses with vegetation, the forced convection may started to develop from 1.5 [m/s] of wind velocity. However, the surface temperature was still decreasing, thus taking 2 [m/s] point is a confident way to express the wind velocity region.
- 2- Convection heat transfer coefficient. —For dry Sunagoke moss, the convection coefficient measured in the indoor experiment (forced convection region) was higher than the average result from outdoor experiment. However, if the upper limit of the average value is taken, the result is comparable with the readings from indoor experiment. Noting 105.2 [W/m²K] for outdoor, and 116.1 [W/m²K] for indoor environment.
- 3- Heat proportions governing heat balance occurred on model houses. —The heat proportion was derived to summarize the contribution of heat acting on a system. Therefore, both indoor and outdoor environment shows similar results since the same model houses were used.

Nevertheless, there were also results that contradicted in indoor and outdoor environments which were:

- 1- Albedo (reflectivity coefficient). —The contradiction of albedo may occurred as a result of different reflection intensity, where the outdoor environment reflected more radiation than indoor environment.

2- Normalized temperature difference. — The normalized temperature difference showed varied results between the two environments due to difference of steady and non-steady state, different base ambient temperature, and environment limitations. Furthermore, the indoor environment only allows certain degree of heat transfer to occur, considering the overall heat capacity of the Artificial Climate Chamber cavity. In contrast, the outdoor environment do not have any limitation in the term of heat exchange.

7-2 Comparison between Green Roof Plants

Through the comparison between plants used in green roof application, the advantageous and disadvantageous can be summarized in the following Table 7-1. Comparisons were made considering only Sunagoke moss without substrate layer, but other plants.

Table 7-1. Summary of comparison between plants used in green roof application.

| | Sunagoke moss | Grass | Sedum | Herbaceous perennials |
|-----------------|--|--|---|--|
| Advantageous | <ul style="list-style-type: none"> • Light-weight • Draught tolerant [31, 43] • Effective in suppressing interior temperature • High albedo • High convection heat transfer coefficient if thin • High water retention [43] • Prolonged evaporation period if thick | <ul style="list-style-type: none"> • High albedo • Moderate convection heat transfer coefficient • High shading area* [36] • Prolonged evaporation period with substrate | <ul style="list-style-type: none"> • High convection heat transfer coefficient [64] • Prolonged evaporation period with substrate • High water retention | <ul style="list-style-type: none"> • High albedo [58] • High shading area* [36] • Prolonged evaporation period with substrate |
| Disadvantageous | <ul style="list-style-type: none"> • Low heat dissipation if thick • Low convection heat transfer coefficient if thick | <ul style="list-style-type: none"> • Necessitate substrate layer • Heavy • High maintenance | <ul style="list-style-type: none"> • Necessitate substrate layer • Heavy • High maintenance | <ul style="list-style-type: none"> • Necessitate substrate layer • Heavy • High maintenance |

*based on comparison of Leaf Area Index (LAI)

7-3 Comparison between Green Roof, High Reflective Roof, and Solar Panel Roof

To compare green roofs with high reflective and solar panel roof, the advantageous, disadvantageous, and initial implementation cost have been summarized in the following Table 7-2. Generally, Sunagoke moss green roof has the similar advantageous as the conventional green roof. However, the advantageous of voluntary soil gives a huge merit in the implementation.

Table 7-2. Comparison between conventional green roof, Sunagoke moss green roof, high reflective roof, and solar panel roof.

| | Conventional Green Roof [65] | Sunagoke Moss Green Roof | High Reflective Roof [65] | Solar Panel Roof [66] |
|-----------------|---|--|--|--|
| Advantageous | <ul style="list-style-type: none"> • Increase solar radiation reflectivity • Interception of solar radiation (photosynthesis) • Reduce interior temperature • Reduce air pollution • Provide shading/ insulation effect • Provide cooling from evapotranspiration • Absorb CO₂, release O₂ • Prevent urban flooding (high water retention) • Offer habitat for animals | <ul style="list-style-type: none"> • Similar advantageous as the conventional green roof • Do not require soil • Light weight • Low initial and running cost • Maintenance free | <ul style="list-style-type: none"> • Highest solar radiation reflection • Less maintenance • Reduce interior temperature • Reduce electricity consumption for cooling | <ul style="list-style-type: none"> • Produce electricity • Reduce electricity consumption • Able to sell electricity • Initial cost is subsidized • Useful during power outages and disasters |
| Disadvantageous | <ul style="list-style-type: none"> • Heavy since require soil layer • High maintenance • Complicated implementation method | | <ul style="list-style-type: none"> • Not effective in energy treatment • Reflected radiation may affect near or taller building • Electric consumption increase for heating (winter) • Less effective in a highly insulated building • Reflectivity decreases with time (stain) | <ul style="list-style-type: none"> • High initial cost • Complicated implementation method • Heavy |
| Initial cost | <ul style="list-style-type: none"> • Grass type: ¥20,000/m² • Sedum type: ¥25,000/m² • Shrub type: ¥35,000/m² | <ul style="list-style-type: none"> • Sunagoke type: ¥9,000/m² [67] | <ul style="list-style-type: none"> • Paint type: ¥4,000/m² • Water resistant sheet type: ¥9,000/m² | <ul style="list-style-type: none"> • Regular type: ¥45,000/m² [68] |

7-4 Future Exploration

To explore further the thermal performance of Sunagoke moss green roof system, the author have drawn several points that can be considered in further investigations.

- 1- New radiation balance to be considered. –The indoor experiments documented in this dissertation were conducted by considering only the radiation model above the green panel. However, the radiation model below the green panel (air layer) has not been taken into account. Therefore, a more detailed radiation model should be proposed. Besides, the effect of radiation scattering on Sunagoke moss surface should also be investigated.
- 2- Other experimental parameters should be examined. –Different ambient temperature scheme (e.g.: colder winter), and lower to zero irradiance (night time) setups are another parameters that interesting to be explored to observe the thermal performance changes. Furthermore, the thicker Sunagoke moss 30mm should be investigated in the laboratory setup, since this dissertation is not included with the evaluation.
- 3- Investigating the water retention, and evapotranspiration capability. –Since water retention is a crucial parameter in reducing Urban Heat Island effect, the parameter should be quantitatively examined, together with the evaporation efficiency of the Sunagoke moss green roof.
- 4- Attempt on the generalization of Sunagoke moss green roof system. –The evaluated data from indoor and outdoor experiments can be further used in generalization of Sunagoke moss green roof system. However, features analysed from points 1 to 3 above need to be clarified first to achieve a more precise generalization.

Acknowledgement

For the very first, the author would like to present his gratitude to Allah and Rasulullah through guiding and supporting him internally to finish his study. Thank you for giving him the opportunity in his life to receive the highest formal education title.

Along conducting this research, the author sincerely appreciate Prof. Dr. Yasuo Katoh for his tremendous supervision and ideas to ensure the success of this research. The author have been extremely lucky to have a supervisor who cared so much about the progress of the work, and promptly responded when asked. Highest thank you, and the author hope that Prof. Dr. Katoh can have a good rest upon the retirement.

The author would also like to express his gratitude to lecturers and professors in Dept. of Mechanical Engineering of Yamaguchi University for providing endless support to his laboratory in conducting researches. Special thanks to Prof. Dr. Hiroshi Katsurayama, Prof. Dr. Makoto Koganei, Prof. Dr. Shinsuke Mochizuki, and Prof. Dr. Kenichiro Tanoue for being a thorough but kind examiners during the three dissertation defends. Upon the completion of this thesis, the author honestly appreciated Dr. Makoto Mizunuma for giving him supervision and facilitating him the experiment equipment at Yamaguchi Prefecture Industrial Technology Institute.

Besides, the author would like to deeply thank his laboratory fellow friends, Kawamata, Nakagawa, Konishi, Nawata, Miyazaki, Nagase, Matsumoto and Nasrullah that assisting him endlessly in completing this thesis. Not to forget his senior: Ishida Satoshi, and juniors: Ruzaini, Taufik, Awata Yusuke, and Wafiyuddin in helping him in the progress. Thank you very much.

To his beloved family and wife, thank you for giving him the incredible support and praying for his success in this dissertation. Father Khalid, mother Normadiah, eldest brother Amir Farhan and family, sister Liyana Adhwa and family, sister Farah 'Aina and youngest brother Ikram Khairi, you all deserve the gratitude. To his wife Nur Atiqah and his son Akira, without you two, the author will not reach to this level. Thank you for cheering him through the ups and downs. There are no words to describe his gratitude.

At this opportunity, the author would like to express his appreciation to Yayasan Pelajaran Mara and Malaysian tax payers for providing him the financial aid. This is the results of the investment, a research for advancement of Malaysia nation. As well to YPM and JUCTe, thank you for the welfare support from the day the author entered Japanese Associate Degree program in 2009.

In the making of this dissertation, together with the journals the author had published, aunties Ramlah and Norizan, friend Evan Nicholas Fernandez, and MPWS Proofreading had contributed to editing and proofreading. Thank you very much. Last but not least, the author appreciate other individuals whom provided assistances whether directly or indirectly in the making of this dissertation. Thank you very much.

References

- [1] L. Kleerekoper, M. Van Esch and T. B. Salcedo, "How to make a city climate-proof, addressing the urban heat island effect," *Resources, Conservation and Recycling*, vol. 64, pp. 30-38, 2012.
- [2] M. A. Fauzi, N. Abdul Malek and J. Othman, "Evaluation of Green Roof System for Green Building Projects in Malaysia," *International Journal of Environmental, Chemical, Ecological, Geological and Geophysical Engineering*, vol. 7, no. 2, pp. 53-59, 2013.
- [3] A. H. Rosenfeld, H. Akbari, S. Bretz, B. L. Fishman, D. M. Kurn, D. Sailor and H. Taha, "Mitigation of urban heat islands: materials, utility programs, updates," *Energy and Buildings*, vol. 22, pp. 255-265, 1995.
- [4] C. P. Tso, "A survey of urban heat island studies in two tropical cities," *Atmospheric Environment*, vol. 30, no. 3, pp. 507-519, 1996.
- [5] S. Niewolt, "The urban microclimate of Singapore," *J. of Trop. Geog.*, vol. 22, pp. 30-37, 1966.
- [6] D. E. Bowler, L. Buyung-Ali, T. M. Knight and A. S. Pullin, "Urban greening to cool towns and cities: A systematic review of the empirical evidence," *Landscape and Urban Planning*, vol. 97, pp. 147-155, 2010.
- [7] C. Aniello, K. Morgan, A. Busbey and L. Newland, "Mapping micro-urban heat islands using Landsat Tm and a GIS," *Comput. Geosci.*, vol. 21, pp. 965-969, 1995.
- [8] J. A. Patz, D. Campbell-Lendrum, T. Holloway and J. A. Foley, "Impact of regional climate change on human health," *Nature*, vol. 438, pp. 310-317, 2005.
- [9] H. Akbari, M. Pomerantz and H. Taha, "Cool surfaces and shade trees to reduce energy use and improve air quality in urban areas," *Solar Energy*, vol. 70, no. 3, pp. 295-310, 2001.
- [10] R. S. Kovats and S. Hajat, "Heat Stress and Public Health: A Critical Review," *Annual Review of Public Health*, vol. 29, no. 1, pp. 41-55, 2008.
- [11] A. J. McMichael, "The urban environment and health in a world of increasing globalization: issues for developing countries," *Bulletin of the World Health Organization*, vol. 78, no. 9, pp. 1117-1126, 2000.
- [12] S. E. Gill, J. F. Handley, A. R. Ennos and S. Pauleit, "Adapting cities for climate change: The role of the green infrastructure," *Built Environment*, vol. 33, no. 1, pp. 115-133, 2007.
- [13] J.-E. Park and H. Murase, "Evapotranspiration efficiency of Sunagoke moss mat for the wall greening on the building," *American Society of Agricultural and Biological Engineers*, vol. 6, pp. 3612-3621, 2008.

- [14] N. Kawakami, H. Murase and H. Fukuda, "Analysis of the transpiration properties in Sunagoke moss," *Acta Horticulturae*, vol. 1011, pp. 473-478, 2013.
- [15] J. A. Clements and S. A. Sherif, "Thermal analysis of roof spray cooling," *International Journal of Energy Research*, vol. 22, pp. 1337-1350, 1998.
- [16] H. Taha, "Urban climates and heat islands: albedo, evapotranspiration, and anthropogenic heat," *Energy and Buildings*, vol. 25, pp. 99-103, 1997.
- [17] E. P. Del Barrio, "Analysis of the green roofs cooling potential in buildings," *Energy and Buildings*, vol. 27, pp. 179-193, 1998.
- [18] A. Niachou, K. Papakonstantinou, M. Santamouris, A. Tsangrassoulis and G. Mihalakakou, "Analysis of the green roof thermal properties and investigation of its energy performance," *Energy and Buildings*, vol. 33, pp. 719-729, 2001.
- [19] S. Gaffin, C. Rosenzweig, L. Parshall, D. Beattie, R. Berghage, G. O'Keeffe and D. Braman, "Energy balance modeling applied to a comparison of green and white roof cooling efficiency," in *Third Annual Greening Rooftops for Sustainable Communities Conference, Awards and Trade Show*, Washington, DC, 2005.
- [20] N. D. VanWoert, D. B. Rowe, J. A. Andresen, C. L. Rugh, R. T. Fernandez and L. Xiao, "Green Roof Stormwater Retention," *Journal of Environmental Quality*, vol. 34, no. 3, pp. 1036-1044, 2004.
- [21] S. Gaffin, C. Rosenzweig, L. Parshall, D. Hillel, J. Eichenbaum-Pikser, A. Greenbaum, R. Blake, R. Beattie and R. Berghage, "Quantifying evaporative cooling from green roofs and comparison to other," in *Forth Annual Greening Rooftops for Sustainable Communities Conference, Awards and Trade Show*, Boston, 2006.
- [22] L. Bengtsson, "Peak flows from thin sedum-moss roof," *Nordic Hydrology*, vol. 36, no. 3, pp. 269-280, 2005.
- [23] L. Bengtsson, L. Grahn and J. Olsson, "Hydrological function of a thin extensive green roof," *Nordic Hydrology*, vol. 36, no. 3, pp. 259-268, 2005.
- [24] K. L. Getter and D. B. Rowe, "The role of extensive green roofs in sustainable development," *HortScience*, vol. 41, no. 5, pp. 1276-1285, 2006.
- [25] D. B. Rowe, M. A. Monterusso and C. L. Rugh, "Assessment of heat-expanded slate and fertility requirements in green roof-substrates," *Horttechnology*, vol. 16, no. 3, pp. 471-477, 2006.
- [26] I. Misaka, H. Suzuki, A. Mizutani, N. Murano and Y. Tashiro, "Evaluation of heat balance of wall greening," *AIJ J. Technol. Des.*, vol. 23, pp. 233-236, 2006.
- [27] J. Coma, G. Pérez, C. Solé, A. Castell and L. F. Cabeza, "Thermal assessment of extensive green roofs as passive tool for energy savings in buildings," *Renewable Energy*, vol. 85, pp. 1106-1115, 2016.

- [28] Y. Kikegawa, Y. Genchi, H. Kondo and K. Hanaki, "Impacts of city-block-scale countermeasures against urban heat-island phenomena upon a building's energy-consumption for air-conditioning," *Applied Energy*, vol. 83, pp. 649-668, 2006.
- [29] E. Oberndorfer, J. Lundholm, B. Bass, R. R. Coffman, H. Doshi, N. Dunnett, S. Gaffin, M. Köhler, K. K. Y. Liu and B. Rowe, "Green Roofs as Urban Ecosystems: Ecological Structures, Functions, and Services," *Bioscience*, vol. 57, no. 10, pp. 823-833, 2007.
- [30] J. C. Berndtsson, "Green roof performance towards management of runoff water quantity and quality: A review," *Ecological Engineering*, vol. 36, pp. 351-360, 2010.
- [31] S. M. Studlar and J. E. Peck, "Extensive green roofs and mosses: Reflection from pilot study in Terra Alta, West Virginia," *Evansia*, vol. 26, no. 2, pp. 52-63, 2009.
- [32] M. E. Bachawati, R. Manneh, R. Belarbi and H. E. Zakhem, "Real-time temperature monitoring for Traditional gravel ballasted and Extensive green roofs: A Lebanese case study," *Energy and Buildings*, vol. 133, pp. 197-205, 2016.
- [33] T. Emilsson and K. Rolf, "Comparison of establishment methods for extensive green roofs in southern Sweden," *Urban Forestry & Urban Greening*, vol. 3, no. 2, pp. 103-111, 2005.
- [34] Y. Suzaki, S. Wakui and K. Iizjima, "On the insulating effect and air temperature moderation by *R. ericoides* moss," *J. Jpn. Soc. Reveget. Tech.*, vol. 30, no. 1, pp. 56-61, 2004.
- [35] M. R. Haferkamp, "Environmental Factors Affecting Plant Productivity," in *Fort Keogh Research Symposium*, Miles City, MT, 1987.
- [36] W. Heinze, "Results of an experiment on extensive growth of vegetation on roofs," *Rasen Grünflächen Begrünungen*, vol. 16, pp. 80-88, 1985.
- [37] N. D. VanWoert, D. B. Rowe, J. A. Andresen, C. L. Rugh and L. Xiao, "Watering regime and green roof substrate design impact *Sedum* plant growth," *Hortscience*, Vols. 659-669, p. 40, 2005.
- [38] F. Madre, A. Vergnes, N. Machon and P. Clergeau, "A comparison of 3 types of green roof as habitats for arthropods," *Ecological Engineering*, vol. 57, pp. 109-117, 2013.
- [39] D. Zirkelbach, S.-R. Mehra, K.-P. Sedlbauer, H.-M. Künzel and B. Stöckl, "A hygrothermal green roof model to simulate moisture and energy performance of building components," *Energy and Buildings*, vol. 145, pp. 79-91, 2017.
- [40] S. N. Ondimu and H. Murase, "Thermal properties of living roof greening material by inverse modeling," *Applied Engineering in Agriculture*, vol. 22, no. 3, pp. 435-441, 2006.
- [41] M. Eksi, D. B. Rowe, I. S. Wichman and J. A. Andresen, "Effect of substrate depth, vegetation type, and season on green roof thermal properties," *Energy and Buildings*, vol. 145, pp. 174-187, 2017.

- [42] S. N. Ondimu and H. Murase, "Combining Galerkin Methods and Neural Network Analysis to Inversely determine Thermal Conductivity of Living Green Roof Materials," *Biosystems Engineering*, vol. 96, no. 4, pp. 541-550, 2007.
- [43] M. Anderson, J. Lambrinos and E. Schroll, "The potential value of mosses for stormwater," *Urban Ecosystem*, vol. 13, pp. 319-332, 2010.
- [44] A. Heim, J. Lundholm and L. Philip, "The impact of mosses on the growth of neighbouring vascular plants, substrate temperature and evapotranspiration on an extensive green roof," *Urban Ecosystem*, vol. 17, pp. 1119-1133, 2014.
- [45] M. T. Bin Ahmad, スナゴケを用いた屋根緑化の熱的性能に関する熱工学的研究, Yamaguchi University Graduation Thesis, 2015.
- [46] M. Akita, M. T. Lehtonen, H. Koponen, E. M. Marttinen and J. P. Valkonen, "Infection of the Sunagoke moss panels with fungal pathogens hampers sustainable greening in urban environments," *Science of The Total Environment*, vol. 409, no. 17, pp. 3166-3173, 2011.
- [47] N. Takahashi, H. Nishina, K. Takayama, S. Futagami, T. Kamura and T. Nakahara, "Analysis for the Effect of Roof Greening in Warehouse by Mean of Simulation," *Environmental Control in Biology*, vol. 51, no. 3, pp. 99-103, 2013.
- [48] S. Quezada-García, G. Espinosa-Paredes, M. Escobedo-Izquierdo, A. Vázquez-Rodríguez, R. Vázquez-Rodríguez and J. Ambriz-García, "Heterogeneous model for heat transfer in Green Roof Systems," *Energy and Buildings*, vol. 139, pp. 205-213, 2017.
- [49] K. Okamoto, スナゴケを用いた屋根緑化の効果に関する熱工学的研究, Yamaguchi University Master Completion Thesis, 2012.
- [50] K. Komizo, スナゴケを用いた屋上緑化パネルの熱的特性に関する研究, Yamaguchi University Graduation Thesis, 2011.
- [51] S. Ishida, スナゴケを用いた屋根緑化の効果に関する熱工学的研究, Yamaguchi University Master Completion Thesis, 2014.
- [52] P. C. Tabares-Velasco and J. Srebric, "The role of plants in the reduction of heat flux through green roofs: laboratory experiments," *ASHRAE Transactions*, vol. 115, no. 2, pp. 793-802, 2009.
- [53] A. Pianella, R. E. Clarke, N. S. Williams, Z. Chen and L. Aye, "Steady-state and transient thermal measurements of green roof substrates," *Energy and Buildings*, vol. 131, pp. 123-131, 2016.
- [54] J. P. Holman, Heat Transfer, 9th ed., New York: McGraw-Hill Higher Education, 2002, pp. 347-348.
- [55] JSME Data Book: Heat Transfer, 5th ed., Tokyo: The Japan Society of Mechanical Engineering, 2009, pp. 52-54.

- [56] "World Weather and Climate Information," [Online]. Available: <https://weather-and-climate.com/average-monthly-Rainfall-Temperature-Sunshine,Tokyo,Japan>. [Accessed 12 7 2017].
- [57] A. Kumar and N. Barthakur, "Convective heat transfer measurements of plants in a wind tunnel," *Boundary-Layer Meteorology*, vol. 2, no. 2, pp. 218-227, 1971.
- [58] J. S. MacIvor and J. Lundholm, "Performance evaluation of native plants suited to extensive green roof conditions in a maritime climate," *Ecological Engineering*, vol. 37, pp. 407-417, 2011.
- [59] R. U. Halwatura, "Effect of turf roof slabs on indoor thermal performance in tropical climates: A life cycle cost approach," *Journal of Construction Engineering*, vol. 2013, pp. 1-10, 2013.
- [60] X. Wang, J. Niu and A. van Paassen, "Raising evaporative cooling potentials using combined cooled ceiling and MPCM slurry storage," *Energy and Buildings*, vol. 40, no. 9, pp. 1691-1698, 2008.
- [61] M. Ikusei, N. Kenichi and Y. Hitoshi, "Evaluation of evaporation ability of the system for mitigating urban heat island," in *The seventh International Conference on Urban Climate*, Yokohama, Japan, 2009.
- [62] R. McMullan, *Environmental Science in Building*, Fifth ed., New York: Palgrave and Hampshire, 2002.
- [63] F. Ghani, "Issues in sustainable architecture and possible solutions," *IJCEE-IJENS*, vol. 12, pp. 21-24, 2012.
- [64] Y. Awata, スナゴケを用いた屋根緑化の反射率を考慮した熱的性能評価, Yamaguchi University Graduation Thesis, 2016.
- [65] *Coolroof Guidebook*, 1st ed., Tokyo: Architectural Institute of Japan, 2013.
- [66] "Solar Partners," [Online]. Available: <https://www.solar-partners.jp>. [Accessed 6 2 2018].
- [67] "mbs," [Online]. Available: <http://www.ryokka.biz/green/index.html>. [Accessed 6 2 2018].
- [68] "Solar power generation comprehensive information," [Online]. Available: <http://standard-project.net/solar/sangyo/menseki.html>. [Accessed 6 2 2018].
- [69] "Emissivity Coefficients of some common Materials," The Engineering ToolBox, [Online]. Available: https://www.engineeringtoolbox.com/emissivity-coefficients-d_447.html. [Accessed 22 12 2017].

Appendix

(I) Calculation for radiation from inner floor and walls of Artificial Climate Chamber.

Experiments to investigate the effects of walls and floor have been conducted by measuring the temperature of walls and floor inside the ACC. The experiments conditions are displayed in Table I, while the location of temperature measuring points are depicted in Fig. I below.

Table I. Experimental conditions for investigating the effect from walls and floor.

| Parameters | Value |
|-----------------------------------|---|
| Ambient Temperature, T_{∞} | 30 [°C] |
| Humidity, RH | 70 [%RH] |
| Irradiance, R_I | 600, 800, 1000 [W/m^2] |
| Wind Velocity, U_{ave} | 0 [m/s] |
| Temperature Measuring Locations | Wall-South (WS) Wall-West (WW) Wall-North (WN) Wall-East (WE) Floor (F) |

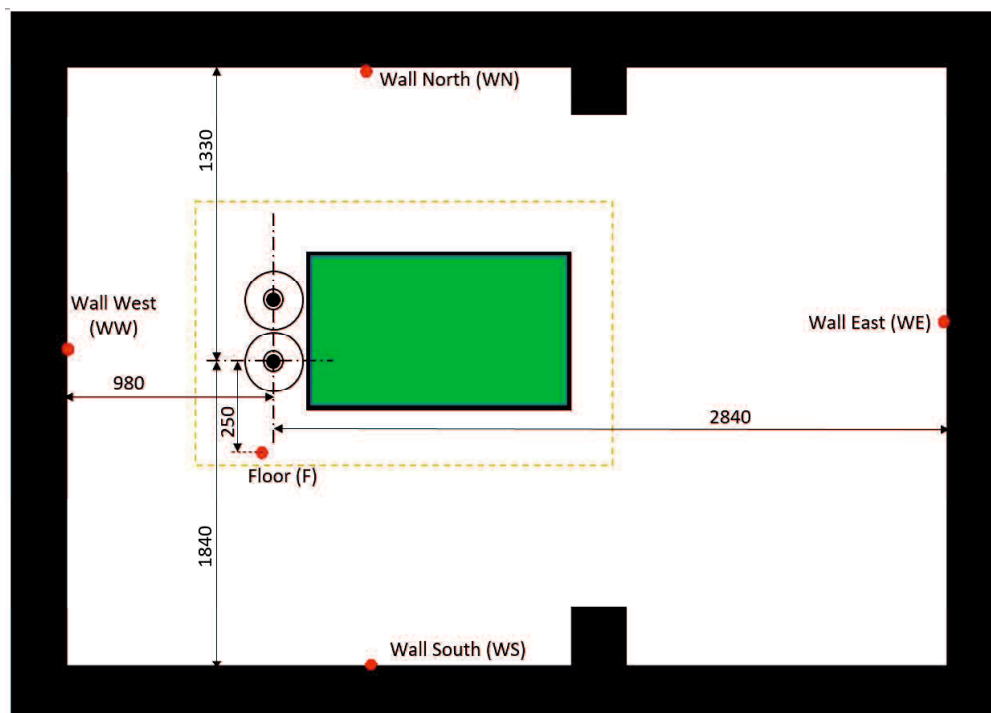


Fig. I. Temperature measuring points on four inner walls and a floor in Artificial Climate Chamber.

Fig. II represents the temperature measurements of each wall and floor, including the reference ambient and Sunagoke moss surface temperatures. As depicted on the graph, Sunagoke moss surface temperatures were highest respective to each irradiance, since Sunagoke moss received the irradiance directly. Meanwhile, the walls and floor temperatures did not exceed the ambient temperature regardless the irradiance.

Considering the material of inner floor and walls is polished stainless steel, the emissivity coefficient is 0.075 (retrieved from https://www.engineeringtoolbox.com/emissivity-coefficients-d_447.html [69]). The calculation for estimated radiation from floor and walls are following the simple radiation model shown as equation below, where the radiation is denoted by Q_x in $[\text{W}/\text{m}^2]$, radiation emitting surface area A , emissivity coefficient ε , Stefan-Boltzmann coefficient σ ($5.6703 \times 10^{-8} [\text{W}/\text{m}^2\text{K}^4]$), and radiating surface temperature $T[\text{K}]$. The results of the radiation calculations are shown in Fig. III, where the radiations from walls and floor were substantially small compared to irradiance and Sunagoke moss surface. For a remark, the calculation for Sunagoke moss used the emissivity 0.9588 of regular plant.

$$Q_x = \varepsilon\sigma T^4$$

From the radiation calculation, radiation percentages were determined by dividing it with the paralleled irradiance, and the results are represented in Fig. IV. As a result, During $600 \text{ W}/\text{m}^2$ of irradiance, the walls and floor radiation were about 5.9%, during $800 \text{ W}/\text{m}^2$, 4.4%, and during $1000 \text{ W}/\text{m}^2$, 3.4%. With these results, the effect from walls and floor were clarified.

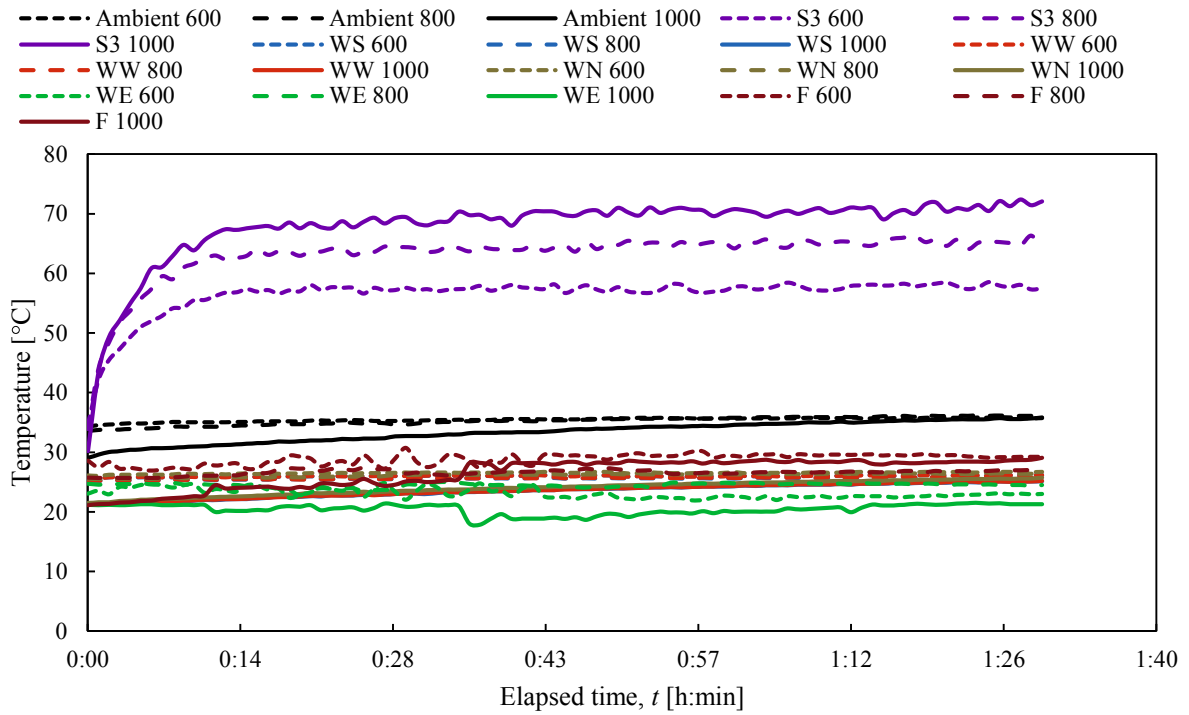


Fig. II. Surface temperature for all walls and floor, including ambient and Sunagoke moss surface temperature measurement, according to each irradiance.

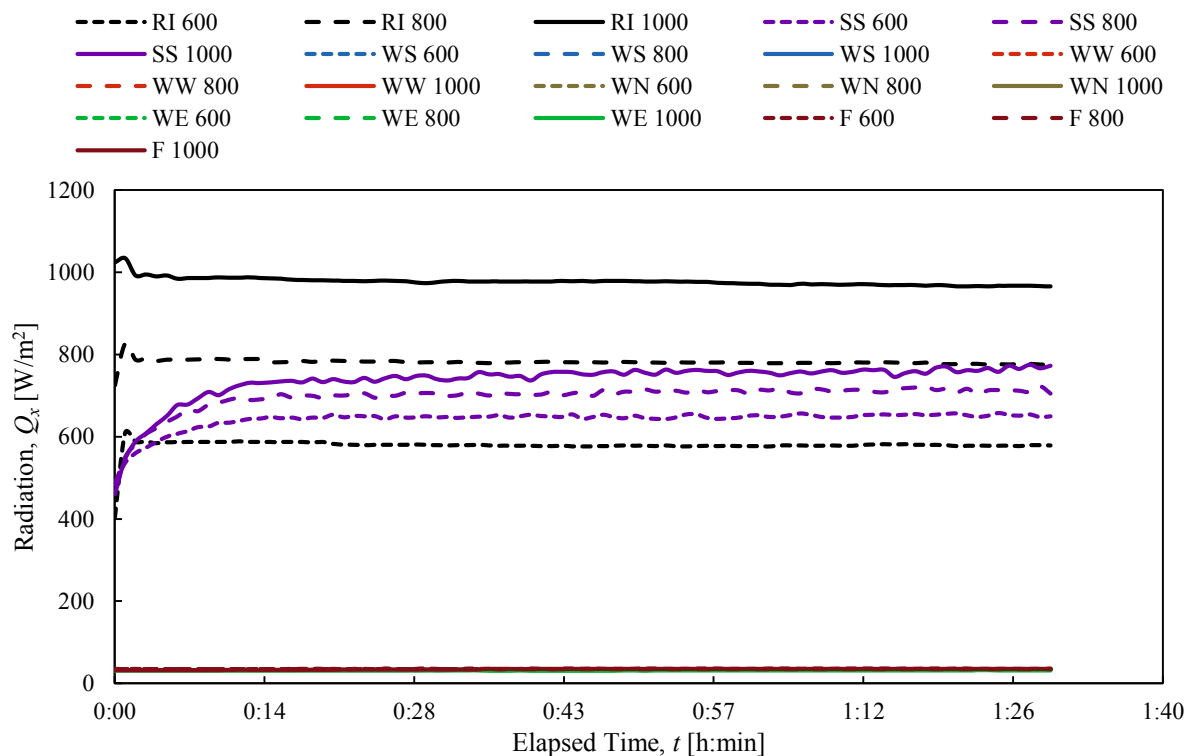


Fig. III. Comparison between radiations emitted by each surface, including irradiances. Irradiances are denoted by black, Sunagoke moss purple, and others are walls and floor.

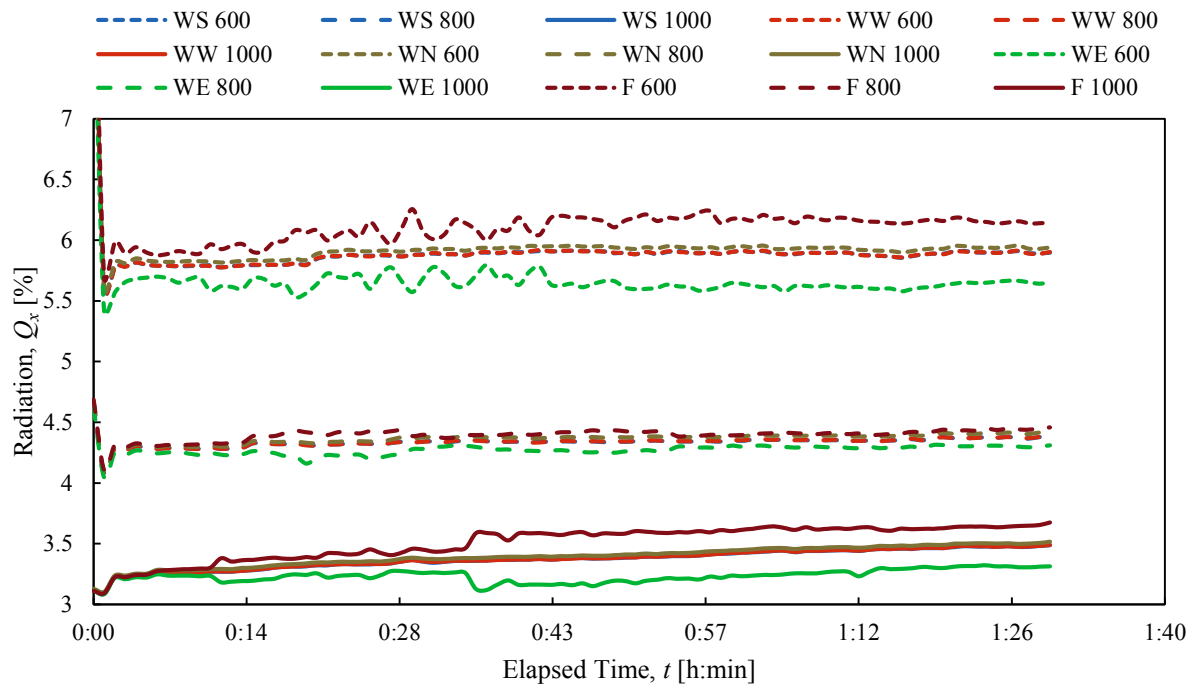


Fig. IV. Walls and floor radiation percentages relative to irradiance.

(II) Definitions

1) The greenhouse effect:

The green house effect is one result of the differing properties of heat radiation when it is generated by bodies at different temperatures. The high temperature sun admits radiation of short wavelength which can pass through atmosphere and through different type materials. Inside the house or other building this heat is absorbed by object, such as plants, which then re-radiate the heat. The objects below the roof are at lower temperature than the sun the radiated heat is of longer wavelengths with cannot penetrate solid material. This re-radiated is therefore trapped and cause the temperature inside the house to rise. The atmosphere surrounding the earth also behaves a large affect around our environment

The climate has significant effects on the energy performance of buildings in both winter and summer, and the durability of building materials. The climate for a building is the set of environment conditions which surround a building and link to the inside of a building by mean of heat transfer. Although the overall features of the climate beyond our control, the design of a building can have a significant influence on the climate behaviour of the building.

2) Heat:

H or Q is a form of energy also called thermal energy in unit joule (J). Is an internal molecules property of materials often forms an intermediate stage in the production of other forms of energy.

3) Thermodynamic Temperature (T):

Is a point on a temperature scale defined by reference to absolute zero and to the triple point of water in unit degree Kelvin (K).

4) Specific heat capacity (C):

The specific heat capacity of a material is the quantity of heat energy require to raise the temperature of 1 kg of that material by 1 degree Kelvin (or 1 degree Celsius) in J/kg K (or J/kg °C).

5) Convection heat:

When the sample exists entirely in a single state of ice, water or steam the temperature raises uniformly as heat is supplied. Therefore, the convection heat is the heat energy absorbed or released from a substance during a change in temperature.

6) Latent heat:

When the sample is changing from one state to supply another the temperature remains constant, even though heat is being supplied. This heat is termed 'latent' because it seems to be hidden. Therefore latent heat is the energy absorbed or released from a substance during a change of state, with no change in temperature.

7) Heat transfer:

Heat energy always tends to transfer from high temperature to low temperature region. Several bodies at different temperature are close together then heat will be exchanged between them until they are at same temperature.

8) Solid state:

The molecules are held together in fixed positions; the volume and shape are fixed.

9) Liquid state:

The molecules are held together but have freedom of movement; the volume is fixed but the shape not fixed.

10) Gas state:

The molecules move rapidly and have complete freedom; the volume and shape not fixed.

11) Conduction:

Is the transfer of heat energy through a material without the molecules of the materials changing their basic positions.

12) Convection:

Is the transfer of heat energy through a material by the bodily movement of particles.

13) Radiation:

Is the transfer of heat energy by electromagnetic waves.